

Universidade do Minho
Escola de Ciências

Inês Catarina Pedro Bártolo

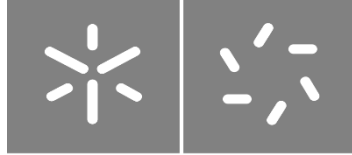
**Particle-based system for Keratinocyte
Growth Factor release in skin models**

**Particle-based system for Keratinocyte
Growth Factor release in skin models**

Inês Catarina Pedro Bártolo

UMinho | 2021

junho de 2021



Universidade do Minho
Escola de Ciências

Inês Catarina Pedro Bártolo

Particle-based system for Keratinocyte Growth Factor release in skin models

Dissertação de Mestrado

Mestrado em Biofísica e Bionanossistemas

Trabalho efetuado sob a orientação de

Doutora Mariana Teixeira Cerqueira

Doutora Elisabete M. S. Castanheira Coutinho

junho 2021

DIREITOS DE AUTOR E CONDIÇÕES DE UTILIZAÇÃO DO TRABALHO POR TERCEIROS

Este é um trabalho académico que pode ser utilizado por terceiros desde que respeitadas as regras e boas práticas internacionalmente aceites, no que concerne aos direitos de autor e direitos conexos.

Assim, o presente trabalho pode ser utilizado nos termos previstos na licença abaixo indicada.

Caso o utilizador necessite de permissão para poder fazer um uso do trabalho em condições não previstas no licenciamento indicado, deverá contactar o autor, através do RepositóriUM da Universidade do Minho.

Licença concedida aos utilizadores deste trabalho



Atribuição-NãoComercial-SemDerivações

CC BY-NC-ND

<https://creativecommons.org/licenses/by-nc-nd/4.0/>

Agradecimentos

Depois de o ano 2019 ter sido tão complicado, onde experienciei a luta do meu pai contra uma maldita doença e a perda física dele e de o ano 2020 trazer uma pandemia mundial e me ter levado a minha avózinha, tenho de agradecer às pessoas que estiveram presentes e me ajudaram direta ou indiretamente para a concretização deste projeto, e me deram força para tal.

Em primeiro lugar, gostaria de agradecer ao Professor Rui Reis pela oportunidade de desenvolver a minha dissertação de mestrado no Instituto de Investigação em Biomateriais, Biodegradáveis e Biomiméticos (I3B's), na Universidade do Minho.

À Doutora Alexandra Marques, por me receber de braços abertos na Skin Team, pelo apoio, motivação e confiança que depositou em mim para a realização deste projeto, onde eu aprendi tanto.

À Doutora Mariana Cerqueira, um obrigada não é o suficiente para expressar o quão agradecida estou por trabalhar ao seu lado. Obrigada pelo apoio, ajuda, paciência, por toda a sabedoria que partilhou comigo, mas principalmente pelo carinho e pelas palavras de motivação que sempre me deu ao longo deste longo período. Não poderia estar mais agradecida por ter uma pessoa como a Mariana para me guiar nesta viagem atribulada.

Um grande obrigada à Professora Elisabete Coutinho. Desde o início do meu mestrado que mostrou um apoio, ajuda e disponibilidade inexplicável.

Agradeço ao projeto SteamTREAT (PTDC/BTM-ORG/28131/2017) pelo apoio financeiro dado à elaboração da minha tese.

Aos meus colegas de laboratório por todos os conhecimentos que partilharam comigo. Um especial agradecimento ao Daniel Rodrigues, por despenderes o teu tempo comigo para me ajudares com a produção das partículas, pela paciência e apoio que sempre me deste, e à Mónica Garcia por me dares os milhões de queratinócitos sempre que precisava, aturares os meus mental breakdowns quando as células não colaboravam comigo, por tudo mesmo!

Mahwish you were the most beautiful surprise in the lab, thank you for being such a good friend since the beginning and for showing your resting bitch face to other people but for being a sweetheart inside. Sara Vieira, obrigada pelo carinho, pela ajuda nas ELISAS, por seres a pessoa mais querida que poderia ter conhecido, és um anjinho. Catarina Vale, por partilhares tantos sorrisos, tantas lágrimas e tantos abraços comigo, por todas as mensagens de apoio e carinho e, em especial pela amizade que me dás diariamente.

Porque “when in doubt, go to the library”, à minha *Library Crew* e a todas as pessoas que já passaram por lá. A todos vocês, obrigada por me terem marcado da maneira mais bonita possível, por

me fazerem rir sempre que os dias eram menos bons e pelo apoio incondicional que tive de todos. Aninha Matos, por seres a minha pessoa preferida de sempre, por estares a meu lado desde o início e por nunca, mas nunca me deixares de apoiar, não há agradecimento possível para ti. Didi, és a menina que está sempre a meu lado, minha companheira das boleias do popó amarelo, sempre pronta a soltar um sorriso enorme que contagia o mundo e que dá os abraçinhos que uma pessoa precisa sempre. Lipoca, caramba, OBRIGADA por tudo, pelos memes diários, pelas minhas mensagens matinais na secretária que me faziam o meu dia de trabalho melhor, pelos cafezinhos que tanto precisava e por seres uma pessoa verdadeiramente bonita, não só no exterior como no interior. Pantunes, obrigada por existires na minha vida, pela ajuda, pelo apoio, pela tua amizade e por todos os momentos de verdadeira felicidade que trazes à minha vida. À Ana Olival por todas as fotos de sobremesas e pratos deliciosos que faz, pelas fotografias de animalinhos que me manda sempre para animar o meu dia e por seres a minha compincha transmontana. À Leonor Ribeiro, por todas as discussões que animavam o meu dia sobre o quão transmontana era, por todas as palavras novas que adicionei ao meu dicionário e por estares sempre presente nesta caminhada. Ao JP, ao Rodrigo e ao Rafa, por serem os palhacinhos que mais alegraram os meus dias.

Às minhas Bitches, Inês e Quelluh, vocês são as minhas melhores amigas, as minhas companheiras para o resto da vida, obrigada por fazerem parte dela.

À Ana Pontes, por seres a pessoa que me acolheu logo no mestrado onde não conhecia ninguém e por nunca me abandonares, por estares a meu lado, sempre disponível para mim e por seres a minha irmã de coração. You are my sister from another mister.

Aos meus Pitéus, Cat, Fill, Joana, Jucu, Machado, Maria, Pedro e Pipa, pela amizade desde pequenina até agora, pelo apoio incondicional que me deram desde sempre, principalmente quando mais precisei e que preciso.

À minha amiga mais antiga, ao meu ombro amigo e à minha companheira para sempre, Maria Pacheco. És a minha força, a minha caixinha dos segredos, a pessoa que melhor me compreende e quem tem sempre a melhor palavra para me dar. És a calma no meio da minha tempestade.

À minha família, por serem o meu apoio e força diária. Tia Lena e tio João, por serem os melhores que existem. Por deixarem tudo e me virem socorrer quando mais precisava, por me mostrarem o verdadeiro significado de família. E um especial obrigada à minha avózinha que me deixou no final do ano 2020 e que foi das pessoas mais lutadoras que já existiu. À Amparo, Zé Manel e Anita por me mostrarem que não é preciso partilharmos o mesmo DNA para sermos da mesma família, por me quererem tanto, mas tanto que nunca me deixaram. A vocês, o meu maior obrigada.

Ao meu namorado, Tó, a ti nem com a maior riqueza que existe neste universo te conseguia pagar e agradecer tudo o que fizeste por mim, és o melhor de mim....não me vou prolongar nas palavras porque sabes verdadeiramente o quão importante és para mim, és o meu pilar (now, i'm crying), corrente de ferro na ostaga da gávea alta. Aos teus pais e à tua maninha, por me adotarem na vossa família, por me aceitarem e por tudo, por tudo mesmo!

Ao meu Loki, por seres o cão mais humano que existe, por me ouvires, me compreenderes e por me dares tanto amor e carinho. És o meu cãopanheiro.

Às pessoas mais importantes da minha vida, por me terem dado a vida, por terem lutado para me darem tudo de bom e o melhor que sempre puderam. MÃE, com letras grandes, és a Mulher mais lutadora que existe, és a força da natureza e o exemplo que carrego para seguir. Devo-te tudo. Não te posso agradecer algo que não consigo retribuir e espero um dia ser metade da pessoa que és. PAI, és a minha estrelinha. Foste tão lutador até ao último segundo, sempre com o maior sorriso do mundo quando me vias. Vou-te lembrar sempre com muito amor e carinho e como o pai que demonstrava o seu amor ao trazer a frutinha e os legumes fresquinhos para eu levar ao domingo para a universidade. Tenho saudades tuas e dedico-te todo o meu sucesso, espero fazer de ti o pai mais orgulhoso de sempre.

Com as lágrimas nos olhos, olho para esta longa jornada como uma jornada em que aprendi a lutar, a sonhar e a ser sempre o melhor que posso ser. Tive o maior apoio do mundo, pois estes tempos foram os mais complicados que alguém pode ter. Com isto tudo, sinto que cumpri com sucesso o que me foi proposto, e que aprendi muito com a minha experiência académica, profissional e pessoal para, que no futuro, consiga ser uma pessoa ainda melhor.

*“But you know, happiness can be found even in the darkest of times, if one only remembers to
turn on the light.”*

STATEMENT OF INTEGRITY

I hereby declare having conducted this academic work with integrity. I confirm that I have not used plagiarism or any form of undue use of information or falsification of results along the process leading to its elaboration.

I further declare that I have fully acknowledged the Code of Ethical Conduct of the University of Minho.

Resumo

A re-epitelização de feridas é um processo dinâmico que compreende a formação de um novo epitélio através de uma rede de sinalização ativa entre diversos fatores de crescimento e tipos celulares. Os principais intervenientes são os queratinócitos (KCs) que migram desde as margens das feridas de modo a restabelecer um epitélio contínuo para, por fim, restaurar a barreira da epiderme. Uma das moléculas mais importantes deste processo é o Fator de Crescimento de KCs (KGF), uma vez que é fundamental para promover a migração e a proliferação destas células. Células estromais, como os fibroblastos da derme, são os principais produtores deste fator, atuando nos KCs através de sinalização parácrina. Diversas estratégias para a entrega deste fator têm sido propostas para melhorar a cicatrização de feridas através da re-epitelização, tendo como objetivo a sua aplicação terapêutica.

Nesta tese foram explorados dois sistemas diferentes: partículas de *gellan gum* (GG) com KGF e *cell sheets* de células estaminais humanas do tecido adiposo (hASCs), como unidades produtoras de KGF. Na primeira abordagem, a otimização dos ensaios de libertação com uma molécula modelo mostraram que em partículas polidispersas foi encapsulada menos proteína, e que uma liofilização posterior permitiu que a libertação da molécula fosse significativamente maior. Após o encapsulamento do KGF nas condições previamente otimizadas, os perfis de libertação controlada foram diferentes, consoante o pH. Em contacto com KCs humanos (hKCs), as partículas foram internalizadas e demonstraram um efeito na proliferação e migração significativamente maior destas células. A neutralização do KGF reduziu a migração dos hKCs, confirmando o efeito estimulatório dependente de KGF. Na segunda estratégia, as hASCs mostraram ser produtoras de KGF em cultura, ao contrário dos hKCs sozinhos. Em co-culturas de hKCs com hASCs (*cell sheet* ou suspensão celular), foi também detetada a presença de KGF, assim como o efeito mitogénico/motogénico nos hKCs. Além disso, ao neutralizar o KGF *in vitro*, uma forte inibição na migração foi observada, confirmando que o efeito estimulatório direto do KGF na melhoria da migração dos hKCs.

Resumindo, os sistemas explorados baseados em KGF mostraram ter impacto na migração e na atividade mitogénica de hKCs, podendo ser explorados no tratamento de feridas em que re-epitelização é insuficiente.

Palavras Chave: Células Estaminais do Tecido Adiposo, Fator de Crescimento de Queratinócitos, Partículas, Pele, Re-epitelização.

Abstract

Wound re-epithelialization is a dynamic process that comprises the formation of new epithelium through an active signaling network between several growth factors and various cell types. The main players are keratinocytes (KCs) that migrate from the wound edges to reestablish a continuous epithelium to ultimately restore epidermal barrier. One of the most important molecules involved in this process is Keratinocyte Growth Factor (KGF) since it is central on promoting both migration and proliferation of KCs. Stromal cells, like dermal fibroblasts, are the main producers of this factor, acting on KCs through paracrine signaling. Multiple strategies to delivery KGF, envisioning therapeutic application, have been proposed to boost wound healing by targeting re-epithelialization.

In this thesis, two different systems were explored: gellan gum (GG) KGF-loaded particles and human adipose stem cells (hASCs) cell sheet constructs as foreseen units for controlled KGF production and consistent release. In the first one, the optimization of the release assays with a model molecule showed that in polydisperse particles less protein was entrapped, and the further lyophilization allowed a significantly higher release of the molecule. Moreover, after entrapment with the optimized conditions, KGF was released in a controlled way exhibiting different release profiles dependent on the pH used. The particles were internalized when in contact with human keratinocytes (hKCs) and lead to their significantly higher proliferation and migration. The neutralization of KGF reduced the migration, confirming the KGF-dependent stimulation effect on cellular migration. In the second strategy, hASCs were able to produce KGF in culture, in opposition hKCs alone. In co-cultures of hKCs with hASCs, in form of cell sheets and cell suspension, KGF was also present and a mitogenic/motogenic effect on hKCs was observed. Additionally, by neutralizing KGF *in vitro*, a strong inhibition on migration was revealed, confirming that the direct stimulatory effect of KGF on hKCs improved migration.

Taking all together, the explored KGF-based systems showed to impact hKCs migration and mitogenic activity, opening the opportunity to treat wounds with impaired re-epithelialization.

Keywords: Human Adipose Stem Cells, Keratinocyte Growth Factor, Particles, Re-epithelialization, Skin.

Table of Contents

Agradecimientos	iii
Resumo	vii
Abstract	viii
Table of Contents	ix
List of Abbreviations	xii
List of Figures	xv
List of Tables	xvi
List of Equations	xvi
1. CHAPTER I. General Introduction	2
1.1. Structural and Physiological Features of Epidermis	2
1.2. Wound Re-epithelialization Process.....	5
1.3. Challenges in the Re-epithelialization of Hard-to-Heal Wounds.....	8
1.4. Keratinocyte Growth Factor as Key Player on Re-epithelialization.....	9
1.5. Keratinocyte Growth Factor Delivery Strategies	10
1.5.1. Topical Application.....	11
1.5.2. Biomaterials-Based Systems	12
1.5.3. Gene Therapy.....	15
1.5.4. Cell Sheets of Adipose Stem Cells as Natural KGF Producers	18
1.5.4.1. Mesenchymal Stem Cells: Adipose Stem Cells.....	18
1.5.4.2. Cell Sheet Technology.....	21
1.5.5. Advantages and Disadvantages of the Presented Strategies.....	22
1.6. Purpose of the Work	25
1.7. References.....	26
2. CHAPTER II. Materials and Methods	41
2.1. Materials	41
2.1.1. Gellan Gum	41
2.1.2. Gellan Gum Particles.....	42
2.1.2.1. Protein loading/release strategies	44

2.1.2.1.1.	Non-Lyophilized Strategy	45
2.1.2.1.2.	Lyophilized Strategy	45
2.2.	<i>In vitro</i> Methodologies	46
2.2.1.	Cell Isolation from Human Tissues	46
2.2.1.1.	Human Adipose Stem Cells Isolation from Adipose Tissue.....	46
2.2.1.2.	Human Keratinocytes Isolation from Skin in Feeder Layer Culture System	47
2.2.1.2.1.	Subculture of Human Keratinocytes	48
2.2.2.	Cell Sheet Fabrication	49
2.2.3.	hKCs and hASCs Direct Contact.....	49
2.2.3.1.	hASCs-CS Based.....	50
2.2.3.2.	Cellular Suspension	50
2.2.4.	hKCs Contact with Gellan Gum Particles.....	50
2.2.4.1.	Internalization of GG Particles by hKCs	51
2.2.4.2.	Effect of GG Particles in hKCs Proliferation.....	51
2.2.5.	Migration Assay	52
2.3.	Methodologies for Particles Characterization and Analysis	53
2.3.1.	Dynamic Light Scattering (DLS) and Zeta Potential (ZP).....	53
2.3.2.	Scanning Transmission Electron Microscopy (STEM).....	53
2.3.3.	Transmission Electron Microscopy (TEM)	54
2.3.4.	Protein Quantification.....	54
2.3.5.	Enzyme-Linked Immunosorbent Assay (ELISA)	55
2.3.6.	Cell Proliferation Assessment.....	56
2.3.7.	Flow Cytometry.....	57
2.3.8.	Immunolabelling.....	58
2.3.8.1.	Immunocytochemistry.....	58
2.3.8.2.	Phalloidin Staining	59
2.3.9.	Quantification of Ki67 Positive Cells.....	59
2.3.10.	Wound Gap Closure <i>in vitro</i>	60
2.4.	Statistical Analysis	60
2.5.	References.....	62
3.	CHAPTER III. Results and Discussion	69
3.1.	Results	69
3.1.1.	Characterization of Gellan Gum Particles	69
3.1.2.	Protein Loading/Release Strategies.....	70

3.1.2.1. Bovine Serum Albumin as a Model Molecule.....	70
3.1.2.1.1. Size Effect.....	70
3.1.2.1.2. Lyophilization Effect.....	71
3.1.2.2. Keratinocyte Growth Factor as Molecule of Interest.....	72
3.1.2.2.1. Lyophilization Effect with pH Variation	72
3.1.3. Biological Assays	74
3.1.3.1. hKCs and Gellan Gum Particles Direct Contact.....	74
3.1.3.1.1. Particles Internalization	74
3.1.3.1.2. KGF and dsDNA Quantification	76
3.1.3.1.3. FGFR2 and Ki67 Expression Markers	77
3.1.3.1.4. Effect on Migration.....	78
3.1.3.2. hKCs and hASCs Direct Contact	80
3.1.3.2.1. Effect on Proliferation and KGF Release.....	80
3.1.3.2.2. FGFR2 and Ki67 Expression Markers	82
3.1.3.2.3. Effect on Migration.....	84
3.2. Discussion	87
3.3. References.....	90
4. CHAPTER IV. General Conclusions and Future Work	98

List of Abbreviations

#		DMEM	Dulbecco's Modified Eagle's Medium - High Glucose
α -MEM	Alpha Minimum Essential Medium	dsDNA	Double-Stranded Deoxyribonucleic Acid
A		E	
A/A	Ascorbic Acid	ECM	Extra Cellular Matrix
ab	Antibody	EDC	N-(3-Dimethylaminopropyl)-N'- Ethylcarbodiimide Hydrochloride
AB	Antibiotic/Antimycotic	EDTA	Ethylenediaminetetraacetic Acid
AOT	Aerosol-OT	EGF	Epidermal Growth Factor
APC	Allophycocyanin	ELP	Elastin-like Peptides
ASCs	Adipose Stem Cells	ELISA	Enzyme-Linked Immunosorbent Assay
B		ESCs	Embryonic Stem Cells
BCA	Bicinchoninic Acid	F	
Biotin-FITC	Biotin (5-Fluorescein) Conjugate	F12	Ham's Nutrient Mixture F12
BSA	Bovine Serum Albumin	Fb	Fibrin
BPE	Bovine Pituitary Extract	FBN	Fibrin Nanoparticles
C		FBS	Fetal Bovine Serum
CK	Cytokeratin	FDA	Food and Drug Administration
CM	Conditioned Medium	FIB-SEM	High-Resolution Field Emission Scanning Electron Microscope with Focused Ion Beam
CS	Cell Sheet	FGF	Fibroblast Growth Factor
CXCL-1	Neutrophil Recruiting Factor	FGF-7	Fibroblast Growth Factor-7
D		FGFR2	Fibroblast Growth Factor Receptor 2
DAPI	4,6-Diamidino-2-Phenyindole	receptor	
	Dilactate	FxCR	Fractional Carbon Dioxide Laser Resurfacing
DBFs	Dermal Fibroblasts		
DLS	Dynamic Light Scattering		

G		M	
g	G-Force	MAA	Methacrylic Acid
GFs	Growth Factors	MCP-1	Monocyte Chemoattractant Protein-1
GG	Gellan Gum	MES	2-N-Morpholino(ethanesulfonic Acid Hydrate) Buffer
GNPs	Gold Nanoparticles	Min	Minutes
H		MMA	Methyl Methacrylate
h	Hour	MMPs	Matrix Metalloproteinases
Has2	Hyaluronan Synthase 2	mRNA	Messenger RNA
hASCs	Human Adipose Stem Cells	MSCs	Mesenchymal Stem Cells
HEMA	Hydroxyethyl Methacrylate	N	
HFF	Human Foreskin Fibroblast	NaV	NeutrAvidin Protein
hKCs	Human Keratinocytes	NHS	N-Hydroxysulfosuccinimide Sodium Salt
I		P	
IL	Interleukin	P	Peptide
IPN	Interpenetrating Polymer Network	PA	Plasminogen Activator
iPSCs	Induced Pluripotent Stem Cells	PBS	Phosphate Buffered Saline
IR	Infrared	PDGF	Platelet-Derived Growth Factor
K		PDI	Polydispersity Index
kDA	Kilodalton	PE	Phycoerythrin
KCs	Keratinocytes	PEG	Poly(ethylene glycol)
KGF	Keratinocyte Growth Factor	Phalloidin	Phalloidin-Tetramethylrhodamine B Isothiocyanate
FITC	Flourescein Isothiocyanate	pl	Isoelectric Point
FSC	Forward Scatter	PLGA	Poly (Lactic-co-Glycolic Acid)
KSFM	Keratinocyte Serum Free Medium	PLLA	Poly (L-Lactic Acid)
		PSCs	Pluripotent Stem Cells
		PVA	Poly (Vinyl Alcohol)

		SVF	Stromal Vascular Fraction
		SEM	Scanning Electron Microscopy
R			
rEGF	Human Recombinant Epidermal Growth Factor	T	
RGD	Arginine-glycine-aspartic acid sequence	TE	Tissue Engineering
RNA	Ribonucleic Acid	TEM	Transmission Electron Microscopy
ROCK inhibitor	Y27632 dihydrochloride	TCPS	Tissue Culture Polystyrene
RT	Room Temperature	TNF- α	Tumor Necrosis Factor Alpha
		tPA	Tissue-Type Plasminogen Activator
		Tris	Tris(Hydroxymethyl)Aminomethane
S			
SB	<i>Stratum Basale</i>	U	
SC	<i>Stratum Corneum</i>	UV	Ultraviolet
SEM	Scanning Electron Microscopy	UP	Ultra Pure
SG	<i>Stratum Granulosum</i>	uPA	Urokinase-Type Plasminogen Activator
SL	<i>Stratum Lucidum</i>		
SS	<i>Stratum Spinosum</i>	V	
SSC	Side Scatter	VEGF	Vascular Endothelial Growth Factor
STEM	Scanning Transmission Electron Microscopy		
SUSP	Cell Suspension	Z	
		ZP	Zeta Potential

List of Figures

CHAPTER I – General Introduction

Figure 1.1 - Schematic representation of the human skin structure.	3
Figure 1.2 - Schematic overview of the structure of the human epidermis.	4
Figure 1.3 - Illustration of the re-epithelialization process.	7
Figure 1.4 - Schematic representation of the mechanism of action of KGF on keratinocytes.....	9

CHAPTER II. Materials and Methods

Figure 2.1 - Chemical structure of deacetylated gellan gum. Adapted from [4].....	41
Figure 2.2 - Schematic overview of GG particles fabrication protocol.	43
Figure 2.3 - Illustration depicting the differences between the termed Non-Lyophilized and Lyophilized strategies for protein release assays.....	45

CHAPTER III - Results and Discussion

Figure 3.1 - STEM micrograph of gellan gum particles.	70
Figure 3.2 - Quantification of the entrapment efficiency (%) and BSA released (%) in particles with different sizes and particles < 1 μm	70
Figure 3.3 - Quantification of entrapment efficiency (%) and BSA released (%) in BSA Lyophilized and BSA Non-Lyophilized conditions.	71
Figure 3.4 - Quantification of the entrapment efficiency (%) and KGF (%) released at different pHs ...	72
Figure 3.5 - KGF released ($\mu\text{g}/\text{mL}$) at different pHs.	73
Figure 3.6 - a) Fluorescence microscopy images of GG particles; Representative density dot plots of hKCs incubated with GG particles; Percentage of FITC expressing hKCs provided by flow cytometry...	74
Figure 3.7 - TEM micrographs of hKCs and gellan gum particles.....	75
Figure 3.8 - Quantification of KGF and dsDNA of hKCs in different conditions.....	76
Figure 3.9 - Representative immunocytochemistry images of the expression of FGFR2 and the expression of Ki67; Ratio of Ki67 positive cells (%).	77
Figure 3.10 - Representative microscopy images showing final gaps of migrating hKCs.....	79
Figure 3.11 - Migration assay conducted using different conditions with hKCs.	80

Figure 3.12 - Quantification of dsDNA, cellular ratio present in co-culture conditions by flow cytometry and KGF.....	81
Figure 3.13 - Representative immunocytochemistry images of the expression of FGFR2 and the expression of Ki67; Ratio of Ki67 positive cells (%).....	83
Figure 3.14 - Representative microscopy images showing final gaps of migrating hKCs.....	85
Figure 3.15 - Migration assay conducted using different conditions with hKCs.	86

List of Tables

CHAPTER I – General Introduction

Table 1.1 - Topical Application of KGF.	11
Table 1.2 - Biomaterials-based strategies for KGF release.	13
Table 1.3 - Gene therapy-based approaches for KGF delivery.	16
Table 1.4 - Adipose Stem Cells as natural source of KGF.	20
Table 1.5 - Advantages and disadvantages of the different strategies for KGF delivery.	22

CHAPTER II. Materials and Methods

Table 2.1 - Panels of antibodies for immunocytochemistry.	59
---	----

CHAPTER III - Results and Discussion

Table 3.1 - Dynamic light scattering parameters: size, polydispersity index and zeta potential.	69
---	----

List of Equations

CHAPTER II. Materials and Methods

<i>Entrapment Efficiency (%) - (Equation 2.1)</i>	55
<i>Protein Released (%) - (Equation 2.2)</i>	55
<i>Ki67 positive cells (%) - (Equation 2.3)</i>	60
<i>Wound Closure (%) - (Equation 2.4)</i>	60

CHAPTER I.

General Introduction

Background**Chapter based on:**

Bártolo I, Reis RL, Marques AP, Cerqueira MT, Keratinocyte Growth Factor-based Strategies for Wound Re-epithelialization, *Tissue Engineering, Part B: Reviews, 2021, accepted*

1.1. Structural and Physiological Features of Epidermis

The skin is the largest organ of the body, representing 10% of the total body mass and a surface area of 1.5-2 m² in adults [1,2]. The principal function of the skin is to protect the body from the external environment. It has also the ability of preventing the entrance of chemical, physical and biological agents and minimize the effects of ultraviolet (UV) radiations, since skin can absorb them, or infrared (IR) radiations as they dissipate the associated heat through the regulation of the blood flux or through sweat [3,4]. There are several barriers like cellular and molecular ones, including antimicrobial, immunological, cellular and enzymatic systems, preventing the entrance of viruses, bacteria, dust or allergens through the human skin unless these barriers are compromised [5,6]. Among the multiple and complex functions of the skin, it has other functions like mediation of sensation, thermoregulation, synthesis of vitamin D, excretion of water and salt, as well as storage of lipids and water [2,6].

The skin consists of three functional layers, epidermis, dermis and hypodermis, also known as subcutaneous tissue, associated with structures such as cutaneous appendages [1,7] (Figure 1.1).

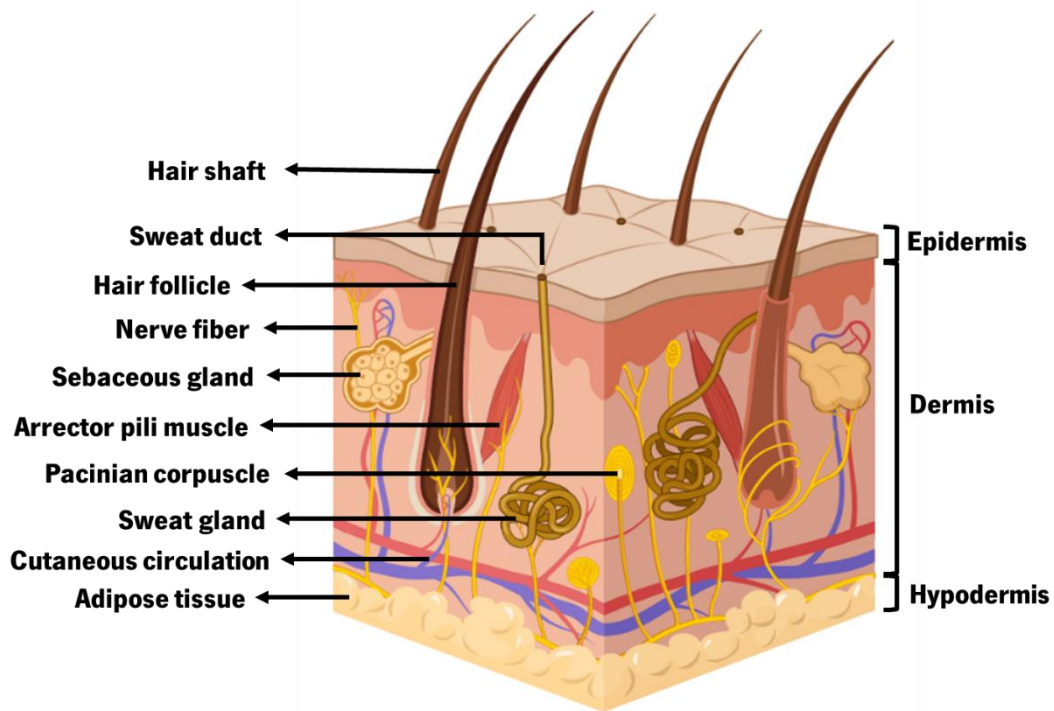


Figure 1.1 - Schematic representation of the human skin structure with the three main components: epidermis, dermis and hypodermis, as well as the associated appendages and blood vessels. This illustration was designed by using elements from BioRender.

The epidermis, being 50-100 μm thick, is organized in several stratified layers: *stratum basale*, *stratum spinosum*, *stratum granulosum*, *stratum lucidum* and *stratum corneum* [6] (Figure 1.2). These layers are mainly composed by KCs in different stages of differentiation, until reaching corneocyte stage in a protein-rich envelope with an outer lipid covering surrounded by an extracellular lipid matrix [2,6]. Besides KCs, which produce keratin and represent more than 90% of the cells in the epidermis, there are also other cell types present and differently distributed in the epidermis such as melanocytes, merkel and langerhans cells. Melanocytes produce pigment granules (melanosomes) containing melanin providing skin and hair pigmentation and protection from UV radiation, whereas, merkel cells play a central function as they work as sensory receptors of the nervous system [7]. Langerhans cells on their turn are antigen-presenting cells that play an important role in immunosurveillance, linked by complex membrane-associated plaques called desmosomes [2,5,7–9].

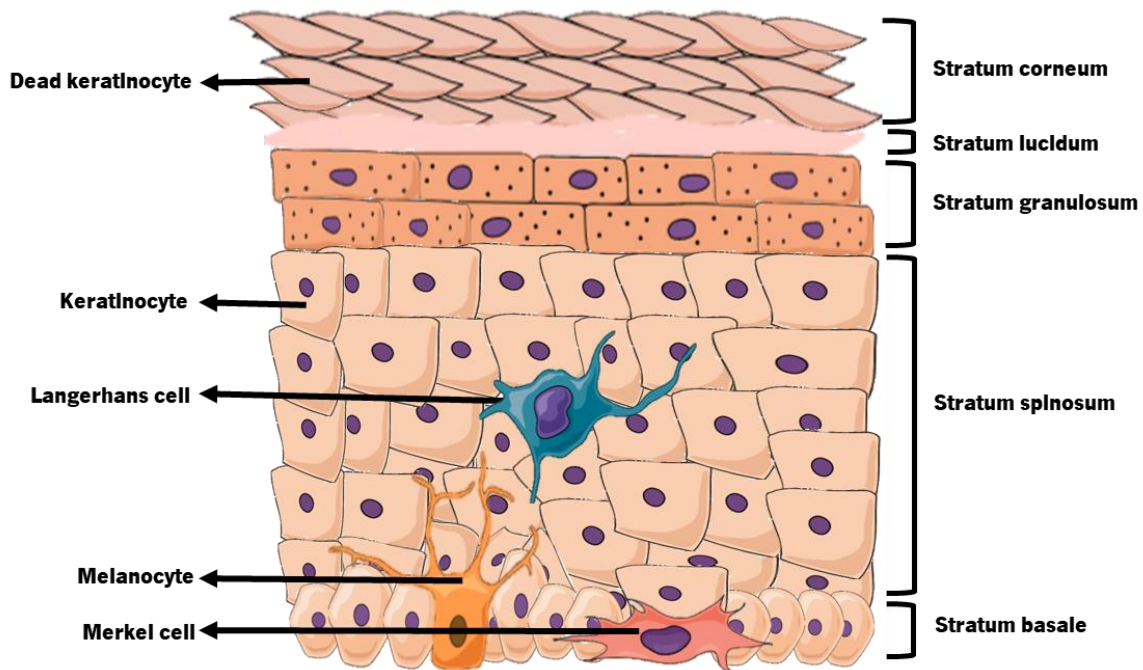


Figure 1.2 - Schematic overview of the structure of the human epidermis depicting its stratified structure with the correspondent layers: *stratum basale*, *stratum spinosum*, *stratum granulosum*, *stratum lucidum* and *stratum corneum*. The associated cell types that are also highlighted. This illustration was designed by using elements from BioRender.

Stratum Basale (SB) is composed by a single sheet of cells (keratinocytes, melanocytes and merkel cells), connected by hemidesmosomes to the underlying basement membrane [7,10]. This layer comprises highly mitotic cells that progressively lose this activity as they move upwards to the upper layers, being composed by gradually more differentiated cells [7]. *Stratum Spinosum (SS)* is organized by 5-10 cell layers of KCs with polyhedral shape and langerhans cells, connected to each other and to SB by desmosomes, where no mitotic activities are detected in KCs being in the beginning of the differentiation process [7,9]. Here, the outer layer of SS start to appear with intracellular membrane-coating granules in the cytosol making the transition between the stratum spinosum and stratum granulosum [9]. *Stratum Granulosum (SG)* is formed by 1-3 layers of cells with two types of granules, keratohyalin granules and lamellar bodies [10]. In the palms and soles, the skin tends to be thicker than in the rest of the body, presenting a clear layer (*Stratum Lucidum, SL*) with 2-3 layers of cells [7]. The last layer - *Stratum Corneum (SC)* - is constituted by 10-15 layers of cells, corneocytes, that are flat dead highly, keratinized cells [2,4,11]. The constitution of the SC creates a barrier for the diffusion of the water, preventing the dispersal of endogenous compounds out of the skin and the permeation of exogenous compounds into the skin [6,11].

The dermis is the largest skin compartment and, like epidermis, varies in thickness (2-3 mm) depending on body location [2,11]. It is responsible for most of the main functions of the skin, such as environmental perception, thermoregulation and immunological defense, as well as water storage and as cushioning against mechanical injuries [2]. Histologically, it is a layer that englobes a wide variety of cell types (like fibroblasts that are responsible for the production of the constituents of ground substance or mast cells, macrophages and Langerhans cells that promote immunity and protect against infection), nerves and blood and lymphatic vessels embedded in a connective tissue network and is separated from the epidermis by a basement membrane [2,6]. Its upper layer, the papillary dermis (100-200 μm thick) has thin bundles of collagen, elastin fibers, fibrocytes, water, electrolytes, plasma proteins and polypeptide complexes [2,11]. Below this layer is the reticular dermis, formed mainly by thick bundles of collagen and elastic fibers. Collagen is in greater quantity and forms 3D networks of fibers that are filled with extracellular matrix (ECM) which is responsible for the high degree of tensile strength of the dermis. Elastin is the second protein that is abundant in the dermis and, like collagen forms a large network and provides elastic properties to the skin [2].

Beneath the dermis lies the third layer, the hypodermis, formed by adipose tissue and areolar fibrous connective tissue, together with blood and lymphatic vessels, nerves and as an energy storage [2,11]. It is the hypodermis that connects the skin to deeper structures such as muscles and bones allowing the movement over them, it also grant thermal insulation and like dermis, providing protective cushion against mechanical trauma [2].

1.2. Wound Re-epithelialization Process

The epidermis exists in a state of equilibrium and forms a protective barrier against the external environment. Upon disruption of the stratum corneum (outmost layer), as in aged, diseased skin or after injuries/wounds, the barrier function is compromised [7,12].

Wounds can be classified following different criteria, as reviewed elsewhere [13–15]. Most of them, apart from e.g. chronic wounds, undergo through a classic and complex multi-step process of healing with interconnected stages that comprises hemostasis, inflammatory, proliferative and remodeling phases [7,16].

Re-epithelialization is initiated by KCs within hours after wounding and continues until full wound closure [17]. A fast restitution of the epidermis and its permeable barrier prevents excessive water lost

and reduces exposure to bacterial infection. This is important to decrease the morbidity and mortality of patients, particularly important when a considerable amount of skin is compromised [18].

Different models have been proposed to explain the migration of KCs over the wound bed: the leapfrog or rolling mechanism [19,20], the tractor-tread or sliding model [21,22], and another one that considers aspects of both theories [23]. According to the leapfrog or rolling mechanism, the migrating suprabasal cells roll over leading basal cells and dedifferentiate to form new leaders at the epidermal tongue that migrate as a cohesive sheet [19,20]. As for the tractor-tread or sliding model, it postulates that KCs from the basal layer move forward in an organized block, while the superficial cells above are passively pulled along [21,22]. The most recent one is a variant of the models above, in which suprabasal cells de-differentiate and participate, together with the basal cells, in the reconstitution of the new epithelium [23]. Although these models propose different mechanisms for wound closure, this is still a controversial topic.

The migrating behavior of KCs is highly dependent on a well-balanced interaction between other cell types and the ECM, occurring through signaling molecules such growth factors (GFs) [24]. Keratinocytes migrate from the wound edges to cover the exposed wound surface, producing Interleukin-1 (IL-1). This cytokine acts in a paracrine and autocrine way, influencing the early steps of migration, proliferation and the expression of an activation-specific set of genes of KCs [25,26]. The KCs-mediated release of IL-1 is the first alert of barrier damage to the surrounding cells, resulting in macrophages recruitment [25]. These cells stimulate dermal fibroblasts (DFBs) also with the IL-1 and Tumor Necrosis Factor Alpha (TNF- α), up-regulating KGF gene expression in DFBs [27]. In response, DFBs secrete KGF and Interleukin-6 (IL-6) inducing KCs to proliferate and migrate towards the wound center [28] (Figure 1.3). Due to the binding of the GFs to KCs, KCs change their phenotype, becoming flat and elongated, more prominent and form peripheral actin filaments as they go from a stationary basal state to a migrating one [29–31].

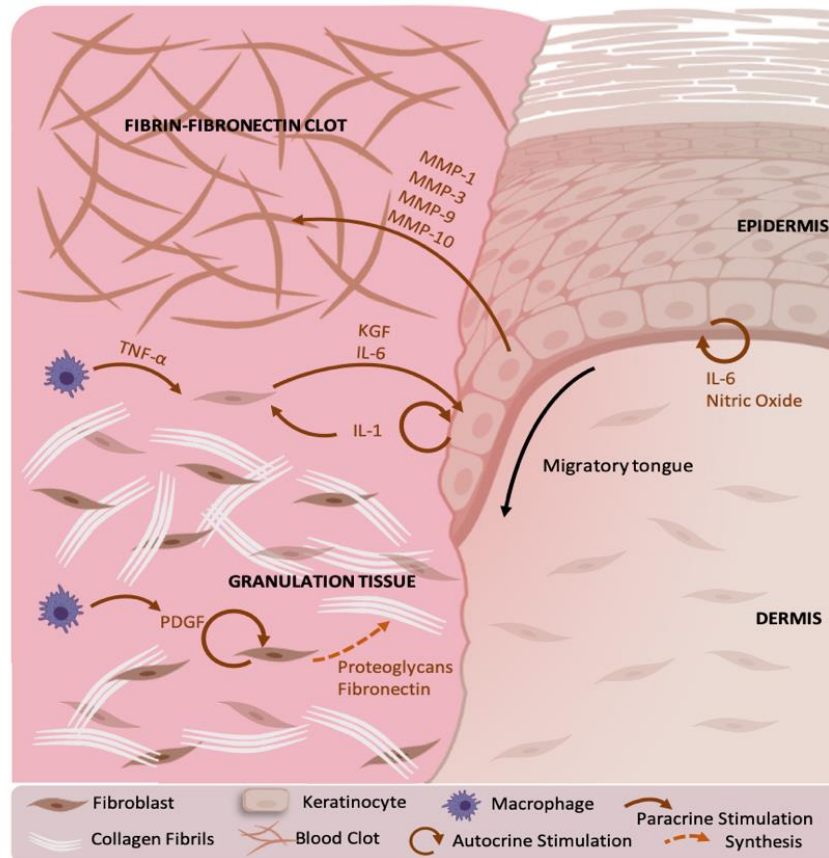


Figure 1.3 - Illustration of the re-epithelialization process, highlighting the main signaling molecules involved. Foremost cellular players at this phase such as keratinocytes, fibroblasts and macrophages are here depicted, as well as the action of the growth factors identified. This image was designed using Power Point by Microsoft.

Alongside, the formation of granulation tissue is of utmost importance for KCs migration. The formation of the provisional matrix is stimulated by Platelet-Derived Growth Factor (PDGF) upon autocrine release from KCs and paracrine production by macrophages that further act on DFBs to induce them to synthesize proteoglycans and fibronectin [16]. Dermal fibroblasts proliferate and synthesize collagen type I, and also increase fibronectin secretion that serves as a template for KCs adhesion [16,32]. Cellular receptors are disposed along the lateral sides of basal KCs and redistributed towards the basal membrane of wound KCs as they come in contact to the dermis. This creates a link between the fibrin-fibronectin clot in the wound space and the collagen-rich dermis [25,33].

In this way, KCs migration is accompanied by ECM degradation mainly through the action of plasmin, that is derived from plasminogen by tissue-type plasminogen activator (tPA) or urokinase-type plasminogen activator (uPA), both up-regulated in the migrating KCs [26]. Matrix metalloproteinases

(MMPs), which are also up-regulated in wound-edge KCs are also responsible for ECM degradation. MMP-1 (collagenase-1) cleaves collagen type I, while MMP-9 (gelatinase-B) cleaves type IV collagen of the basal lamina [26]. Non-collagenous proteins, like fibronectin, are also cleaved by MMPs, such MMP-3 (stromelysin-1) and MMP-10 (stromelysin-2), expressed by migrating KCs [18,26]. The proliferation and migration of KCs during all this process is also due to their ability to secrete IL-6 and nitric oxide (NO), which provides an additional positive stimulation to perpetuate the process until the injury site is covered [16] (Figure 1.3). Epidermal migration ceases once a monolayer of KCs is created and enters on proliferative mode. Further on, neoformed epithelium begins to mature in order to restore the barrier function [26,31].

1.3. Challenges in the Re-epithelialization of Hard-to-Heal Wounds

An impaired re-epithelialization is observed in several pathological wound scenarios that often lead to chronicity, such as diabetes, burns or other highly traumatic wounds. Chronic wounds, despite having different causes, present a set of common characteristics. They often have high incidence of bacterial biofilms, creating a continuous state of inflammation, and excessive proteolysis that causes extreme degradation of critical growth factors, receptors and/or ECM [34,35]. This highly destructive environment not only prevents wound closure, inhibits migration of DFBs and synthesis of granulation tissue, but also attracts more inflammatory cells, leading to an unresolved inflammatory loop. In this adverse scenario, KCs are highly dysfunctional, and despite being greatly proliferative as a result of c-myc activation and overexpression [36], they are unable to migrate efficiently due to the damaged structural elements of ECM and uncontrolled signaling cascades of a high inflammatory state. This frequently results in parakeratosis and hyperkeratosis, as proliferative KCs accumulate throughout suprabasal layers undergoing abnormal differentiation [37]. Their reduced migration is attributed to the dysfunctional ECM with elevated MMPs activity that degrades fibronectin and tenascin-C and reduce levels of laminin 332, which is a crucial substrate for KC migration. All of this together results in compromised re-epithelialization and consequently healing failure in the most hard-to-heal wounds [38,39]. An overview of therapeutic approaches to treat these wounds have been recently reviewed elsewhere and will not be explored here as they go beyond this review topic [25].

1.4. Keratinocyte Growth Factor as Key Player on Re-epithelialization

The Fibroblast Growth Factor (FGF) family, to which KGF belongs to, is one of the eight families that has a special role in wound healing [15]. FGF family comprises 23 members (22 of them identified in humans), characterized by a central core of 140 amino acids showing high homology among all family members and high affinity for heparin and heparin-like glycosaminoglycans [40]. FGF stimulate the migration and proliferation of endothelial cells critical for angiogenesis and are produced by inflammatory cells, vascular endothelial cells, fibroblasts and keratinocytes [41,42]. In particular, Fibroblast Growth Factor-7 (FGF-7) or KGF is produced by various types of mesenchymal cells but not by epithelial cells, acting as an epithelium-specific growth factor mediator [43,44].

In skin wounds in specific, KGF stimulates KCs to migrate and proliferate, promoting skin re-epithelialization [27]. After wounding, DFBs start to produce KGF that is going to bind to KCs membrane, more specifically on FGFR2 receptor (FGFR2-IIIb), a tyrosine kinase receptor [45] (Figure 1.4).

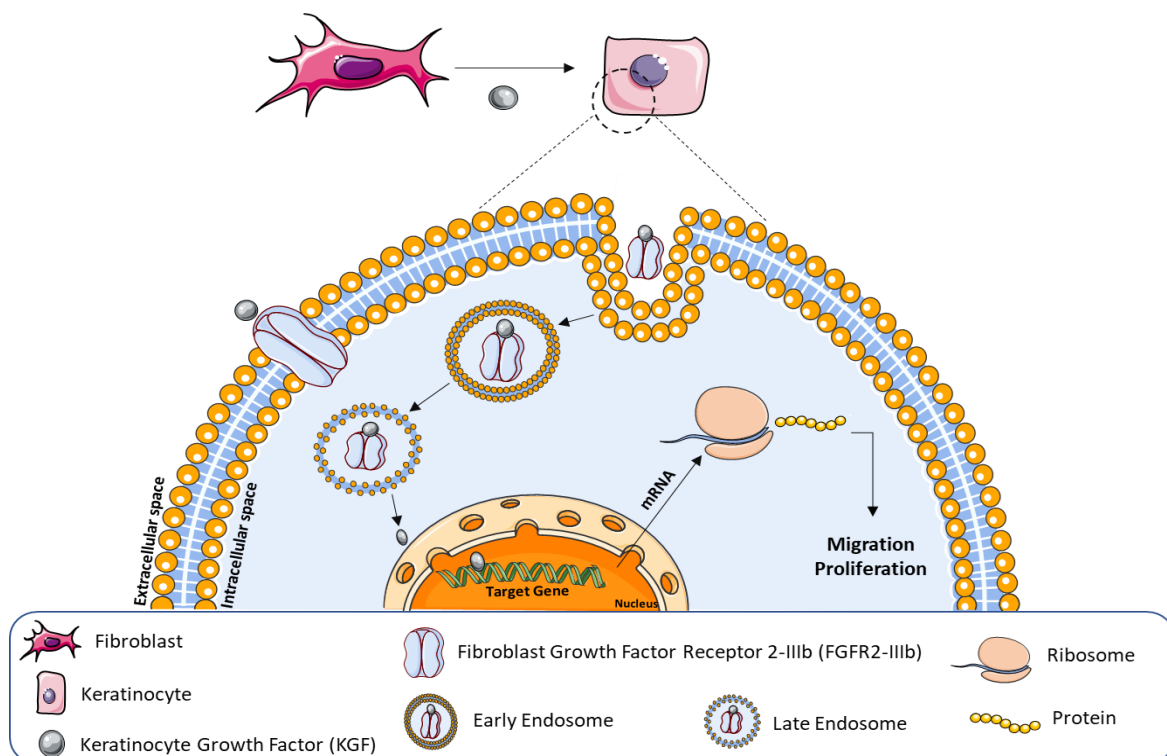


Figure 1.4 - Schematic representation of the mechanism of action of KGF on keratinocytes. KGF is released by fibroblasts and actuates on keratinocytes through binding to the receptor FGFR2-IIIb. This, through a cascade of events and upregulation of targeted genes in the nucleus, the migration and proliferation of keratinocytes is promoted, which is crucial for the re-epithelialization process in the cutaneous wound healing context. This illustration was designed by using elements from Servier Medical Art.

This receptor is expressed in KCs throughout the stratum basale and in the hair follicles but not in DFBs, suggesting once more its role as a paracrine mediator of mesenchymal-epithelial interactions [46,47]. In general, the binding of this GF to the receptor leads to the transduction into secondary signals and activation of pathways that control various features of subcellular biology and cellular function. In details, the binding between KGF and its receptor induces a tyrosine phosphorylation in the receptor that leads to the clustering of the ligand-receptor complex in clathrin-coated pits that are endocytosed [48,49]. The complex passes through an early and late endocytic pathway to perinuclear structures, with subsequent transportation to the lysosomal degradative compartment [50]. The receptors are still active in the late endosome due to the slow kinetics of degradation, where the receptor is ubiquitinated by KGF, leading to a degradative pathway of the receptor [50]. At the nucleus KGF induces the salvage pathway and the expression of some enzymes important for *de novo* synthesis, meaning that it is able to stimulate the synthesis of the enzymes involved in nucleotide biosynthesis during wound healing. This should allow the production of sufficient amount of nucleotides necessary for deoxyribonucleic acid (DNA) replication, ribonucleic acid (RNA) synthesis and, consequently in KCs proliferation [43]. In addition to proliferation, it has been shown that KGF promotes KCs migration. In part it could be mediated via metalloproteinase stromelysin-2, that modulates KCs motility by degradation of proteins involved in cell–cell and cell–matrix adhesion, allowing the re-epithelialization to occur [51].


1.5. Keratinocyte Growth Factor Delivery Strategies

The success of GF-based therapeutic approaches for wound healing is often hampered by issues such as instability, safety, efficacy and high-costs [52]. When in the form of recombinant proteins, GFs have low stability in physiological environment, short half-life, rapid diffusion/degradation which results in a low effective dose *in vivo*. Environmental factors like temperature, pH, ionic strength, hydrolysis or oxidation are known to affect their shelf life [53]. Thus, GFs have to be repeatedly injected at a supraphysiological dose, so the concentration in the wound sites is maintained [54,55]. In turn, uncontrolled *in situ* concentrations are also associated to serious side effects that have raised safety concerns. Therefore, more sophisticated delivery systems that allow precise, controlled and localized release, and yet ensuring safety, clinical efficiency and convenience of handling [4], are required to improve GF-based strategies and to fully promote their therapeutical potential [52].

1.5.1. Topical Application

Topical application of KGF has been tested not only to address its impact in cutaneous re-epithelialization [56–58] (Table 1.1), but also on other types of epithelia like, tracheal, tympanic membrane and cornea [59–61].

Table 1.1 - Topical Application of KGF.

 TOPICAL APPLICATION			
SYSTEM	MODEL	OUTCOME	REF
KGF Solution	<i>In vitro</i> , hKCs	Stimulation of hKCs migration; Increased levels of plasminogen activator	56
	<i>In vitro</i> , REK cell line (newborn KCs, rat)	Enhanced cell migration; Accumulation of intermediate size hyaluronan; Increased hyaluronan synthase 2	58
	<i>In vitro</i> , organotypic model with REK cell line (newborn KCs, rat)	Up-regulation of hyaluronan synthase 2/3 and CD44 in the spinous cell layer; Inhibited expression of keratin 10	
	<i>In vivo</i> , partial-thickness wounds in pigs	Higher rate of re-epithelialization; Thicker epidermis	57
	<i>In vivo</i> , full-thickness wounds in pigs	Thicker epidermis, deep rete ridges; Better developed hemidesmosomes in basal KCs	

In skin, the potential effect of KGF was assessed *in vitro* by measuring randomized migration and plasminogen activator (PA) activity of hKCs in response to the growth factor. The authors showed that the stimulation of hKCs migration by KGF was dose dependent. The treatment of 1 nM of KGF, showed to increase cell numbers, as well as the PA activity, which is known to be correlated with boosted KCs proliferation and migration [56]. In line with these observations, KGF (0.1–100 ng/ml final concentrations) applied to REK cell line monocultures (rat newborn KCs) enhanced KCs migration.


Alongside, an increased hyaluronan synthesis through hyaluronan synthase 2 (Has2) was observed, suggesting that hyaluronan plays an essential role in the KGF-stimulated motility of KCs. KGF (2 and 20 ng/mL with re-application)-treated stratified organotypic cultures of the same cell line showed accumulation of hyaluronan in stratum spinosum and a delay on KCs terminal differentiation [58]. Further data in a porcine model revealed that topically applied KGF promotes re-epithelialization of both partial and full-thickness excisional wounds [57]. In partial wounds, the application of 200 µg/mL of KGF stimulated the re-epithelialization rate, which was associated with epidermal thickening, when compared to control wounds [57]. On the other side, thicker epidermis with deep rete-ridges, better development of tonofilaments and hemidesmosomes in basal KCs with no delay on their differentiation was observed in the majority of KGF-treated full-thickness wounds (200 µg/mL in a re-application regimen) [57].

1.5.2. Biomaterials-Based Systems

The use of biomaterials, as delivery systems, are important tools for the administration of GFs in order to enable a controlled spatial-temporal delivery [55,62]. These biomaterials can be processed differently into hydrogels, different size-ranged particles, membranes or scaffolds, depending on the strategy and the purpose of the study [62].

The effect of different types of hydrogels loaded with KGF has been studied either *in vitro* and/or *in vivo* on full-thickness wounds (Table 1.2).

Table 1.2 - Biomaterials-based strategies for KGF release.

				
	SYSTEM	MODEL	OUTCOME	REF
(HYDRO)GELS	Aloe Vera-derived hydrogels with bonded KGF	<i>In vitro</i> , Balb/MK cell line (KCs, mouse)	KGF successfully stabilized; No effect on cell proliferation	63
	Gelatin hydrogel modified with PEGylated RGD and soluble KGF-1 (RGD-IPN+KGF)	<i>In vivo</i> , full-thickness wounds on rats	No significant differences in the rate of wound contraction; Prevented the entry of foreign bodies	64
	Fibrin gels with KGF conjugated to a peptide for covalent binding	<i>In vitro</i> , 4MBr-5 cell line (bronchial lung epithelial cells, Rhesus monkey)	Faster closure in wound healing assay <i>in vitro</i>	65
		<i>In vivo</i> , full-thickness excisional wounds on athymic mice	Enhanced re-epithelialization; Improved granulation tissue	
	HEMA-based hydrogels bonded with KGF	-----	No <i>in vitro</i> or <i>in vivo</i> assays were performed	66
	Skin micro autografts in a KGF-loaded gel	Randomized Clinical Trial, skin ulcers of 30 participants	Status unknown; No published results	76
PARTICLES	Gold nanoparticles with crosslinked KGF	<i>In vitro</i> , HaCaT cell line (KCs, human)	Biocompatible system; Improved cellular proliferation	68
		<i>In vivo</i> , full-thickness wounds on rat	Enhanced re-epithelialization	
	Fibrin nanoparticles covalently coupled with KGF	<i>In vitro</i> , primary hDFBs	Enhanced cell migration	69
		<i>In vivo</i> , full-thickness excisional wounds on mice	Thicker epidermal layers; Improved healing	
	Self-assembled nanoparticles of KGF-ELP fusion protein	<i>In vitro</i> , hKCs and hDFBs	Increased proliferation of hKCs, but not hDFBs	70
		<i>In vivo</i> , full-thickness excisional wounds on diabetic mice	Enhanced re-epithelialization and granulation	
MEMBRANES	Collagen membranes with immobilized KGF and bFGF	<i>In vitro</i> , HaCaT cell line (KCs, human) and primary hDFBs	Enhanced cell proliferation and faster migration	72
		<i>Ex vivo</i> , rat skin for explant migration assay	KGF loaded membrane enhanced cell migration	
		<i>In vivo</i> , full-thickness excisional wounds on rats	Higher epidermal thickness; Organized dermal-epidermal structures, Mature appendages in dual factor (KGF and bFGF) application	
	PLGA/Aerosol-OT and PLLA/Aerosol-OT membrane with incorporated KGF	<i>In vitro</i> , HaCaT cell line (KCs, human)	Both polymer matrices, when formulated with AOT, sustained cell growth	73
	Hybrid chitosan-silica dressing with adsorbed KGF	<i>In vitro</i> , primary hKCs	Higher proliferation of hKCs and attachment of hybrid dressing than single chitosan	74
		<i>In vivo</i> , full-thickness on athymic mice	Accelerated wound closure; Thicker epidermis	
Silk membranes functionalized with KGF (and other growth factors)	<i>In vitro</i> , wounded organotypic models	Higher KCs migration and stratification	75	

Legend: IPN - interpenetrating polymer network, PEG - poly(ethylene glycol), RGD - tripeptide Arg-Gly-Asp, HEMA - Hydroxyethyl)methacrylate, ELP - sequence motif derived from the hydrophobic domain of tropoelastin, PLGA - Poly-lactic-co-glycolic acid.

Aloe Vera-derived hydrogels were proposed as approaches to stabilize KGF (5 µg/mL) against the degradative environment of the wound and to promote KCs proliferation [63]. Although no effect on cell proliferation was observed, these hydrogels were non-cytotoxic to mouse KC line Balb/MK and KGF was successfully bonded to the hydrogels [63]. In another work, a hydrogel of gelatin modified with PEGylated RGD and 3.3 ng/mL of soluble KGF (RGD+IPN+KGF), also did not reveal a significant alteration in the closure rate of rat full-thickness wounds. Yet, those structures acted as scaffolds for the deposition and organization of the dermal ECM [64]. The targeting of large full-thickness and chronic wounds has been also attempted. Fibrin gels with KGF conjugated to a peptide (Fb-P-KGF) for covalent binding significantly increased the closure rate and enhanced re-epithelialization of full-thickness wounds. This effect was promoted by KGF (150 ng) that was released after the degradation of the fibrin by the cells present in the wound [65]. Interestingly, Sen-Britain *et al.*, [66] questioned whether the interaction of the KGF with hydrogels altered native protein conformation and release, which can compromise its interaction with the receptor and therefore its biological activity. In fact, (hydroxyethyl)methacrylate (HEMA)-based hydrogels with methyl methacrylate (MMA) depicted the KGF at a more native-like orientation than those with methacrylic acid (MAA). Despite this, release profiles were undistinguishable supporting the urging for downstream studies to validate their (lack of) activity in terms of wound re-epithelialization.

Particle-based systems have been also proposed for the delivery of KGF with the rationale of allowing sustained and long-term administration of KGF (Table 2) [62,67]. Keratinocyte growth factor (5 ng/mL) linked to 60 nm diameter gold nanoparticles (KGF-GNPs) were shown to directly target KCs by coupling to the receptor in their cell membrane [68]. Importantly, KGF-GNPs promoted KCs proliferation at a significantly higher level than soluble KGF (5 ng/mL). When applied to rat full-thickness wounds, KGF-GNPs lead to a higher re-epithelialization than GNPs or KGF (5 ng/mL) alone [68]. In a different work, fibrin nanoparticles coupled with KGF (FBN-KGF) (10 pmol) enhanced cell migration *in vitro* greater than FBN alone or the same dosage of soluble KGF. Moreover, in a mice full-thickness wound model, FBN-KGF particles treatment lead to a thicker epidermis and an overall improved healing, compared with all the control conditions [69]. Others showed that self-assembled nanoparticles of elastin-like peptides (ELP) conjugated with KGF (50 ng/mL) increased proliferation of hKCs, but not hDFBs. Furthermore, KGF-ELP nanoparticles incorporated in a fibrin hydrogel avoided wound drying and boosted the re-epithelialization of full-thickness excisional wounds in diabetic mice, opposing KGF application alone, where no differences to the control were observed [70].

Membranes have been extensively used for wound dressings and to incorporate GFs in order to maximize their assimilation [71]. Collagen membranes have been considered due to their analog character of ECM, providing a natural substrate for cellular attachment and proliferation. In accordance, membranes of collagen with tethered KGF provided a favorable *in vitro* environment for initial hKCs and hDFBs adhesion and proliferation. This effect was further confirmed in an *ex vivo* wounded rat skin, in which, KGF-loaded collagen membranes (10 ng/cm²) presented an enhanced migration. Moreover, treatment of rat wounds with KGF-loaded membranes (10 ng/cm²) lead to a thicker neoformed epidermis and vascular networks. Moreover, an organized dermal-epidermal and mature appendages were also observed in dual loading of bFGF (10 µg/cm²) and KGF (10 ng/cm²) onto a collagen scaffold [72]. Using the same dosage, PLGA and poly (L-lactic acid) (PLLA) polymers membranes formulated with Aerosol-OT (AOT) and 10 ng/mL of KGF showed different profiles of GF release depending on the formulation. PLGA/AOT/KGF membrane exhibited faster release rate of KGF when comparing to PLLA/AOT/KGF, but no further data on the effect on epithelial cells is provided than proliferation [73]. The outcomes of chitosan-silica membranes containing up to 100 µg of KGF. A higher proliferation of hKCs and increased attachment was observed *in vitro* in the hybrid dressing in relation to the chitosan alone. Mice full-thickness wounds treat with these membranes showed an overall accelerated wound closure along with a thicker epidermis, in comparison to the controls (chitosan membrane with KGF and hybrid membrane only) [74]. In the same line, silk membranes functionalized with KGF (and several other GFs) supported macrophage secretion of neutrophil recruiting factor (CXCL-1) and monocyte chemoattractant protein 1 (MCP-1) without production of pro-inflammatory cytokines. Moreover, KGF-loaded and Vascular Endothelial Growth Factor (VEGF)-loaded silk membranes applied to a wound organotypic model promoted the highest KCs migration and stratification, when compared with other GFs-loaded membranes [75].


Despite all the pre-clinical work presented above, there is just one ongoing registered translational work. It was setup as a randomized clinical trial was established to treat skin ulcers either using skin micro grafts with a solution of KGF or by a standard treatment comprising skin grafts. Nonetheless no results have been published so far, and the status of the trial is currently unknown [76].

1.5.3. Gene Therapy

The use of viral or non-viral vectors to introduce into DFBS and KCs genetic material encoding for the protein of interest into DFBS and KCs (Table 1.3) is another relevant strategy for KGF delivery [77].

This technique has been explored either by applying the modified gene into the host tissue (*in vivo*) [78–82], or by cellular transfection with further cell delivery to the host skin (*ex vivo*) [82–84].

Table 1.3 - Gene therapy-based approaches for KGF delivery.

 GENE THERAPY			
APPLICATION METHOD/SYSTEM	MODEL	OUTCOME	REF
Injection non-viral liposomal complex at wound edge (KGF cDNA construct)	<i>In vivo</i> , scald burns on rats	Dermal and epidermal regeneration improved; Increased synthesis of collagen IV	78, 79
Naked DNA injection with intradermal electroporation (KGF-1 plasmid)	<i>In vivo</i> , full-thickness excisional wounds on diabetic mice	Wound healing rate enhanced; Intact and mature epithelium	85
Topical application after microdermabrasion (KGF-1 plasmid)	<i>In vivo</i> , microdermabrasion in mice skin	Increased skin strength – improved ductility, toughness and tensile strength	81
Different Virus-mediated gene transfer approaches (KGF adenoviral injection; fibrin matrix: adenoviral immobilization or transfected fibroblasts)	<i>In vivo</i> , skin-humanized model in athymic mice	Faster re-epithelialization in all delivery systems; Higher reproducibility in genetically modified fibroblast-containing matrix with overall wound healing enhancement	82
Bioengineered skin (KGF-transformed keratinocytes incorporated in acellular dermis)	<i>In vivo</i> , full-thickness wounds on athymic mice	Thicker and hyperproliferative epidermis	83
Biomembrane containing keratinocytes (KGF-transfected HaCaT)	<i>In vivo</i> , superficial 2 nd -degree burns burn in pigs	Faster re-epithelialization	84
In vitro-transcribed (IVT) modified KGF-encoded mRNA (KGF-mRNA transfected HaCaT)	<i>In vitro</i> , HaCaT cell line (KCs, human)	High KGF protein release (transient); Faster migration in wound healing assay	86

Administration of KGF as liposomal cDNA was one of non-viral strategies explored. The non-viral liposomal complex (KGF cDNA 2.2 µg) was weekly injected (during 4 weeks) in the wound edge of scalded burns in rats leading to a successful transfection and subsequent KGF expression in DFBs, macrophages and KCs [78]. Epidermal regeneration was improved by 170% in rats receiving the KGF cDNA constructs and dermal remodeling was further enhanced in these animals by an increased collagen deposition, when

compared with vehicle administration only. A subsequent study conducted by some of the authors showed that KGF administered as a liposomal cDNA in a similar setup, also impacted the level of several GFs leading to dermal regeneration, and increased neovascularization [79]. Both studies [78,79] indicate that delivering KGF as a non-viral liposomal cDNA gene complex effectively enhanced dermal and epidermal regeneration. In another non-viral transfection-based study KGF was delivered into full-thickness excisional mice diabetic wounds via naked DNA injection with subsequent intradermal electroporation [85]. This technique was applied in order to improve the transfection efficiency so that a single dosing regimen could be utilized, and a much smaller application of DNA would be required. With just a single injection of KGF DNA plasmid, KGF expression was detected and over 90% of wounds healed in the presence of KGF versus 40% in the untreated group. Histological analysis demonstrated an intact and mature epithelium, compared with untreated wounds that displayed an incomplete epithelium with unresolved inflammation. In another approach, based on the application of needle free vector application after microdermabrasion, authors also aimed to improve the transfection efficiency of topically delivered DNA plasmid [81]. This technique has been used to increase skin permeability for drug delivery by overcoming the obstacle of protective skin without damaging the structural integrity or skin components. Multiple topical applications of KGF-1 plasmid following microdermabrasion of mice skin resulted in increased levels of KGF-1 messenger RNA (mRNA) and protein, primarily localized in the epidermis and hair follicles. This procedure ultimately significantly improved three biodynamic parameters of skin strength. However, the correlation of this outcome with transfected cells could not be established.

A virus-mediated KGF delivery comparative study was conducted to assess the efficacy of different gene transfer approaches in a skin-humanized model in athymic mice [82]. Three distinct delivery strategies for KGF gene were investigated: intradermal adenoviral injection, adenoviral vector immobilized in a fibrin carrier, and KGF-adenoviral gene-transferred hDFBs embedded in a fibrin matrix. An overproduction of KGF protein was detected in all the delivery systems along with re-epithelialization enhancement. Despite the enhancement in all the conditions, direct gene delivery strategies exhibited variability in transfection efficacy. While genetically modified hDFBs in a fibrin carrier appeared to be the most reliable, avoiding also the direct exposure to viral vectors.

Bioengineered skin substitutes were created with normal hKCs (control) or hKCs transfected with recombinant retrovirus encoding KGF. Bioengineered Skin with Gene-Modified hKCs secreted significant higher levels of KGF and accelerated wound closure *in vitro*, in relation to the control. After transplantation on mice full-thickness wounds, modified substitutes formed a thicker and hyperproliferative epidermis

that self-heals more rapidly than the control condition. Moreover, this strategy appeared also to affect vascularization, as athymic mice transplanted with this bioengineered skin displayed an enhanced revascularization via secretion of VEGF, which was overexpressed [83].

Aiming to address the best KGF-transfected cell type to better stimulate KCs metabolism, both immortalized hKCs (HaCaT cell line) and hDFBs (KMST-6 cell line) were lipofected with KGF-1 plasmid [84]. Keratinocyte growth factor-expressing clones were selected using an air–liquid interface test system and interestingly HaCaT cells displayed stronger transgene expression compared to transfected fibroblasts. Whether it was related to the transfection efficacy or to the autocrine signaling on hKCs being more effective than paracrine via hDFBs it was not unraveled. The most effective HaCaT clone was then incubated on a membrane carrier and applied to superficial second degree burns in pigs. Wounds treated with the membrane containing transfected HaCaT cells significantly diminished the required period to achieve a complete re-epithelialization, when compared with wounds covered with untransfected cells. In untreated sites, the double amount of time was required until a thin epithelium was detected [84].

The future of gene therapy for wound healing will require consistent and safe delivery methods. To circumvent associated safety issues, an *in vitro*-transcribed modified KGF mRNA strategy, was investigated. This approach relies on using a transient effect rather than interfering with the DNA of the nucleus [86]. KGF-mRNA transfected HaCaTs cell line and human foreskin fibroblast (HFF) exhibited a high KGF protein release that was sufficient to significantly improve re-epithelialization in the performed scratch assays. Although being good indicators, no further *in vivo* studies have been performed and therefore it is still premature to extrapolate conclusions at the wound site.

1.5.4. Cell Sheets of Adipose Stem Cells as Natural KGF Producers

1.5.4.1. Mesenchymal Stem Cells: Adipose Stem Cells



Stem cells are cells with the unique ability of self-renewal and differentiation capability, existing in both embryos and adult cells [87]. They can be divided according to their differentiation capacity that is intimately linked with the state of development. Totipotent stem cells, like zygote, are able to divide and differentiate into cells to form an entire organism. Pluripotent stem cells (PSCs) are capable of forming tissues from all embryonic germ layers, except placenta [87,88]. Embryonic stem cells (ESCs) located in human blastocysts and induced pluripotent stem cells (iPSCs) are examples of pluripotent cells, where the latter are artificially generated from somatic cells [87,89]. Multipotent stem cells have a reduced potency comparing to PSCs as they can only specialize in some cells of a more restricted subset of cell

lineages. One example is hematopoietic stem cells, which can give rise to several types of blood cells, becoming oligopotent stem cells [87,88]. These cells can differentiate into several cell types, like myeloid stem cells that divides into white blood cells but not into red blood cells. Unipotent cells are known to have the narrowest differentiation capabilities and the ability to divide repeatedly, being capable of only forming one cell type, e.g. dermatocytes [87].

Adult stem cells are undifferentiated cells that reside among differentiated cells in a tissue or organ and have the proficiency to renew themselves and differentiate into specialized cell types, being multipotent or unipotent stem cells [89]. One of the functions of these cells is to promote tissue regeneration like in wound healing, to release of GFs and to modulate immune responses [90–92]. Mesenchymal stem cells (MSCs), originally isolated and characterized from mouse bone marrow by Friedenstein *et al.* [93], are adult multipotent cell population capable of differentiating into mesodermal cell lineages such adipocyte, muscle, tendon, osteocyte and chondrocyte [34,89]. Although there are many sources of MSCs, the amount of tissue that can be retrieved is limited and a few cells can be harvested [94]. Adipose-derived stem cells (ASCs), have become one of the most promising stem cells populations identified so far since they are abundant and can be easily harvested in larger quantities with less donor-site morbidity [94–96]. Human adipose stem cells can secrete numerous GFs and cytokines (CKs), including KGF, that are critical for wound healing, where enhanced tissue granulation, macrophage recruitment and improved vascularization have been also reported, helping improving wound healing [92,97,98].

Taking in account the numerous advantages that hASCs provide to wound re-epithelialization, this strategy has been widely explored in different works, including as a natural source of KGF. Under this scope, different *in vitro* and *in vivo* with the involvement of KGF have been carried out and are summarized in Table 1.4.

Table 1.4 - Adipose Stem Cells as natural source of KGF.

 ADIPOSE STEM CELLS 			
APPLICATION METHOD/SYSTEM	MODEL	OUTCOME	REF
hASCs- Conditioned Medium	<i>In vitro</i> , primary KCs and HaCaT cell line	Migration and proliferation significantly enhanced; MMP-2 and MMP-9 induced; KGF mRNA expression and protein significantly higher; Ki67 expression increased	99
hASCs in collagen type I matrix	<i>In vitro</i> , organotypic culture model	Expression of several cytokines; Significantly reduced expression of Ki67 upon exposure to neutralizing antibody against KGF	
hASCs embedded in collagen type I matrix	<i>In vivo</i> , full-thickness on immunodeficient mice	Promoted re-epithelialization; More effective wound closure; Less inflammation	
hASCs- Conditioned Medium	<i>In vivo</i> , cutaneous wound on human skin	Presence of KGF in CM; Less erythema and hyperpigmentation; Reduced transient adverse effects; Increased levels of transepidermal water loss	100
hASCs- CS	<i>In vivo</i> , excisional wounds on mice with delayed healing	Full re-epithelialization of wounds; Formation of appendages in the neoformed matrix; Up-regulation of KGF	97
	<i>In vivo</i> , diabetic wounds on Zucker Diabetic Fatty Rat	Secretion of several cytokines, namely KGF; Significantly accelerated healing; Increased blood vessel density and dermal thickness	114

Conditioned medium (CM) of hASCs showed to significantly enhance migration and proliferation of KCs, together with increased levels of KGF mRNA and protein expression, when compared both to control and with CM from hDFb. To prove KGF involvement, KCs were exposure to the CM in the presence of a neutralizing antibody against KGF, and delay in cellular proliferation and a decreased expression of Ki67 was observed in those conditions. Further on, hASCs as potential cells to replace hDFbs, incorporated in the collagen type I matrix showed to sustain proliferative epidermis. However, when in the presence of the neutralizing antibody against KGF the expression of Ki67 decreased, as well as expression of other cytokeratins. These observations support the inductive effect of hASCs on KCs proliferation through secretion of KGF. Moreover, when applied to mice full-thickness wounds these

constructs promoted an enhanced re-epithelialization and more effective wound closure, when hASCs were present [99]. To evaluate the effectiveness and benefits of CM of hASCs on wound healing after fractional carbon dioxide laser resurfacing (FxCr) on human skin, CM was topically applied on FxCr-treated sites for one hour [100]. Herein the presence of KGF was found in CM of hASCs, where the treated sites showed less erythema and hyperpigmentation, reducing transient adverse effects and increased levels of trans-epidermal water loss, indicating impaired skin barrier function.

1.5.4.2. Cell Sheet Technology

In order to overcome the drawbacks such inefficient delivery of cells, cell sheet (CS) engineering appears as a powerful tool in the regenerative medicine area [97,101]. This technique has been used in corneal reconstruction, esophageal transplantation by endoscopy, tracheal replacement, tissue-engineered cardiac patches, vascularized thick tissues formed by multi-step transplantation and creation of organ-like structures [102–108]. This original scaffold-free approach was first described by Okano *et al.*, [109]. It involves cell culture until confluency in a temperature-responsive polymer coated surface that with further temperature decrease, changes its hydrophilicity leading to cellular spontaneous detachment as a monolayer [110]. These CS allow noninvasive cellular harvesting embedded in their own ECM, facilitating the direct transplantation to host tissues since the ECM acts as a natural scaffold yet retaining cell-cell and cell-ECM junctions [92,97,111–113].

Taking advantage of the CS technology together with the attractive properties for wound healing related with hASCs, CS constructs were tested on full-thickness excisional mice skin wounds with delayed healing [97]. The CS obtained using thermoresponsive surfaces showed to be more stable and easily manageable comparing to the ones produced with standard cell culture surface, due to the natural adhesive character of the CS. Although both strategies had no significant effect over wound closure, hASCs-CS lead not only to full re-epithelialized wounds but also to the formation of appendages in the neoformed matrix. In wounds treated with CS obtained from the thermoresponsive surfaces an up-regulation of KGF was detected which could possibly influencing the formation of a thicker epidermis with a higher degree of maturation characterized by the presence of rete ridges-like structures, as well the significant number of hair follicles observed after transplantation. This methodology allowed not only the production of hASCs-CS in a short time, envisioning the potential of the method in clinical setting but also the re-epithelialization with high number of hair follicles and the presence of rete ridge-like structures. Cell sheets of hASCs were further used to treat diabetic wounds. For that, they were transplanted into full-

thickness wounds of a xenogeneic model of type 2 diabetes, the Zucker Diabetic Fatty Rat (ZDF rat) [114]. Several cytokines were found to be secreted by hASCs sheets, namely KGF. The healing of the wound was significantly accelerated in the transplantation group from day 3 onward comparing to the control, and after 14 days after transplantation, was detected an increased blood vessel density and dermal thickness, also compared to the control. The xenogeneic hASCs sheets allowed for an accelerated healing of large wounds, promoting angiogenesis and the paracrine effects by secreted GFs.

1.5.5. Advantages and Disadvantages of the Presented Strategies

Despite the relevant outcomes on re-epithelialization enhancement, one of the main drawbacks associated to the topical application of KGF is related with the low diffusion and the consequent need of high dosage (e.g. around 10 times superior than biomaterial-based strategies) and repeated administration (Table 1.5).

Table 1.5 - Advantages and disadvantages of the different strategies for KGF delivery.

STRATEGIES	ADVANTAGES	DISADVANTAGES
TOPICAL APPLICATION	<ul style="list-style-type: none"> – Low risk of systemic adverse events; – Convenient to use and easy to apply. 	<ul style="list-style-type: none"> – Short half-life; – Need of repeated injections; – Lack of dosage control; – Rapid diffusion; – Application at supraphysiological concentrations.
BIOMATERIALS-BASED	<ul style="list-style-type: none"> – High versatility of application; – Incorporation of KGF at lower dosages; – Sustained delivery; – Protection to external insults. 	<ul style="list-style-type: none"> – Efficacy related with the type of biomaterial/processing conditions;
GENE THERAPY	<ul style="list-style-type: none"> – High transduction efficiency; – Sustained gene expression; – Specific Targeting. 	<ul style="list-style-type: none"> – Virus-associated toxicity; – High costs; – Complicated manufacturing.
ADIPOSE STEM CELLS (CELL SUSPENSION)	<ul style="list-style-type: none"> – Natural producer of GFs; – Various harvest sites; – Additional paracrine signaling potential – Low risk of rejection. 	<ul style="list-style-type: none"> – Limited expansion <i>in vitro</i>; – Heterogeneous population of cells; – Low engraftment ; – Low survival.

In the skin wound healing context, the need of exaggerated high doses is intimately related with the high proteolytic environment that tend to lyse the topically applied GFs. Recombinant human platelet-derived growth factor BB (becaplermin), the only GF-based drug for skin wound healing approved by US Food and Drug Administration (FDA) as adjuvant treatment of diabetic foot ulcers [115], is a strong example of the high dosage ($100 \mu\text{g}/\text{cm}^2$) and need of reapplication (alternate days). Although effective, its use has been limited by the high cost and by post-marketing reports of an increased rate of mortality secondary to cancer in patients treated with three or more tubes of becaplermin. To our knowledge, no evidences on the associated mechanisms have been reported, but possibly uncontrolled feedback loops for unbalanced concentration could be leading to the malignances observed.

Medical application of KGF in specific has been successfully used in several preclinical models of radiation and chemotherapy-induced mucositis, and developed into commercial medicine (i.e. Palifermin) [116], however more effective delivery systems are needed to ensure safe treatments and open the possibility to target skin wounds. KGF is under control of a feedback loop which reenforces the strict need for controlled delivery approaches. Both paracrine and autocrine signaling may be important for the action of KGF in normal tissues, and in the most cases the action of KGF via the autocrine signaling was not observed. These facts determine that the expression level of KGF by epithelial cells is high in some cancer tissues and the autocrine loop may be enhanced due to hyperplasia or tumorigenesis [117]. However, the detailed mechanisms remain to be unraveled.

Biomaterials can be highly appealing vehicles to provide a controlled dosage in a sustained manner deliver of GFs, minimizing some of the issues mentioned above. They can be processed as hydrogels, particles and membranes showing high versatility in different types of wounds like epidermal, superficial/deep partial-thickness, and full-thickness wounds [65,68,72]. Among the described studies of KGF-biomaterials systems, the overall range of KGF concentration drops significantly, comparing with topically applied KGF dosages (highest of $100 \mu\text{g}$ for chitosan-silica membranes [74] and lowest $3.3 \text{ ng}/\text{mL}$ in PEGylated RGD gelatin hydrogel [64]). Most of the studies promoted an overall enhancement of the re-epithelialization process, but KGF dosages varied significantly, being difficult to establish the correlation of minimal dose/maximum efficacy. In the case of the hydrogels explored, only one type of hydrogel allowed the improvement of the environment for efficacious wound closure [65]. It seems, that in these 3D structures the concentration of KGF was not fundamental since no response regarding re-epithelialization was obtained with the highest concentration ($5 \mu\text{g}$) and the lowest (3.3 ng), and only occurring with the intermediate KGF concentration (150 ng). While it is difficult to compare all those

systems in terms of KGF dosage, one must also consider that their release profile is potentially different due to the nature of the membrane biomaterial. This was for example confirmed with PLGA and PLLA membranes formulated with equal 10 ng/mL of KGF. Each polymer formulation released biologically relevant levels of KGF, although with different times release kinetics. PLGA/AOT/KGF film is potentially a better formulation for a rapid time frame (within 72 hours) protein drug release, given its propensity to release protein early after exposure to solution [73]. Nonetheless, whether the achieved differences, like those potentially attained in any other of the explored strategies, are sufficient to efficiently foster wound re-epithelialization is yet to be determined. In this regard, not only the type of biomaterial used and its processing method interfere with GFs release and dose needed, but it is also determinant the GFs incorporation methodology, via adsorption or covalent binding. While the controlled release in adsorbed-based KGF strategies occurs via diffusion from 3D (hydrogels) or 2D (membranes); when KGF is covalently bound, the release is strongly dependent on the biomaterial degradation or other triggering stimuli.

Gene therapy is a potent methodology for KGF delivery and highly relevant to surpass some of the issues related with control and efficacy. Either by transfecting native cells directly at wound site [78,79,81,82] or by using an *ex-vivo* model [82–84] before cell transplantation, this technique reported highly transduction of KGF. This ensured high levels of KGF in a continuous manner. Of course, gene therapy opens the discussion on serious safety related issues and complicated manufacturing. However, the exploitation of alternative delivery methods to virus-mediated ones, as well as by using mRNA [86], instead of DNA, are just examples of the effort made to move this strategy to a clinical side.

The use of hASCs demonstrated to have various advantages to target wound healing, as these cells are natural producers of relevant GFs and cytokines, can be easily harvested from various sites and have low risk of rejection due to their immunoprivileged nature [118,119]. However, the conventional cell transplantation normally involves the need of a great cell number that is often hampered due a limited expansion *in vitro* and a heterogeneous population of cells. Moreover, traditional cell application via injection on the wound sites lead to low engraftment efficiency due to fast diffusion, poor localization to the host tissue, damage from enzymatic digestion, and shear cell death [101,113,120]. By contrast, cells sheets formed by cell sheet technology can overcome these problems since native ECM adhesive properties allow promote cell engraftment to the host tissues, including wound sites [121].

1.6. Purpose of the Work

Currently, multiple therapeutic strategies to delivery KGF have been proposed to boost the healing process by targeting re-epithelialization. This has been achieved through a range of different approaches, such as topical application, using controlled release-based methods with different biomaterials (hydrogels, particles and membranes), through gene therapy techniques, and also, via the use of stem cells.

Taking this in consideration, this thesis is focused on the study of two different strategies for KGF delivery in the context of skin re-epithelialization. The first one comprises the development of a particle-based system, whereas the second one explores the use of adipose stem cells as natural producers of KGF. For that, gellan gum particles were produced to release KGF, while for the second strategy cell sheets of adipose stem cells were generated. After fine tuning these systems, the amount of KGF was quantified for precise predicted administration and the potential of both approaches on KCs motogenesis and proliferation were assessed *in vitro*.

1.7. References

- [1] M.E. Lane, Nanoparticles and the skin–applications and limitations., *J. Microencapsul.* 28 (2011) 709–16. <https://doi.org/10.3109/02652048.2011.599440>.
- [2] D. Voegeli, Understanding the main principles of skin care in older adults., *Nurs. Stand.* 27 (2012) 59–60, 62–4, 66–8. <https://doi.org/10.7748/ns2012.11.27.11.59.c9414>.
- [3] B. Baroli, Penetration of nanoparticles and nanomaterials in the skin: Fiction or reality?, *J. Pharm. Sci.* 99 (2010) 21–50. <https://doi.org/10.1002/jps.21817>.
- [4] B. Zhang, X. Liu, C. Wang, L. Li, L. Ma, C. Gao, Bioengineering Skin Constructs, in: *Stem Cell Biol. Tissue Eng. Dent. Sci.*, Elsevier, 2015: pp. 703–719. <https://doi.org/10.1016/C2011-0-07350-7>.
- [5] S. Eyerich, K. Eyerich, C. Traidl-Hoffmann, T. Biedermann, Cutaneous Barriers and Skin Immunity: Differentiating A Connected Network., *Trends Immunol.* 39 (2018) 315–327. <https://doi.org/10.1016/j.it.2018.02.004>.
- [6] T.W. Prow, J.E. Grice, L.L. Lin, R. Faye, M. Butler, W. Becker, E.M.T. Wurm, C. Yoong, T.A. Robertson, H.P. Soyer, M.S. Roberts, Nanoparticles and microparticles for skin drug delivery., *Adv. Drug Deliv. Rev.* 63 (2011) 470–91. <https://doi.org/10.1016/j.addr.2011.01.012>.
- [7] D.T. Nguyen, D.P. Orgill, G.F. Murphy, The pathophysiologic basis for wound healing and cutaneous regeneration, in: *Biomater. Treat. Ski. Loss*, Elsevier, 2009: pp. 25–57. <https://doi.org/10.1533/9781845695545.1.25>.
- [8] R.R. Wickett, M.O. Visscher, Structure and function of the epidermal barrier, *Am. J. Infect. Control.* 34 (2006) S98–S110. <https://doi.org/10.1016/j.ajic.2006.05.295>.
- [9] K. Walters, M. Roberts, The Structure and Function of Skin, in: *Dermatological Transdermal Formul.*, 2002: pp. 1–39. <https://doi.org/10.1201/9780824743239.ch1>.
- [10] G.K. Menon, New insights into skin structure: scratching the surface, *Adv. Drug Deliv. Rev.* 54 (2002) S3–S17. [https://doi.org/10.1016/S0169-409X\(02\)00121-7](https://doi.org/10.1016/S0169-409X(02)00121-7).

- [11] O.G. Jepps, Y. Dancik, Y.G. Anissimov, M.S. Roberts, Modeling the human skin barrier–towards a better understanding of dermal absorption., *Adv. Drug Deliv. Rev.* 65 (2013) 152–68. <https://doi.org/10.1016/j.addr.2012.04.003>.
- [12] P. Martin, Wound healing–aiming for perfect skin regeneration., *Science.* 276 (1997) 75–81. <https://doi.org/10.1126/science.276.5309.75>.
- [13] N.J. Percival, Classification of Wounds and their Management, *Surg.* 20 (2002) 114–117. <https://doi.org/10.1383/surg.20.5.114.14626>.
- [14] C.K. Sen, Human Wounds and Its Burden: An Updated Compendium of Estimates, *Adv. Wound Care.* 8 (2019) 39–48. <https://doi.org/10.1089/wound.2019.0946>.
- [15] S. Tejiram, S.L. Kavalukas, J.W. Shupp, A. Barbul, Wound healing, in: *Wound Heal. Biomater.*, Elsevier, 2016: pp. 3–39. <https://doi.org/10.1016/B978-1-78242-455-0.00001-X>.
- [16] G. Broughton, J.E. Janis, C.E. Attinger, The Basic Science of Wound Healing, *Plast. Reconstr. Surg.* 117 (2006) 12S-34S. <https://doi.org/10.1097/01.prs.0000225430.42531.c2>.
- [17] I. Pastar, O. Stojadinovic, N.C. Yin, H. Ramirez, A.G. Nusbaum, A. Sawaya, S.B. Patel, L. Khalid, R.R. Isseroff, M. Tomic-Canic, Epithelialization in Wound Healing: A Comprehensive Review, *Adv. Wound Care.* 3 (2014) 445–464. <https://doi.org/10.1089/wound.2013.0473>.
- [18] R.A.F. Clark, Wound Repair, in: *Princ. Tissue Eng.*, Fourth Edi, Elsevier, 2014: pp. 1595–1617. <https://doi.org/10.1016/B978-0-12-398358-9.00076-8>.
- [19] W.S. Krawczyk, A PATTERN OF EPIDERMAL CELL MIGRATION DURING WOUND HEALING, *J. Cell Biol.* 49 (1971) 247–263. <https://doi.org/10.1083/jcb.49.2.247>.
- [20] R.D. Paladini, K. Takahashi, N.S. Bravo, P.A. Coulombe, Onset of re-epithelialization after skin injury correlates with a reorganization of keratin filaments in wound edge keratinocytes: defining a potential role for keratin 16., *J. Cell Biol.* 132 (1996) 381–97. <https://doi.org/10.1083/jcb.132.3.381>.
- [21] G.P. Radice, The spreading of epithelial cells during wound closure in *Xenopus* larvae, *Dev. Biol.* 76 (1980) 26–46. [https://doi.org/10.1016/0012-1606\(80\)90360-7](https://doi.org/10.1016/0012-1606(80)90360-7).

- [22] D.T. Woodley, Reepithelialization, in: R.A.F. Clark (Ed.), *Mol. Cell. Biol. Wound Repair*, 2nd ed., Springer US, Boston, MA, 1988: pp. 339–354. https://doi.org/10.1007/978-1-4899-0185-9_10.
- [23] M.L. Usui, R.A. Underwood, J.N. Mansbridge, L.A. Muffley, W.G. Carter, J.E. Olerud, Morphological evidence for the role of suprabasal keratinocytes in wound reepithelialization, *Wound Repair Regen.* 13 (2005) 468–479. <https://doi.org/10.1111/j.1067-1927.2005.00067.x>.
- [24] A. Michopoulou, P. Rousselle, How do epidermal matrix metalloproteinases support re-epithelialization during skin healing?, *Eur. J. Dermatology.* 25 (2015) 33–42. <https://doi.org/10.1684/ejd.2015.2553>.
- [25] P. Rousselle, F. Braye, G. Dayan, Re-epithelialization of adult skin wounds: Cellular mechanisms and therapeutic strategies, *Adv. Drug Deliv. Rev.* 146 (2019) 344–365. <https://doi.org/10.1016/j.addr.2018.06.019>.
- [26] M.-C. Miller, J. Nanchahal, Advances in the Modulation of Cutaneous Wound Healing and Scarring, *BioDrugs.* 19 (2005) 363–381. <https://doi.org/10.2165/00063030-200519060-00004>.
- [27] A. Tang, B.A. Gilchrist, Regulation of keratinocyte growth factor gene expression in human skin fibroblasts., *J. Dermatol. Sci.* 11 (1996) 41–50. [https://doi.org/10.1016/0923-1811\(95\)00418-1](https://doi.org/10.1016/0923-1811(95)00418-1).
- [28] H. Smola, G. Thiekötter, N.E. Fusenig, Mutual induction of growth factor gene expression by epidermal-dermal cell interaction., *J. Cell Biol.* 122 (1993) 417–29. <https://doi.org/10.1083/jcb.122.2.417>.
- [29] E.A. O'Toole, Extracellular matrix and keratinocyte migration, *Clin. Exp. Dermatol.* 26 (2001) 525–530. <https://doi.org/10.1046/j.1365-2230.2001.00891.x>.
- [30] R.A.F. Clark, Overview and General Considerations of Wound Repair, in: *Mol. Cell. Biol. Wound Repair*, Springer US, Boston, MA, 1998: pp. 3–33. https://doi.org/10.1007/978-1-4615-1795-5_1.

- [31] G.S. Schultz, G.A. Chin, L. Moldawer, R.F. Diegelmann, R. Fitridge, M. Thompson, Principles of wound healing, in: R. Fitridge, M. Thompson (Eds.), *Mech. Vasc. Dis.*, University of Adelaide Press, Adelaide, 2011: pp. 423–450. <https://doi.org/10.1017/UPO9781922064004.024>.
- [32] G. Henry, W.L. Garner, Inflammatory mediators in wound healing, *Surg. Clin. North Am.* 83 (2003) 483–507. [https://doi.org/10.1016/S0039-6109\(02\)00200-1](https://doi.org/10.1016/S0039-6109(02)00200-1).
- [33] R. Grose, C. Hutter, W. Bloch, I. Thorey, F.M. Watt, R. Fässler, C. Brakebusch, S. Werner, A crucial role of β 1 integrins for keratinocyte migration in vitro and during cutaneous wound repair, *Development*. 129 (2002) 2303–2315. <https://doi.org/10.1242/dev.129.9.2303>.
- [34] D. Chen, H. Hao, X. Fu, W. Han, Insight into Reepithelialization: How Do Mesenchymal Stem Cells Perform?, *Stem Cells Int.* 2016 (2016) 1–9. <https://doi.org/10.1155/2016/6120173>.
- [35] T.N. Demidova-Rice, M.R. Hamblin, I.M. Herman, Acute and Impaired Wound Healing, *Adv. Skin Wound Care*. 25 (2012) 304–314. <https://doi.org/10.1097/01.ASW.0000416006.55218.d0>.
- [36] O. Stojadinovic, H. Brem, C. Vouthounis, B. Lee, J. Fallon, M. Stallcup, A. Merchant, R.D. Galiano, M. Tomic-Canic, Molecular Pathogenesis of Chronic Wounds: The Role of β -Catenin and c-myc in the Inhibition of Epithelialization and Wound Healing, *Am. J. Pathol.* 167 (2005) 59–69. [https://doi.org/10.1016/S0002-9440\(10\)62953-7](https://doi.org/10.1016/S0002-9440(10)62953-7).
- [37] O. Stojadinovic, I. Pastar, S. Vukelic, M.G. Mahoney, D. Brennan, A. Krzyzanowska, M. Golinko, H. Brem, M. Tomic-Canic, Deregulation of keratinocyte differentiation and activation: a hallmark of venous ulcers, *J. Cell. Mol. Med.* 12 (2008) 2675–2690. <https://doi.org/10.1111/j.1582-4934.2008.00321.x>.
- [38] M.L. Usui, J.N. Mansbridge, W.G. Carter, M. Fujita, J.E. Olerud, Keratinocyte Migration, Proliferation, and Differentiation in Chronic Ulcers From Patients With Diabetes and Normal Wounds, *J. Histochem. Cytochem.* 56 (2008) 687–696. <https://doi.org/10.1369/jhc.2008.951194>.

- [39] M.S. Ågren, H.H. Steenfos, S. Dabelsteen, J.B. Hansen, E. Dabelsteen, Proliferation and Mitogenic Response to PDGF-BB of Fibroblasts Isolated from Chronic Venous Leg Ulcers is Ulcer-Age Dependent¹¹ Presented in part at the Gordon Research Conference on Wound Repair July 2–7 1995 and at an IBC meeting on Fibrosis in Washington, J. Invest. Dermatol. 112 (1999) 463–469. <https://doi.org/10.1046/j.1523-1747.1999.00549.x>.
- [40] N. Itoh, D.M. Ornitz, Fibroblast growth factors: from molecular evolution to roles in development, metabolism and disease, J. Biochem. 149 (2011) 121–130. <https://doi.org/10.1093/jb/mvq121>.
- [41] N. Ferrara, H.-P. Gerber, J. LeCouter, The biology of VEGF and its receptors, Nat. Med. 9 (2003) 669–676. <https://doi.org/10.1038/nm0603-669>.
- [42] G. Seghezzi, S. Patel, C.J. Ren, A. Gualandris, G. Pintucci, E.S. Robbins, R.L. Shapiro, A.C. Galloway, D.B. Rifkin, P. Mignatti, Fibroblast growth factor-2 (FGF-2) induces vascular endothelial growth factor (VEGF) expression in the endothelial cells of forming capillaries: an autocrine mechanism contributing to angiogenesis., J. Cell Biol. 141 (1998) 1659–73. <https://doi.org/10.1083/jcb.141.7.1659>.
- [43] H.D. Beer, M.G. Gassmann, B. Munz, H. Steiling, F. Engelhardt, K. Bleuel, S. Werner, Expression and function of keratinocyte growth factor and activin in skin morphogenesis and cutaneous wound repair., J. Investig. Dermatology. Symp. Proc. 5 (2000) 34–9. <https://doi.org/10.1046/j.1087-0024.2000.00009.x>.
- [44] A.T. Grazul-Bilska, M.L. Johnson, J.J. Bilski, D.A. Redmer, L.P. Reynolds, A. Abdullah, K.M. Abdullah, Wound healing: the role of growth factors., Drugs Today (Barc). 39 (2003) 787–800. <https://doi.org/10.1358/dot.2003.39.10.799472>.
- [45] U. auf dem Keller, M. Krampert, A. Kümin, S. Braun, S. Werner, Keratinocyte growth factor: effects on keratinocytes and mechanisms of action, Eur. J. Cell Biol. 83 (2004) 607–612. <https://doi.org/10.1078/0171-9335-00389>.
- [46] Tissue expression of FGFR2 - Staining in skin - The Human Protein Atlas, (n.d.). <https://www.proteinatlas.org/ENSG00000066468-FGFR2/tissue/skin>.

- [47] S. Werner, Keratinocyte Growth Factor: A Unique Player in Epithelial Repair Processes, *Cytokine Growth Factor Rev.* 9 (1998) 153–165. [https://doi.org/10.1016/S1359-6101\(98\)00010-0](https://doi.org/10.1016/S1359-6101(98)00010-0).
- [48] C. Marchese, P. Mancini, F. Belleudi, A. Felici, R. Gradini, T. Sansolini, L. Frati, M.R. Torrisci, Receptor-mediated endocytosis of keratinocyte growth factor, *J. Cell Sci.* 111 (1998) 3517–3527. <https://doi.org/10.1242/jcs.111.23.3517>.
- [49] F. Belleudi, M. Ceridono, A. Capone, A. Serafino, C. Marchese, M. Picardo, L. Frati, M.R. Torrisci, The endocytic pathway followed by the keratinocyte growth factor receptor., *Histochem. Cell Biol.* 118 (2002) 1–10. <https://doi.org/10.1007/s00418-002-0424-0>.
- [50] F. Belleudi, L. Leone, V. Nobili, S. Raffa, F. Francescangeli, M. Maggio, S. Morrone, C. Marchese, M.R. Torrisci, Keratinocyte Growth Factor Receptor Ligands Target the Receptor to Different Intracellular Pathways, *Traffic.* 8 (2007) 1854–1872. <https://doi.org/10.1111/j.1600-0854.2007.00651.x>.
- [51] M. Madlener, C. Mauch, W. Conca, M. Brauchle, W.C. Parks, S. Werner, Regulation of the expression of stromelysin-2 by growth factors in keratinocytes: implications for normal and impaired wound healing, *Biochem. J.* 320 (1996) 659–664. <https://doi.org/10.1042/bj3200659>.
- [52] Z. Wang, Z. Wang, W.W. Lu, W. Zhen, D. Yang, S. Peng, Novel biomaterial strategies for controlled growth factor delivery for biomedical applications, *NPG Asia Mater.* 9 (2017) e435–e435. <https://doi.org/10.1038/am.2017.171>.
- [53] T. Arakawa, S.J. Prestrelski, W.C. Kenney, J.F. Carpenter, Factors affecting short-term and long-term stabilities of proteins., *Adv. Drug Deliv. Rev.* 46 (2001) 307–26. [https://doi.org/10.1016/s0169-409x\(00\)00144-7](https://doi.org/10.1016/s0169-409x(00)00144-7).
- [54] P.E. Clayton, I. Banerjee, P.G. Murray, A.G. Renehan, Growth hormone, the insulin-like growth factor axis, insulin and cancer risk, *Nat. Rev. Endocrinol.* 7 (2011) 11–24. <https://doi.org/10.1038/nrendo.2010.171>.
- [55] P. Korja, Delivery of growth factors for tissue regeneration and wound healing., *BioDrugs.* 26 (2012) 163–75. <https://doi.org/10.2165/11631850-000000000-00000>.

- [56] R. Tsuboi, C. Sato, Y. Kurita, D. Ron, J.S. Rubin, H. Ogawa, Keratinocyte Growth Factor (FGF-7) Stimulates Migration and Plasminogen Activator Activity of Normal Human Keratinocytes, *J. Invest. Dermatol.* 101 (1993) 49–53. <https://doi.org/10.1111/1523-1747.ep12358892>.
- [57] L. Staiano-Coico, J.G. Krueger, J.S. Rubin, S. D'limi, V.P. Vallat, L. Valentino, T. Fahey, A. Hawes, G. Kingston, M.R. Madden, Human keratinocyte growth factor effects in a porcine model of epidermal wound healing., *J. Exp. Med.* 178 (1993) 865–878. <https://doi.org/10.1084/jem.178.3.865>.
- [58] S. Karvinen, S. Pasonen-Seppänen, J.M.T. Hyttinen, J.-P. Pienimäki, K. Törrönen, T.A. Jokela, M.I. Tammi, R. Tammi, Keratinocyte Growth Factor Stimulates Migration and Hyaluronan Synthesis in the Epidermis by Activation of Keratinocyte Hyaluronan Synthases 2 and 3, *J. Biol. Chem.* 278 (2003) 49495–49504. <https://doi.org/10.1074/jbc.M310445200>.
- [59] B.N. Gomperts, J.A. Belperio, M.C. Fishbein, M.P. Keane, M.D. Burdick, R.M. Strieter, Keratinocyte Growth Factor Improves Repair in the Injured Tracheal Epithelium, *Am. J. Respir. Cell Mol. Biol.* 37 (2007) 48–56. <https://doi.org/10.1165/rcmb.2006-03840C>.
- [60] S.-I. Ishimoto, T. Ishibashi, D.P. Bottaro, K. Kaga, Direct Application of Keratinocyte Growth Factor, Basic Fibroblast Growth Factor and Transforming Growth Factor- α During Healing of Tympanic Membrane Perforation in Glucocorticoid-treated Rats, *Acta Otolaryngol.* 122 (2002) 468–473. <https://doi.org/10.1080/00016480260092246>.
- [61] C. Sotozono, T. Inatomi, M. Nakamura, S. Kinoshita, Keratinocyte growth factor accelerates corneal epithelial wound healing in vivo., *Invest. Ophthalmol. Vis. Sci.* 36 (1995) 1524–9. <http://www.ncbi.nlm.nih.gov/pubmed/7601632>.
- [62] F. Oyarzun-Ampuero, A. Vidal, M. Concha, J. Morales, S. Orellana, I. Moreno-Villoslada, Nanoparticles for the Treatment of Wounds., *Curr. Pharm. Des.* 21 (2015) 4329–41. <https://doi.org/10.2174/1381612821666150901104601>.
- [63] Y. Ni, D. Turner, K. Yates, I. Tizard, Stabilization of Growth Factors Relevant to Wound Healing by a Plant Cell Wall Biomaterial, *Planta Med.* 73 (2007) 1260–1266. <https://doi.org/10.1055/s-2007-990225>.

- [64] H. Waldeck, A.S. Chung, W.J. Kao, Interpenetrating polymer networks containing gelatin modified with PEGylated RGD and soluble KGF: Synthesis, characterization, and application in vivo critical dermal wound, *J. Biomed. Mater. Res. Part A.* 82A (2007) 861–871. <https://doi.org/10.1002/jbm.a.31054>.
- [65] D.J. Geer, D.D. Swartz, S.T. Andreadis, Biomimetic Delivery of Keratinocyte Growth Factor upon Cellular Demand for Accelerated Wound Healing in Vitro and in Vivo, *Am. J. Pathol.* 167 (2005) 1575–1586. [https://doi.org/10.1016/S0002-9440\(10\)61242-4](https://doi.org/10.1016/S0002-9440(10)61242-4).
- [66] S. Sen-Britain, W.L. Hicks, R. Hard, J.A. Gardella, Differential orientation and conformation of surface-bound keratinocyte growth factor on (hydroxyethyl)methacrylate, (hydroxyethyl)methacrylate/methyl methacrylate, and (hydroxyethyl)methacrylate/methacrylic acid hydrogel copolymers, *Biointerphases.* 13 (2018) 06E406. <https://doi.org/10.1116/1.5051655>.
- [67] W. ABDELWAHED, G. DEGOBERT, S. STAINMESSE, H. FESSI, Freeze-drying of nanoparticles: Formulation, process and storage considerations☆, *Adv. Drug Deliv. Rev.* 58 (2006) 1688–1713. <https://doi.org/10.1016/j.addr.2006.09.017>.
- [68] A. Pan, M. Zhong, H. Wu, Y. Peng, H. Xia, Q. Tang, Q. Huang, L. Wei, L. Xiao, C. Peng, Topical Application of Keratinocyte Growth Factor Conjugated Gold Nanoparticles Accelerate Wound Healing., *Nanomedicine.* 14 (2018) 1619–1628. <https://doi.org/10.1016/j.nano.2018.04.007>.
- [69] I. Muhamed, E.P. Sproul, F.S. Ligler, A.C. Brown, Fibrin Nanoparticles Coupled with Keratinocyte Growth Factor Enhance the Dermal Wound-Healing Rate., *ACS Appl. Mater. Interfaces.* 11 (2019) 3771–3780. <https://doi.org/10.1021/acsami.8b21056>.
- [70] P. Korja, H. Yagi, Y. Kitagawa, Z. Megeed, Y. Nahmias, R. Sheridan, M.L. Yarmush, Self-assembling elastin-like peptides growth factor chimeric nanoparticles for the treatment of chronic wounds., *Proc. Natl. Acad. Sci. U. S. A.* 108 (2011) 1034–9. <https://doi.org/10.1073/pnas.1009881108>.
- [71] C. Kao, Use of concentrate growth factors gel or membrane in chronic wound healing: Description of 18 cases, *Int. Wound J.* 17 (2020) 158–166. <https://doi.org/10.1111/iwj.13250>.

- [72] Y. Qu, C. Cao, Q. Wu, A. Huang, Y. Song, H. Li, Y. Zuo, C. Chu, J. Li, Y. Man, The dual delivery of KGF and bFGF by collagen membrane to promote skin wound healing., *J. Tissue Eng. Regen. Med.* 12 (2018) 1508–1518. <https://doi.org/10.1002/term.2691>.
- [73] S.A. Burns, R. Hard, W.L. Hicks, F. V Bright, D. Cohan, L. Sigurdson, J.A. Gardella, Determining the protein drug release characteristics and cell adhesion to a PLLA or PLGA biodegradable polymer membrane, *J. Biomed. Mater. Res. Part A.* 94A (2010) 27–37. <https://doi.org/10.1002/jbm.a.32654>.
- [74] J. Oh, E. Lee, Engineered dressing of hybrid chitosan-silica for effective delivery of keratin growth factor and acceleration of wound healing, *Mater. Sci. Eng. C.* 103 (2019) 109815. <https://doi.org/10.1016/j.msec.2019.109815>.
- [75] M. Bienert, M. Hoss, M. Bartneck, S. Weinandy, M. Böbel, S. Jockenhövel, R. Knüchel, K. Pottbacker, M. Wöltje, W. Jahnen-Dechent, S. Neuss, Growth factor-functionalized silk membranes support wound healing in vitro, *Biomed. Mater.* 12 (2017) 045023. <https://doi.org/10.1088/1748-605X/aa7695>.
- [76] A. Cruz, C. Ramos, *ClinicalTrials.gov*, Eff. Comp. Ski. Micro-Grafts vs Meshed Split Thick. Ski. Grafts. (2016). <https://clinicaltrials.gov/ct2/show/study/NCT02813213?term=Keratinocyte+growth+factor&draw=2&rank=19>.
- [77] E. Gorell, N. Nguyen, A. Lane, Z. Siprashvili, Gene Therapy for Skin Diseases, *Cold Spring Harb. Perspect. Med.* 4 (2014) a015149–a015149. <https://doi.org/10.1101/cshperspect.a015149>.
- [78] M.G. Jeschke, G. Richter, F. Höfstädter, D.N. Herndon, J.-R. Perez-Polo, K.-W. Jauch, Non-viral liposomal keratinocyte growth factor (KGF) cDNA gene transfer improves dermal and epidermal regeneration through stimulation of epithelial and mesenchymal factors., *Gene Ther.* 9 (2002) 1065–74. <https://doi.org/10.1038/sj.gt.3301732>.
- [79] C.T. Pereira, D.N. Herndon, R. Rocker, M.G. Jeschke, Liposomal Gene Transfer of Keratinocyte Growth Factor Improves Wound Healing by Altering Growth Factor and Collagen Expression, *J. Surg. Res.* 139 (2007) 222–228. <https://doi.org/10.1016/j.jss.2006.09.005>.

- [80] G.P. Marti, P. Mohebi, L. Liu, J. Wang, T. Miyashita, J.W. Harmon, KGF-1 for Wound Healing in Animal Models, in: *Electroporation Protoc.*, 2008: pp. 383–391. https://doi.org/10.1007/978-1-59745-194-9_30.
- [81] C. Dou, F. Lay, A.M. Ansari, D.J. Rees, A.K. Ahmed, O. Kovbasnjuk, A.E. Matsangos, J. Du, S.M. Hosseini, C. Steenbergen, K. Fox-Talbot, A.T. Tabor, J.A. Williams, L. Liu, G.P. Marti, J.W. Harmon, Strengthening the Skin with Topical Delivery of Keratinocyte Growth Factor-1 Using a Novel DNA Plasmid, *Mol. Ther.* 22 (2014) 752–761. <https://doi.org/10.1038/mt.2014.2>.
- [82] M.J. Escámez, M. Carretero, M. García, L. Martínez-Santamaría, I. Mirones, B. Duarte, A. Holguín, E. García, V. García, A. Meana, J.L. Jorcano, F. Larcher, M. Del Río, Assessment of Optimal Virus-Mediated Growth Factor Gene Delivery for Human Cutaneous Wound Healing Enhancement, *J. Invest. Dermatol.* 128 (2008) 1565–1575. <https://doi.org/10.1038/sj.jid.5701217>.
- [83] G. Erdag, D.A. Medalie, H. Rakhorst, G.G. Krueger, J.R. Morgan, FGF-7 Expression Enhances the Performance of Bioengineered Skin, *Mol. Ther.* 10 (2004) 76–85. <https://doi.org/10.1016/j.ymthe.2004.04.013>.
- [84] J. Kopp, G.Y. Wang, P. Kulmburg, S. Schultze-Mosgau, J.N. Huan, K. Ying, H. Seyhan, M.D. Jeschke, U. Kneser, A.D. Bach, S.D. Ge, S. Dooley, R.E. Horch, Accelerated Wound Healing by In vivo Application of Keratinocytes Overexpressing KGF, *Mol. Ther.* 10 (2004) 86–96. <https://doi.org/10.1016/j.ymthe.2004.04.016>.
- [85] G. Marti, M. Ferguson, J. Wang, C. Byrnes, R. Dieb, R. Qaiser, P. Bonde, M. Duncan, J. Harmon, Electroporative transfection with KGF-1 DNA improves wound healing in a diabetic mouse model, *Gene Ther.* 11 (2004) 1780–1785. <https://doi.org/10.1038/sj.gt.3302383>.
- [86] M. Denzinger, A. Link, J. Kurz, S. Krauss, R. Thoma, C. Schlensak, H.P. Wendel, S. Krajewski, Keratinocyte Growth Factor Modified Messenger RNA Accelerating Cell Proliferation and Migration of Keratinocytes, *Nucleic Acid Ther.* 28 (2018) 335–347. <https://doi.org/10.1089/nat.2018.0737>.
- [87] W. Zakrzewski, M. Dobrzyński, M. Szymonowicz, Z. Rybak, Stem cells: Past, present, and future, *Stem Cell Res. Ther.* 10 (2019) 68. <https://doi.org/10.1186/s13287-019-1165-5>.

- [88] L.A. Fortier, Stem Cells: Classifications, Controversies, and Clinical Applications, *Vet. Surg.* 34 (2005) 415–423. <https://doi.org/10.1111/j.1532-950X.2005.00063.x>.
- [89] M. Prochazkova, M.G. Chavez, J. Prochazka, H. Felfy, V. Mushegyan, O.D. Klein, Embryonic Versus Adult Stem Cells, in: *Stem Cell Biol. Tissue Eng. Dent. Sci.*, Elsevier, 2015: pp. 249–262. <https://doi.org/10.1016/B978-0-12-397157-9.00020-5>.
- [90] C. Ribeiro, V. Correia, P. Martins, F.M. Gama, S. Lanceros-Mendez, Proving the suitability of magnetoelectric stimuli for tissue engineering applications, *Colloids Surfaces B Biointerfaces.* 140 (2016) 430–436. <https://doi.org/10.1016/j.colsurfb.2015.12.055>.
- [91] M.T. Cerqueira, R.P. Pirraco, A.P. Marques, Stem Cells in Skin Wound Healing: Are We There Yet?, *Adv. Wound Care.* 5 (2016) 164–175. <https://doi.org/10.1089/wound.2014.0607>.
- [92] Y.C. Lin, T. Grahovac, S.J. Oh, M. Ieraci, J.P. Rubin, K.G. Marra, Evaluation of a multi-layer adipose-derived stem cell sheet in a full-thickness wound healing model, *Acta Biomater.* 9 (2013) 5243–5250. <http://dx.doi.org/10.1016/j.actbio.2012.09.028>.
- [93] A.J. Friedenstein, U.F. Deriglasova, N.N. Kulagina, A.F. Panasuk, S.F. Rudakowa, E.A. Luriá, I.A. Ruadkow, Precursors for fibroblasts in different populations of hematopoietic cells as detected by the *in vitro* colony assay method., *Exp. Hematol.* 2 (1974) 83–92. <http://www.ncbi.nlm.nih.gov/pubmed/4455512>.
- [94] Z. Si, X. Wang, C. Sun, Y. Kang, J. Xu, X. Wang, Y. Hui, Adipose-derived stem cells: Sources, potency, and implications for regenerative therapies, *Biomed. Pharmacother.* 114 (2019) 108765. <https://doi.org/10.1016/j.biopha.2019.108765>.
- [95] N. Kosaric, H. Kiwanuka, G.C. Gurtner, Stem cell therapies for wound healing, *Expert Opin. Biol. Ther.* 19 (2019) 575–585. <https://doi.org/10.1080/14712598.2019.1596257>.
- [96] W.U. Hassan, U. Greiser, W. Wang, Role of adipose-derived stem cells in wound healing, *Wound Repair Regen.* 22 (2014) 313–325. <https://doi.org/10.1111/wrr.12173>.

- [97] M.T. Cerqueira, R.P. Pirraco, T.C. Santos, D.B. Rodrigues, A.M. Frias, A.R. Martins, R.L. Reis, A.P. Marques, Human Adipose Stem Cells Cell Sheet Constructs Impact Epidermal Morphogenesis in Full-Thickness Excisional Wounds, *Biomacromolecules*. 14 (2013) 3997–4008. <https://doi.org/10.1021/bm4011062>.
- [98] M.T. Cerqueira, A.P. Marques, R.L. Reis, Using stem cells in skin regeneration: possibilities and reality., *Stem Cells Dev*. 21 (2012) 1201–14. <https://doi.org/10.1089/scd.2011.0539>.
- [99] V.-I. Alexaki, D. Simantiraki, M. Panayiotopoulou, O. Rasouli, M. Venihaki, O. Castana, D. Alexakis, M. Kampa, E.N. Stathopoulos, E. Castanas, Adipose Tissue-Derived Mesenchymal Cells Support Skin Reepithelialization through Secretion of KGF-1 and PDGF-BB: Comparison with Dermal Fibroblasts, *Cell Transplant*. 21 (2012) 2441–2454. <https://doi.org/10.3727/096368912X637064>.
- [100] B.-R. Zhou, Y. Xu, S.-L. Guo, Y. Xu, Y. Wang, F. Zhu, F. Permatasari, D. Wu, Z.-Q. Yin, D. Luo, The Effect of Conditioned Media of Adipose-Derived Stem Cells on Wound Healing after Ablative Fractional Carbon Dioxide Laser Resurfacing, *Biomed Res. Int*. 2013 (2013) 1–9. <https://doi.org/10.1155/2013/519126>.
- [101] M.M. McLaughlin, K.G. Marra, The use of adipose-derived stem cells as sheets for wound healing, *Organogenesis*. 9 (2013) 79–81. <https://doi.org/10.4161/org.24946>.
- [102] J. Yang, M. Yamato, T. Shimizu, H. Sekine, K. Ohashi, M. Kanzaki, T. Ohki, K. Nishida, T. Okano, Reconstruction of functional tissues with cell sheet engineering., *Biomaterials*. 28 (2007) 5033–43. <https://doi.org/10.1016/j.biomaterials.2007.07.052>.
- [103] K. Nishida, M. Yamato, Y. Hayashida, K. Watanabe, N. Maeda, H. Watanabe, K. Yamamoto, S. Nagai, A. Kikuchi, Y. Tano, T. Okano, Functional bioengineered corneal epithelial sheet grafts from corneal stem cells expanded ex vivo on a temperature-responsive cell culture surface, *Transplantation*. 77 (2004) 379–385. <https://doi.org/10.1097/01.TP.0000110320.45678.30>.
- [104] R. Takagi, M. Yamato, N. Kanai, D. Murakami, M. Kondo, T. Ishii, T. Ohki, H. Namiki, M. Yamamoto, T. Okano, Cell sheet technology for regeneration of esophageal mucosa., *World J. Gastroenterol*. 18 (2012) 5145–50. <https://doi.org/10.3748/wjg.v18.i37.5145>.

- [105] M. Hasegawa, M. Yamato, A. Kikuchi, T. Okano, I. Ishikawa, Human Periodontal Ligament Cell Sheets Can Regenerate Periodontal Ligament Tissue in an Athymic Rat Model, *Tissue Eng.* 11 (2005) 469–478. <https://doi.org/10.1089/ten.2005.11.469>.
- [106] N. Sekiya, G. Matsumiya, S. Miyagawa, A. Saito, T. Shimizu, T. Okano, N. Kawaguchi, N. Matsuura, Y. Sawa, Layered implantation of myoblast sheets attenuates adverse cardiac remodeling of the infarcted heart, *J. Thorac. Cardiovasc. Surg.* 138 (2009) 985–993. <https://doi.org/10.1016/j.jtcvs.2009.02.004>.
- [107] K. Matsuura, A. Honda, T. Nagai, N. Fukushima, K. Iwanaga, M. Tokunaga, T. Shimizu, T. Okano, H. Kasanuki, N. Hagiwara, I. Komuro, Transplantation of cardiac progenitor cells ameliorates cardiac dysfunction after myocardial infarction in mice, *J. Clin. Invest.* 119 (2009) 2204–17. <https://doi.org/10.1172/JCI37456>.
- [108] S. Masuda, T. Shimizu, M. Yamato, T. Okano, Cell sheet engineering for heart tissue repair, *Adv. Drug Deliv. Rev.* 60 (2008) 277–285. <https://doi.org/10.1016/j.addr.2007.08.031>.
- [109] T. Okano, N. Yamada, H. Sakai, Y. Sakurai, A novel recovery system for cultured cells using plasma-treated polystyrene dishes grafted with poly(N-isopropylacrylamide), *J. Biomed. Mater. Res.* 27 (1993) 1243–1251. <https://doi.org/10.1002/jbm.820271005>.
- [110] T. Okano, N. Yamada, M. Okuhara, H. Sakai, Y. Sakurai, Mechanism of cell detachment from temperature-modulated, hydrophilic-hydrophobic polymer surfaces, *Biomaterials.* 16 (1995) 297–303. [https://doi.org/10.1016/0142-9612\(95\)93257-E](https://doi.org/10.1016/0142-9612(95)93257-E).
- [111] M. Costa, R.P. Pirraco, M.T. Cerqueira, R.L. Reis, A.P. Marques, Growth Factor-Free Pre-vascularization of Cell Sheets for Tissue Engineering, in: *Methods Mol. Biol.*, 2016: pp. 219–226. https://doi.org/10.1007/7651_2016_362.
- [112] M.E.L. Lago, M.T. Cerqueira, R.P. Pirraco, R.L. Reis, A.P. Marques, Skin in vitro models to study dermal white adipose tissue role in skin healing, in: *Ski. Tissue Model. Regen. Med.*, Elsevier, 2018: pp. 327–352. <https://doi.org/10.1016/B978-0-12-810545-0.00014-0>.
- [113] J. Na, S.Y. Song, J.D. Kim, M. Han, J.S. Heo, C.E. Yang, H.O. Kim, D.H. Lew, E. Kim, Protein-Engineered Large Area Adipose-derived Stem Cell Sheets for Wound Healing, *Sci. Rep.* 8 (2018) 15869. <https://doi.org/10.1038/s41598-018-34119-x>.

- [114] M. Hamada, T. Iwata, Y. Kato, K. Washio, S. Morikawa, H. Sakurai, M. Yamato, T. Okano, Y. Uchigata, Xenogeneic transplantation of human adipose-derived stem cell sheets accelerate angiogenesis and the healing of skin wounds in a Zucker Diabetic Fatty rat model of obese diabetes, *Regen. Ther.* 6 (2017) 65–73. <https://doi.org/10.1016/j.reth.2017.02.002>.
- [115] R.S. Rees, M.C. Robson, J.M. Smiell, B.H. Perry, Becaplermin gel in the treatment of pressure ulcers: a phase II randomized, double-blind, placebo-controlled study., *Wound Repair Regen.* 7 (1999) 141–7. <https://doi.org/10.1046/j.1524-475x.1999.00141.x>.
- [116] S. Vadhan-Raj, J.D. Goldberg, M. Perales, D.P. Berger, M.R.M. Brink, Clinical applications of palifermin: amelioration of oral mucositis and other potential indications, *J. Cell. Mol. Med.* 17 (2013) 1371–1384. <https://doi.org/10.1111/jcmm.12169>.
- [117] Z. Wen-jing, Y. Li, L. Xue-dong, Z. Dong, Issues within Keratinocyte Growth Factor (KGF) research, *J. For. Res.* 16 (2005) 335–338. <https://doi.org/10.1007/BF02858203>.
- [118] J.R. Yu, J. Navarro, J.C. Coburn, B. Mahadik, J. Molnar, J.H. Holmes, A.J. Nam, J.P. Fisher, Current and Future Perspectives on Skin Tissue Engineering: Key Features of Biomedical Research, Translational Assessment, and Clinical Application, *Adv. Healthc. Mater.* 8 (2019) 1801471. <https://doi.org/10.1002/adhm.201801471>.
- [119] A.M. Hocking, N.S. Gibran, Mesenchymal stem cells: Paracrine signaling and differentiation during cutaneous wound repair, *Exp. Cell Res.* 316 (2010) 2213–2219. <https://doi.org/10.1016/j.yexcr.2010.05.009>.
- [120] D.J. Mooney, H. Vandenberg, Cell Delivery Mechanisms for Tissue Repair, *Cell Stem Cell.* 2 (2008) 205–213. <https://doi.org/10.1016/j.stem.2008.02.005>.
- [121] G. CHEN, Y. QI, L. NIU, T. DI, J. ZHONG, T. FANG, W. YAN, Application of the cell sheet technique in tissue engineering, *Biomed. Reports.* 3 (2015) 749–757. <https://doi.org/10.3892/br.2015.522>.

CHAPTER II.

Materials and Methods

CHAPTER II. Materials and Methods

This chapter provides an overview on the materials and the biological assays performed throughout this thesis. Moreover, it aims at describing detailed protocols for all the techniques used, both in the formulation of the different strategies and in the characterization of the outcomes achieved.

2.1. Materials**2.1.1. Gellan Gum**

Gellan gum is an anionic exopolysaccharide of natural origin secreted from *Shingomonas elodea*, and consists on repeating tetra saccharide units of glucose, glucuronic acid and rhamnose residues in a 2:1:1 ratio (Figure 2.1), resembling ECM glycosaminoglycan composition [1–3].

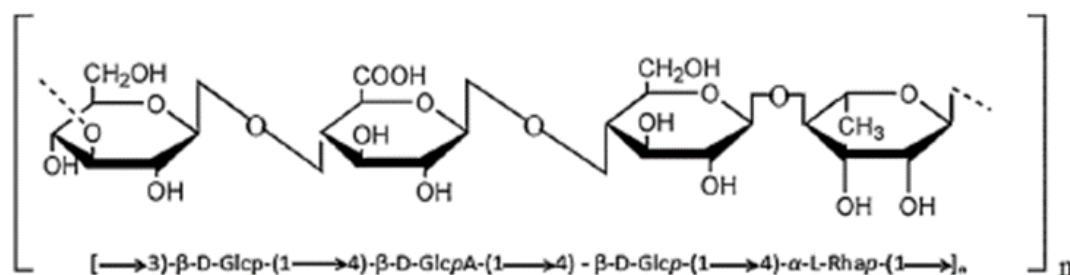


Figure 2.1 - Chemical structure of deacetylated gellan gum. Adapted from Prajapati *et al.* [4].

Industrially, glyceryl and acetyl substituents are removed by fermentation medium with hot alkaline solution obtaining a deacetylated polymer with $2\text{-}3 \times 10^5$ Da, soluble in both hot and cold water [4,5]. The deacetylation results in change of soft, elastic and thermoreversible to a firm, brittle and with higher thermal stability gels, and depending on the degree of deacetylation, GG can be high acyl (partially deacetylated) or low acyl (highly deacetylated) [4–6]. Due to the low number of acyl groups on GG low acyl, hydration depends on the type and concentration of the ions, being soluble in deionized water at room temperature [4]. At low temperatures, GG forms an orderly double helix structure, while at higher temperatures, it presents a single polysaccharide chain, reducing significantly the viscosity of the solution, which means that it undergoes through a thermally reversible coil to double helix transition, thus forming hydrogels [4,6].

Gellan Gum is a biodegradable, biocompatible and non-toxic polymer with pH between 2-10, being resistant to the action of different enzymes like pectinase, amylase, cellulase, papain and lipase [4]. It is widely used in different industries, such as pharmacy, biomedicine, food and tissue engineering (TE) [4]. In tissue engineering, in particular, it has been mostly used as a material for cartilage reconstructions, working as injectable carriers for autologous cells transplantation [7,8], for bone regeneration as GG microspheres grafted within gelatin to delivery cells [9], for dental cavity fillings after tooth extraction as sponges [10], for rheumatoid arthritis treatment and for artificial veins design as gellan sulfate materials [11,12], for wound healing by using spongy-like hydrogels, in order to recreate cellular microenvironment contributing to re-epithelialization and neovascularization [13–15]. Thus, GG has shown to be a material with versatile processing methodologies that has been explored in a wide range of applications.

2.1.2. Gellan Gum Particles

As described, GG can be differently processed giving rise to distinct platforms for cell and drug delivery to the desired location [5]. Gellan Gum beads and capsules have been studied due their potential of carrying drugs and produced with the help of an aqueous solution of Ca^{2+} ions, forming a three-dimensional network by cross-linking the polymer chains [5].

Gellan Gum particles were obtained by using the technique double emulsion water-in-oil-in-water (Figure 2.2) [16]. For each reaction, 1 mL of 1% (w/v) gelzan (Sigma-Aldrich, Portugal) solution was prepared and kept at 90 °C under stirring for 30 minutes. After stabilization at 40 °C, a drop of tween-20 (Sigma-Aldrich, Portugal) was added to prevent the formation of soluble aggregates [17]. GG solution was emulsified with 3 mL of 0.5% (v/v) span-80 (Sigma-Aldrich, Portugal) in chloroform (Fisher Scientific, UK) as a second liquid phase [18], using ultraturrax (T18 BASIC, IKA) for 3 minutes to homogenize. Following that, GG solution and 5 mL of 60% (w/v) calcium chloride (CaCl_2 ; Merck, Germany), were dropped wise crosslinked, forming direct bridges between pairs of double helix due to the exposure to Ca^{2+} [19], to 15 mL of 3.5% (w/v) poly(vinyl alcohol) (PVA; Sigma-Aldrich, Portugal) for suspension polymerization and stabilization [20,21], with continuous stirring. Chloroform was removed using a rotatory vacuum evaporator, and the solution passed through a 100 μm strainer (Falcon, USA) in order to avoid aggregates. To recover the particles, centrifugation was performed for 1 hour at 13751 g and then, after discarding the supernatant and the pellet resuspended with deionized water, the solution was passed through a 70 μm strainer (Falcon, USA). The particles were washed with deionized water for extra 3 times by

centrifugation for 10 minutes at 13751 g to remove PVA and ions Ca^{2+} , obtaining polydisperse particles. Then, the selection of the particles ($< 1 \mu\text{m}$) was performed by passing the particles through strainers (pluriSelect Life Science, Germany) with different sizes, 10 μm , 5 μm and 1 μm . In the end, the polydisperse particles and particles $< 1 \mu\text{m}$ were freeze-dried for a week and kept at room temperature (RT).

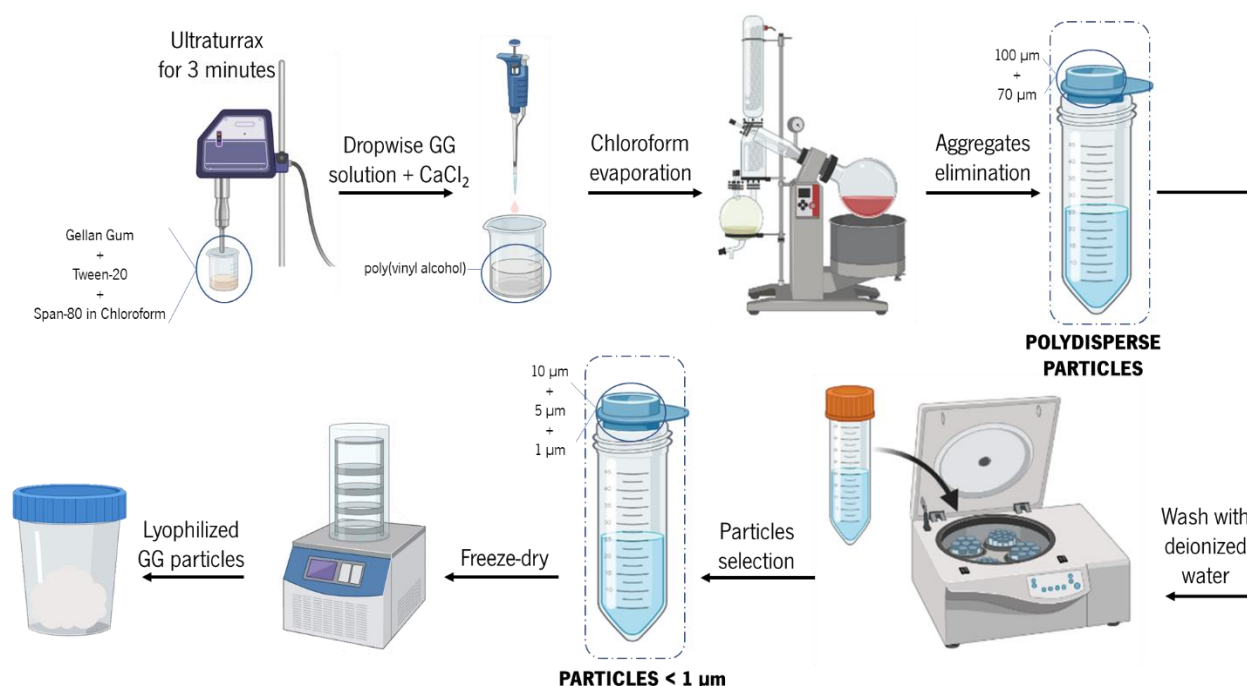


Figure 2.2 - Schematic overview of GG particles fabrication protocol for polydisperse particles and particles $< 1 \mu\text{m}$.

Nanoparticles in aqueous suspensions tend to become physically unstable leading to aggregation/particle fusion and therefore the objective of freeze-drying the particles is to improve their physical and chemical stability by removing the water [21]. The process of freeze-drying the particles consists of three steps: freezing (solidification), primary drying (ice sublimation) and secondary drying (desorption of unfrozen water), where, in the end, the particles exhibit all the physical and chemical characteristics preserved, acceptable relative humidity and long-term stability [21].

Ultraviolet light, was chosen as a sterilization method, given that the particles exceed the maximum range of filtration for sterilization ($> 0.22 \mu\text{m}$). Ultraviolet light sterilization is widely used to sterilize microorganisms in several fields, since they absorb UV light and the DNA is destroyed, leading to disinfection [22]. To assess the feasibility of UV light exposure to sterilize these particles, they were placed

inside a petri dish and sealed with parafilm. Inside a laminar flow chamber (BH-EN 2000 S/D, Faster), the particles were exposed with UV light ($\lambda \approx 254$ nm) for 15 minutes, and after that time, the petri dish was flipped over and exposed again for 15 minutes more and saved until further use. To further test if UV sterilization was successful, the particles were resuspended in alpha Minimum Essential Medium (α -MEM; Fisher Scientific, USA). Through the Streak Plate Procedure, designed to grow and isolate pure cultures of bacteria or colonies [23], drops of the particles' suspension were released in an agar plate and spread over the petri dish. In the end the plate was incubated for 24 hours upside down, so that the condensation did not drip on the colonies. After 24 hours, not a single colony was observed on the agar plate, meaning that the sterilization was successfully accomplished.

2.1.2.1. Protein loading/release strategies

The preliminary experiences were performed with Bovine Serum Albumin (BSA; Sigma-Aldrich, Portugal). This protein besides its similar properties, molecular weight and amino acid sequence to human serum albumin [122], the low cost associated to its purification and use makes this protein appealing in a variety of laboratory applications. After that, the assays were performed with KGF, that was selected for this project as it is known to be a strong candidate for wound re-epithelialization, as explained throughout the thesis. Before loading KGF (PeproTech, USA) on GG particles, KGF was reconstituted, according to manufacturer indications. To reconstitute KGF, the vial was centrifugated prior to opening and 500 μ L of Phosphate Buffered Saline (PBS; Sigma-Aldrich, Portugal) was added to have a concentration of 0.1 mg/mL. To extend the storage to 3 months, a solution 0.1% (w/v) of BSA was added and aliquots were prepared and stored at -80 °C. For both proteins, two different strategies for the release were studied opening a possibility for two different therapeutic approaches. One where the particles with entrapped protein were ready to use (Lyophilized), and the other one where the particles had no protein/drug incorporated but with possibility of adding the protein at the time of application (Non-Lyophilized) (Figure 2.3).

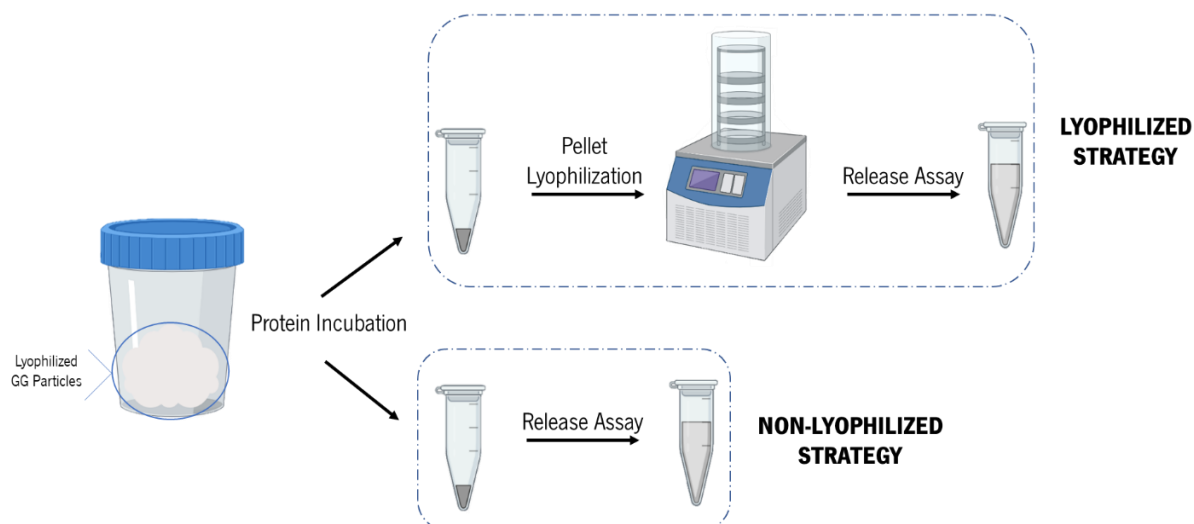


Figure 2.3 - Illustration depicting the differences between the termed Non-Lyophilized and Lyophilized strategies for protein release assays, performed after the last step of the particle's fabrication protocol.

2.1.2.1.1. Non-Lyophilized Strategy

Non-lyophilized strategy consisted on incubating the protein using the particles after the production. Briefly, four conditions (10 μg , 5 μg , 1 μg and 0 μg) for the loading of the particles were prepared, each one of it on 1 mg of GG particles. The particles were incubated with a stock solution of 0.05% (w/v) BSA in PBS with a total volume of 100 μL . The particles were incubated overnight with agitation at 37 $^{\circ}\text{C}$. The samples were centrifugated for 10 minutes at 12.3 g and the supernatant was removed and saved at -80 $^{\circ}\text{C}$, corresponding to the amount of BSA not loaded. To each sample 1300 μL of Sodium Chloride (NaCl; Panreac, Spain), pH=7.4 was added. The particles were resuspended and incubated at 37 $^{\circ}\text{C}$ under agitation. At each time point (1 hour, 3 hours, 6 hours, 9 hours, 24 hours, 48 hours and 72 hours), samples were centrifugated for 10 minutes at 12.3 g and 160 μL were removed and saved at -80 $^{\circ}\text{C}$.

2.1.2.1.2. Lyophilized Strategy

This strategy refers to the use to the same process as above, but with a subsequent step of lyophilization after protein incorporation, aiming at a ready-to-use approach. After analysis of the results obtained with BSA, as explained in the subsection above, the condition of 10 $\mu\text{g}/\text{mL}$ was the only concentration where the release values were within the range of the standard curve of Micro BCA assay and being so, it was selected to be used in further studies with KGF. In this sense, KGF release profile

(with previously tested BSA concentration) was performed for non-lyophilized and lyophilized strategies using NaCl with different pH (4, 7.4 and 10) to study the release profile in these different scenarios.

The incubation and release of both proteins was done as explained before (see section 2.1.2.1.1.). After the incubation of the proteins and the supernatant removed, the particles were freeze-dried for 24 hours and then ready to use. Then, the particles were resuspended in NaCl and the release performed, as described above (see section 2.1.2.1.1.).

2.2. *In vitro* Methodologies

2.2.1. Cell Isolation from Human Tissues

Human skin samples were obtained from abdominoplasty surgeries, while human subcutaneous adipose tissue was obtained from liposuction procedures. These surgeries were performed at Hospital São João (Porto, Portugal) with informed consent and under a collaboration protocol with 3B's Research Group approved by the ethical committees of both institutions.

2.2.1.1. Human Adipose Stem Cells Isolation from Adipose Tissue

Human adipose stem cells represent an interesting cell type in cutaneous wound healing scenario, as they can secrete a range of favorable angiogenic factors, inducing skin neovascularization, is immune-privileged, stimulates the production of anti-inflammatory cytokines, is multi-potent, reduces wound contraction, attenuating scar formation, and induces keratinization, and thus in better skin healing [25–27].

Subcutaneous adipose tissue obtained from liposuction procedures were transported in PBS (Sigma-Aldrich, Portugal) with 10% Antibiotic/Antimycotic (AB; Fisher Scientific, USA), under controlled temperature conditions, and processed within 24 hours after collection. Samples were washed with PBS, in order to remove most of the blood and incubated with 0.05% Collagenase Type II (Sigma-Aldrich, UK) under agitation for 45 minutes at 37 °C. The digested samples were filtered and centrifuged at 800 g for 10 minutes to pellet the stromal vascular fraction (SVF) that was resuspended with red blood cell lysis buffer (155 mM of Ammonium Chloride, 12 mM of Potassium Bicarbonate and 0.1 M of Ethylenediaminetetraacetic Acid, all from Sigma-Aldrich, Germany) in distilled water, incubated for 10 minutes at room temperature and centrifugated at 300 g for 5 minutes.

The supernatant was then discarded and red blood cells-free SVF was resuspended in α -MEM, supplemented with 10% Fetal Bovine Serum (FBS; Life Technologies, Netherlands) and 1% AB, and plated in T150 cm² flasks. hASCs were selected by adherence to tissue culture polystyrene (TCPS) surfaces 5 days after isolation and harvested at 90% confluence along the passages.

2.2.1.2. Human Keratinocytes Isolation from Skin in Feeder Layer Culture System

Feeder-Layer Culture System

The cell line 3T3-J2 is a subclone of the original mouse embryonic fibroblast line from a Swiss mouse [28] and it was kindly provided by Professor Fiona Watt laboratory at King's College London. Cells of this sub-clone are known to, after mitotic inactivation, support epithelial cells, namely keratinocytes, acting as feeder cells [29].

Before inactivation, each T75 flask is harvested with $1-2 \times 10^5$ cells, until reaching confluency with approximately $3-6 \times 10^6$ cells. To inhibit the proliferation, 4 $\mu\text{g}/\text{mL}$ of Mitomycin C (Sigma-Aldrich, UK) was added to the confluent flask and incubated for 2 hours at 37 °C, medium was removed, and the flasks washed with 0.02% Ethylenediaminetetraacetic acid (EDTA; Sigma-Aldrich, Portugal). Then, cells were harvested in 0.05% Trypsin-EDTA (Fisher Scientific, USA) and divided into a T75 flask with the optimal density of 1.8×10^6 cells.

hKCs Isolation

Skin Samples, with adjacent adipose tissue, were collected in sterile containers with 100 mL solution of PBS with 10% AB, transported under controlled temperature conditions and processed within 24 hours after collection. Skin tissue was disposed from the adjacent adipose tissue, washed with PBS, cut in small fragments (roughly 1 cm²) and incubated overnight in Dispase (2.4 U/mL) (BD Biosciences, USA) in PBS with 1% AB at 4 °C.

After enzymatic digestion with dispase, epidermis was carefully peeled off, using forceps, and further digested by 0.05% Trypsin-EDTA. After an incubation period of 5-7 minutes at 37 °C, digested tissue was filtrated through a sterile 100 μm cell strainer (Falcon, USA) and centrifugated at 420 g for 5 minutes. The supernatant was discarded, the pellet resuspended in FAD medium and the cell suspension was filtered again through a 100 μm cell strainer and 0.3×10^6 cells plated into T75 cm² tissue culture

flasks (Falcon, USA), on top of feeders, prepared as described above. FAD medium consists of Dulbecco's Modified Eagle's Medium - high glucose (DMEM; Sigma-Aldrich, UK) and Dulbecco's Modified Eagle's Medium - high glucose/Ham's Nutrient Mixture F12 (DMEM/F12; Sigma-Aldrich, UK) (3:1), supplemented with 1.8×10^{-4} M of Adenine Hemisulfate Salt (Sigma-Aldrich, UK), 10% of non-activated FBS, Insulin (5 μ g/mL) (Sigma-Aldrich, UK), 1% of L-Glutamine (200 mM) (Fisher Scientific, USA), 1.8 mM of Calcium Chloride (Merck, UK), 1% of Penicillin-Streptomycin 10k/10k (Lonza, Switzerland) and HCE cocktail. This cocktail comprises Hydrocortisone (0.05 μ g/mL) (Sigma-Aldrich, UK), 10^{-10} M of Cholera Enterotoxin (Sigma-Aldrich, USA) and 10 ng/mL of Recombinant Human Epidermal Growth Factor (rEGF; PeproTech, USA). Approximately 7 days after plating, prior to confluence, hKCs were trypsinized and then sub-cultured either in a feeder-layer system, for expansion, or feeder-free hKCs culture, for the different subsequent studies.

2.2.1.2.1. Subculture of Human Keratinocytes

Feeder-Layer Culture System

For the sub-culture of hKCs, $2-3 \times 10^5$ of hKCs were placed on T75 inactivated feeders previously prepared, where they grow as colonies. After confluency of hKCs, feeders were removed and hKCs were trypsinized. For that, FAD medium was discarded, and cells were washed with 1X PBS and then with 0.02% EDTA. Fresh 2.5 mL of EDTA was added and incubated for 5 minutes at 37 °C, selectively detaching the feeders from the flask by gentle aspiration with a pipette, leaving hKCs alone in the flask. For the detachment of hKCs, 2.5 mL of 0.05% Trypsin-EDTA was added to the T75 flask and incubated for about 5-10 minutes at 37 °C. To inactivate the Trypsin, 5 mL of FAD medium was added, and the cells were transferred to a centrifuge tube. hKCs were recovered by centrifugation at 200 g for 5 minutes, supernatant was discarded, and further cultured at $2-3 \times 10^5$ density on T75 flask with inactivated feeders in FAD medium.

Feeder-Free hKCs Culture

In the feeder-free system, hKCs were detached from feeder layers, as explained above, with additional 2 times centrifugation before resuspension in Keratinocyte Serum Free Medium (KSFM; Fisher Scientific, USA) supplemented with the Human Keratinocyte Growth Supplement Kit (Fisher Scientific, USA) containing 5 ng/mL of rEGF, 50 μ g/mL of Bovine Pituitary Extract (BPE), and with 1% AB.

Additionally, for expansion in this system, Y27632 dihydrochloride (ROCK inhibitor; Enzo Life Sciences, USA) was added to culture medium at a concentration of 1% (v/v), as this inhibitor is known to regulate the differentiation and proliferation of hKCs, leading to the inhibition of the differentiation and promotion of proliferation [30,31].

2.2.2. Cell Sheet Fabrication

Cell sheet engineering was proposed by Okano *et al.* [32] with several applications in biomedical field as a scaffold-free tissue engineering, since the cell's self-extracellular matrix acts as a natural scaffold, retaining cell-cell and cell-ECM junctions, which have been also pointed out to enhance cellular residence time and to promote full thickness skin wound regeneration when using either MSCs or skin-related lineages [25,33].

For CS fabrication, 3×10^5 cells of hASCs were plated on a 6-well plate and cultured for 5 days in α -MEM medium, supplemented with 10% FBS, 1% AB and 50 $\mu\text{g}/\text{mL}$ of Ascorbic Acid (A/A; Wako Pure Chemical Industries, USA), at 37 °C in humidified atmosphere with 5% CO_2 . By adding A/A to the culture media, collagen production was stimulated, leading to the production and organization of ECM, and therefore, to the formation of a confluent hASCs layer with a thick collagenous matrix, as previously described [25].

2.2.3. hKCs and hASCs Direct Contact

Direct co-cultures of hASCs-hKCs were performed using different methodologies to promote the contact between these cell types: via cell sheet (hASCs cell sheet on top of a confluent monolayer of hKCs) and via cell suspension (cell suspension on top of a confluent monolayer of hKCs). The production of KGF from these co-cultures was quantified in the resultant CM after different culture periods (48 and 72 hours). In order to have a precise quantification and to assess the co-culture effects, adequate controls comprising hASCs and hKCs monocultures were also performed. Furthermore, for accurate normalization of the amount of KGF released, cell proliferation effect was quantified by DNA assay quantification, and contribution of the two cell types in culture was assessed by flow cytometry with exclusive identity markers, as further described.

hASCs were isolated from subcutaneous adipose tissue as explained on section 2.2.1.1. and cultured with α -MEM medium supplemented with 10% FBS, 1% AB at 37 °C in humidified atmosphere

with 5% CO₂. The medium was changed every 2-3 days until 90 % confluency was reached, and the cells were used at passage 2 to 4. Human keratinocytes were isolated from skin tissue as explained on section 2.2.1.2., used at passage 1 to 3 and at density of 1.5×10^5 cells/well, were plated on a 12-well plate and cultured for 5 days with 500 μ L of KSFM and ROCK inhibitor at 37 °C in humidified atmosphere with 5% CO₂.

2.2.3.1. hASCs-CS Based

After 5 days, the contact of hASCs-CS on top of hKCs was performed with the help of the tip of the micropipette the cell sheet was detached from the well and the keratinocytes were washed with 1X PBS. The previously obtained CS was placed on top with a combination of 1:1 KSFM / α -MEM (total 500 μ L) for 48 hours and 72 hours.

2.2.3.2. Cellular Suspension

Prior to the contact of the cell suspension, hKCs were washed with 1X PBS, then a suspension of hASCs at density of 5×10^4 cells/well was seeded on top of the hKCs with 1:1 KSFM/ α -MEM (total 500 μ L) for 48 hours and 72 hours.

Control condition comprising hASCs was done the same day as the fabrication of the cell sheets, at density of 1.5×10^5 cells/well with 500 μ L of α -MEM medium. The control of hKCs was also performed using the same cellular density with 500 μ L of KSFM plus ROCK inhibitor, and both controls cultured for 5 days.

For either co-culture methodology used, at each time point, the CM was removed and centrifugated for 10 minutes at 366 g. The supernatant was filtered with the help of a syringe and a 0.22 μ m filter (TPP, Switzerland), then stored at -80 °C until further usage.

2.2.4. hKCs Contact with Gellan Gum Particles

The internalization and proliferation induced by GG particles were assessed and described in the subsequent sections.

2.2.4.1. Internalization of GG Particles by hKCs

The internalization was evaluated both through flow cytometry and transmission electron microscopy (TEM).

For flow cytometry analysis, GG particles functionalized with a fluorescent conjugate, Biotin (5-fluorescein) conjugate (Biotin-FITC; Sigma-Aldrich, Portugal) were used. To achieve a more stable and stronger immobilization, N-(3-Dimethylaminopropyl)-N'-ethylcarbodiimide hydrochloride/N-Hydroxysulfosuccinimide sodium salt (EDC/NHS; Sigma-Aldrich, Portugal) was used as a linker to enhance the efficiency of the binding. EDC reacts with carboxylic groups (from protein or substrate) generating an unstable reactive ester, O-acylisourea. In combination of NHS, a semi-stable amine-reactive NHS-ester is formed. These species can interact with the amine groups (from the protein or substrate) establishing a covalent bond between the protein [34], which in this case is NeutrAvidin Protein (NaV; Thermo Fisher Scientific, USA), that will in the end be linked with Biotin-FITC. NaV was used to decrease the background in biotin-binding. For that, 1 mg of particles was dissolved in 1 mL of 2-N-morpholino(ethanesulfonic acid hydrate) buffer (MES; Sigma-Aldrich, USA), 100 μ L of 4% (w/v) EDC in MES buffer and 100 μ L of 4.8% (w/v) NHS in MES buffer and incubated for 1 hour at RT. Then the particles were washed 3 times with 1 mL of PBS, in which were centrifugated at 18000 g for 10 minutes between the washes. The particles were resuspended in 500 μ L of 0.1% (w/v) NaV and incubated for 4 hours at RT in the dark. After, the particles were again washed 3 times as explained before, and resuspended 155 μ L of 0.01% (w/v) of Biotin-FITC, added 345 μ L of PBS and incubated overnight at 4 °C. The next day, 3 more washes were performed, the particles were dissolved in KSFM to put in contact with hKCs and to be observed by Transmitted and Reflected Light Microscope with Apotome 2 (Axio Imager Z1m, Zeiss). The particles analyzed by TEM did not contain any fluorescence. For both assays, hKCs at density of 3.75×10^5 cells/well, were plated on a 6-well plate and cultured for 48 hours in KSFM and ROCK inhibitor at 37 °C in humidified atmosphere with 5% CO₂. Then, the medium was discarded and 2 mL of 5% (v/v) GG particles functionalized with Biotin-FITC or 2 mL of 5% (v/v) GG particles without the functionalization was added to the wells. After 72 hours, the cells were analyzed by flow cytometry and by TEM.

2.2.4.2. Effect of GG Particles in hKCs Proliferation

After analyzing the results of the release assays with 10 μ g of KGF incubated on the particles, having a maximum release of 5 μ g after 72 hours, the concentration of 10 ng was chosen to proceed

with the in vitro assays, as was already proven to be effective [35]. Particles without KGF were used as control condition.

For the particles with KGF, they were incubated with 20 μL of KGF and 80 μL of KSFM, overnight with agitation at 37 °C. While the ones without the KGF were incubated with 100 μL of KSFM, overnight with agitation at 37 °C. After, they were centrifugated for 10 minutes at 12.3 g the supernatant was removed and were resuspended in 10 mL of KSFM.

Human KCs at density of 7.4×10^4 cells/well, were plated on a 24-well plate and cultured for 24 hours in KSFM and ROCK inhibitor at 37 °C in humidified atmosphere with 5% CO_2 . Then, the medium was discarded and 500 μL of 5% (v/v) KGF-loaded particles or 500 μL of 5% (v/v) GG particles without KGF in KSFM was added to the wells. Control wells with KGF-loaded particles and without cells were used to assess the amount of KGF released to the culture medium. After 72 hours, the medium was saved to further be analyzed by ELISA, some cells frozen to -80 °C for the DNA to be quantified and other were fixed and placed at 4 °C to see if proliferation and receptor markers were present.

2.2.5. Migration Assay

For the migration assay, culture inserts 2 well 24 ibiTreat, μ -plate 24 well were used to mimic the wound gap in a real scenario. In this sense, the effect of CM from hKCs and hASCs direct co-cultures, respective monoculture controls and GG particles were tested. Furthermore, in order to validate the contribution of KGF in the observed outcomes, Keratinocyte Growth Factor Antibody (KGF ab; Fisher Scientific, USA) (0.6 $\mu\text{g}/\text{mL}$), was included and additional wells with this antibody and CM mentioned above were tested.

The assay was performed according to manufacturer's instructions. In detail, 7×10^4 hKCs were plated by adding 70 μL to each well of ibidi insert in KSFM and ROCK inhibitor, at 37 °C in humidified atmosphere with 5% CO_2 . After 24 hours, ibidi inserts were removed, carefully washed with PBS, and 250 μL of medium from the conditions mentioned above were added.

This migration assay was monitored immediately and up to 20 hours by live imaging using an Inverted Microscope with Incubation (Axio Observer, Zeiss). Images were acquired every 30 minutes and processed with ZEN 3.1 (blue edition) software (Zeiss, Germany), and the closure of the wound gap was analyzed by beWound software (Biomedical Engineering Solutions Research Group, University of Minho, Portugal).

2.3. Methodologies for Particles Characterization and Analysis

2.3.1. Dynamic Light Scattering (DLS) and Zeta Potential (ZP)

The determination of the average hydrodynamic diameter, polydispersity index and surface charge are crucial for proper characterization of the particles, and for that, dynamic light scattering and zeta potential measurements were performed. In DLS, a monochromatic beam of light scatters in all directions creating fluctuations due to the Brownian motion of the molecules in solution, and in conjugation with the Stokes-Einstein equation, the particle size can be determinate [36,37]. Zeta Potential is a key parameter that controls the electrostatic interaction in particle dispersions by using the technique of micro-electrophoresis, which can be employed for understanding the physical stability of the suspension [38]. Laser Doppler electrophoresis is used to measure small frequency shifts in the scattered light that arise from the movement of the particles in an applied electric field, and then, calculating ZP or surface charge [38].

Briefly, 1 mg of GG particles were resuspended in 1 mL of ultra-pure water (UP; Milli-Q Direct 16, Millipore) then placed on a cuvette (Sarstedt, Germany) carefully to avoid the formation of bubbles. Zetasizer Nano ZS (Malvern Instruments, UK), using the parameters of temperature 25 °C and dispersant water the size and polydispersity index were measured. For the surface charge determination, the parameters were the same but on the cuvette was placed on top a Folded Capillary Zeta Cell (Malvern Instruments Inc., USA).

2.3.2. Scanning Transmission Electron Microscopy (STEM)

Scanning transmission electron microscopy (STEM) is a powerful and indispensable microscopic method that allows to study of materials at atomic resolution [39]. The principle of this technique works on the same basis as the normal scanning electron microscopy (SEM), by forming a focused beam of electrons that is scanned across the sample [40]. The difference is the sample is thinned such that the majority of electrons are transmitted, and the scattered electrons detected helps forming an image without any carbon support film or treatment of the sample [39,40].

Herein, the samples were diluted at 0.5 mg/mL in UP water followed by a further dilution of 1:20 and placed to dry on copper grids (TED PELLA Inc., USA) for further observation. Particle size and morphology were analyzed with a High-Resolution Field Emission Scanning Electron Microscope with

Focused Ion Beam (FIB-SEM) (AURIGA COMPACT, ZEISS, Germany), with an acceleration voltage of 20 kV and magnification of x50.00 k.

2.3.3. Transmission Electron Microscopy (TEM)

Transmission electron microscopy (TEM) provides images of the ultrastructure and organization of the components of tissue, cells and organisms [41]. A fine electron beam is created by a high-voltage, electric current-heated tungsten filament, focused by magnetic lenses. The electron beam passes through an ultrafine plastic section where the tissue and cellular components are fixed [42]. The electron-electron interactions between the beam and the sample transform the electrons into scattered or unscattered electrons, that are focused with magnetic lenses and then projected on a screen to generate a shadow image of variable darkness based on the density of unscattered electrons [41,42].

In this work, the cells were washed with PBS 1X and fixed with 2.5% glutaraldehyde and 2% paraformaldehyde in 0.1 M sodium cacodylate buffer (pH=7.4) for 20 minutes. With a cell scraper, the cells were removed from the wells and transferred to a falcon. Samples were then processed at Histology and Electron Microscopy unit at i3S (University of Porto) and were visualized under a Transmission Electron Microscope Jeol JEM 1400.

2.3.4. Protein Quantification

In order to quantify the amount of BSA and KGF released at each time point, Micro BCA™ Protein Assay Kit was performed according to the manufacturer's instructions (Fisher Scientific, USA). Micro BCA assay is a common method to measure proteins in solution from 0.5 µg/mL to 10 µg/mL and when a protein is placed in an alkaline environment containing Cu²⁺, the peptide bonds of the protein react with Cu²⁺ atoms, leading to the reduction of Cu²⁺ to Cu⁺, within the complexation sites of the protein [43]. Bicinchoninic acid (BCA), the detection reagent, is a sensitive, stable, water-soluble compound and highly specific for Cu⁺, establishing a 2:1 complex with Cu⁺. This results in a purple stable and highly colored complex with an absorbance at 562 nm, which increases proportionally to the protein concentration [43].

Briefly, standards were prepared at concentrations ranging from 0 µg/mL to 20 µg/mL in NaCl, pH=7.4. In each well of 96-well plate, 150 µL of standards or samples, and 150 µL of working reagent were added. The plate was sealed and incubated for 2 hours at 37 °C. After the incubation time, the plate was left to cool at room temperature and then, the absorbance was measured at 562 nm in a microplate reader (Synergy HT, Bio-Tek). The protein concentration of each sample was calculated from

the standard curve which relates the protein (Bovine Serum Albumin) concentration with the absorbance intensity. The assay was performed three independent times for each approach.

The entrapment efficiency, was calculated by the following equation:

$$\text{Entrapment Efficiency (\%)} = \frac{(\text{Total of Protein-Free Protein})}{\text{Total Protein}} \times 100 \quad (\text{Equation 2.1})$$

Where the total protein corresponded to the concentration initially incubated in the particles and the free protein to the concentration found in the supernatant removed after the incubation of the protein.

The concentration released by the particles was calculated taking in account the percentage of the entrapment efficiency, using the following equation:

$$\text{Protein Released (\%)} = \frac{\text{Micro BCA concentration}}{\text{Entrapment Efficiency}} \times 100 \quad (\text{Equation 2.2})$$

Where the Micro BCA concentration corresponded to the values obtained from the standard curve.

2.3.5. Enzyme-Linked Immunosorbent Assay (ELISA)

Enzyme-Linked Immunosorbent Assay (ELISA) is a powerful assay used for the detection and quantification of soluble substances such as proteins, peptides, antibodies, and hormones. The antigen (target macromolecule) is immobilized on a solid surface (microplate) and then complexed with an antibody that is linked to a reporter enzyme. The detection is possible with the measurement of the activity of the reporter enzyme via incubation with the appropriate substrate to produce a measurable product. The most crucial element of an ELISA is a highly specific antibody-antigen interaction [44], making it possible to detect a specific protein in culture medium, in opposition to Micro BCA. This assay was used to analyze the KGF present in the medium, either released from GG particles in contact with hKCs and in the CM recovered from direct contact between hASCs and hKCs and respective monoculture controls.

Human KGF/FGF-7 DuoSet ELISA (R&D Systems, USA) assay was performed according to the manufacturer's instructions. The wash buffer was prepared by dissolving 0.05% Tween 20 (Sigma-Aldrich, USA) in DPBS solution previously filtered. The washing steps were performed three times. The blocking

buffer was prepared by diluting reagent diluent concentrate (R&D Systems, USA) in ultra-pure water. Briefly, the wells of Nunc MaxiSorp 96-well plate (Thermo-Fisher, USA) were coated with 100 μ L of capture antibody, overnight at room temperature. The wells were washed three times with 400 μ L of wash buffer and then, 300 μ L of blocking buffer (reagent diluent) was incubated for 1 hour at room temperature. The wells were again washed three times and 100 μ L of standards diluted in reagent diluent, at concentrations ranging from 0 to 2000 pg/ml, and samples with unknown KGF concentration were added to the coated wells, in triplicate for 2 hours, at room temperature, so that the antigen from the samples binded to the immobilized antibody at the bottom of the wells. After incubation, the washing step was performed and 100 μ L of detection antibody was added to the wells for additional 2 hours, at room temperature, in order to bind to the captured antigen. Afterwards, the wells were again washed and Streptavidin-HRP was added for 20 minutes, at room temperature, protected from light and washed again. After this, 100 μ L of substrate solution composed of a 1:1 mix of color reagent A and color reagent B from the kit was added to each well and incubated for 20 minutes, protected from light, having a blue shading on the top four standard wells, while the remaining standards continued clear. To complete the procedure, 50 μ L of stop solution was added to each well, and the color immediately changed to yellow. The absorbance was immediately read on a microplate reader (Synergy HT, Bio-Tek) at 450 nm, 540 nm and 570 nm, and then, the 570 nm absorbance was subtracted to 450 nm for correction of optical imperfections in the plate.

2.3.6. Cell Proliferation Assessment

The assessment of cell proliferation is essential in numerous biological studies, being an important indicator of cells health. Fluorochromes that interacts with DNA are commonly used to measure the number of cells by quantifying their DNA [45]. Cell proliferation was assessed using a fluorometric quantification Kit (Quant-iT™, PicoGreen®; Molecular Probes, Invitrogen, USA). PicoGreen is a fluorescence dye that binds specifically to double-stranded DNA (dsDNA). When bound to dsDNA, the dye is excited at 480 nm and emits at 520 nm [45].

Both hKCs and hASCs co-cultures, monocultures controls and hKCs after contact with GG particles-loaded/non-loaded with KGF (see section 2.2.3. and 2.2.4.) were analyzed, and at each time point, the samples were washed 2X with PBS and the adhered cells of the cell sheets were lysed by using 1mL/well of Lysis Buffer and the other cell types with UP water. The Lysis Buffer consists of 10 mM of Tris(hydroxymethyl)aminomethane (Tris; Thermo-Fisher, UK), 1 mM EDTA (Sigma-Aldrich, Portugal) and

0.2% (v/v) of Triton X-100 (Thermo-Fisher, Germany) on ultrapure water, pH=8 and filtered with 0.22 µm filter. The 6-well plate were saved at -80 °C for at least 30 minutes or until further use. Before starting the DNA quantification, the samples were transferred to 37 °C for 30 minutes, and the process of freeze at -80 °C and thaw at 37 °C was repeated one more time. The volume of samples of the cell sheets was transferred to eppendorfs tubes and placed in an ultrasound bath for 15 minutes without temperature to remove all cell content.

Reagents from the kit were prepared according to the manufacturer's instructions. DNA standards, provided by the kit, were prepared in lysis buffer or in ultrapure water at concentrations ranging from 0 to 2 µg/mL for the standard curve. In each well of a white opaque 96-wells plate, 28.7 µL of sample or standard (n=3), 71.3 µL of PicoGreen solution and 100 µL of TE buffer were added. Plates were incubated in dark for 10 minutes and, then, the fluorescence was read in a microplate reader (Synergy, HT, Bio-TEK) with an excitation wavelength of 485/20 nm and emission wavelength of 528/20 nm. DNA concentration of each sample was calculated from the standard curve, which relates the DNA concentration with the fluorescence intensity.

2.3.7. Flow Cytometry

Flow cytometry is a technique that provides rapid multi-parametric analysis of single cell or particles in solution, regarding to the characterization of the surface and intracellular markers expressed or not in a certain cell population [46,47]. Each cell is analyzed for visible light scatter and one or multiple fluorescence parameters. Visible light is measured in two directions, the forward direction (Forward Scatter or FSC), which indicates the relative size of the cell and Side Scatter (SSC), which indicates the internal complexity or granularity of the cell [46]. The fluorescence measurement can be through transfection and expression of fluorescent proteins (e.g. Green Fluorescent Protein), staining with fluorescent dyes (e.g. Propidium Iodide) or staining with fluorescent conjugated antibodies (e.g. CD3 FITC) [46]. To label antibodies, fluorochromes are used namely, FITC, phycoerythrin (PE) and allophycocyanin (APC). The fluorochrome chosen depends on the laser to be used, where FITC excitation/emission maxima approx. 495/520 nm, PE excitation/emission maxima approx. 565/578 nm and APC excitation/emission maxima approx. 650/660 nm [47], which can be analyzed in most flow cytometry analyzer.

In order to detect the number of hASCs and hKCs in the co-culture assays (see section 2.2.3.), flow cytometry was used as an indirect form to assess that cellular ratio present via the expression of

CD90. This antigen is known to be strongly expressed in MSCs cells, and negative in hKCs [48,49]. Cellular monocultures of these cell types were used as controls to confirm the full or lack of CD90 expression.

To obtain a single-cell suspension, hASCs cell sheet cultured on top of hKCs was dissolved in 3 mL of 70 µg/mL of Collagenase (Sigma-Aldrich, UK) in α -MEM for 20 minutes at 37 °C, under agitation. While for plated cells, these, were washed with 1X PBS and harvested with 0.05% Trypsin-EDTA. For the cell sheet co-culture condition, the dissolved cell sheet and the hKCs were mixed and passed through a 70 µm strainer. All the conditions were centrifuged at 300 g for 5 minutes, and the supernatant was discarded and resuspended in 500 µL of Acquisition Buffer (PBS + 1% Formalin). Each condition was divided in two tubes, a control (unstained), and the tubes with cells stained for APC Mouse Anti-Human CD90 (BD Biosciences, USA). For hKCs and hASCs, 2 µL of the antibody was used, for the cell sheets and the suspension, 5 µL of antibody was used.

Samples were incubated for 30 minutes, at RT and protected from light. Then 2 mL of PBS was added to each tube, and the samples centrifuged at 500 g for 5 minutes. The supernatant was discarded, and the cells were resuspended in 300 µL of acquisition buffer.

All the samples were run in a FACS Aria III cell sorter (BD Biosciences, Belgium) and data was analyzed using FACS Diva 7.0 software. Furthermore, flow cytometry technique was used to detect internalization of functionalized particles with FITC in hKCs. As described on 2.2.4.1, the functionalized/non-functionalized particles with FITC were placed in contact with hKCs for 72 hours and then cells were harvested with trypsin and the cell suspension was run in FACS Aria III cell sorter and further analyzed in FACS Diva 7.0 software for FITC signal.

2.3.8. Immunolabelling

2.3.8.1. Immunocytochemistry

After each time point, samples (see Table 2.1) were washed three times with PBS and fixed with 1 mL of 10% (v/v) of Formalin (Thermo Fisher Scientific, USA) for 30 minutes at room temperature. After fixation time, samples were washed with PBS and left with PBS solution at 4 °C until use.

Cellular permeabilization was performed with 0.2% of Triton X-100 for 15 minutes at room temperature when targeting an intracellular antigen, Ki67 (abcam, UK). Non-specific binding was blocked in all conditions by using Normal Horse Serum 2.5% (Vector Laboratories, UK) and incubated for 40

minutes at RT. Cells were incubated with primary antibodies (see concentrations Table 2.1), diluted in 0.2% of Triton X-100 with a few drops of Normal Horse Serum 2.5% for 1 hour, RT. After that, cells were washed three times with PBS for 5 minutes. A secondary antibody was used to bind the primary antibodies, for fluorescent detection (1:500) and incubated for 1 hour at RT, washed again three times with PBS for 5 minutes. Nuclei cell were stained with 4,6-diamidino-2-phenylindole dilactate (DAPI; Biotium, USA) (1:1000) for 15 minutes, protected from light at RT. Samples were washed again to remove the excess of staining.

Table 2.1 - Panels of antibodies and conditions used to stain cell cultures by immunocytochemistry.

Tested Samples	Antibody (Reactivity/Host)	Antibody Dilution	Detection Method
hKCs hASCs hASCs-CS hASCs-suspension	Ki67 (abcam, UK), (Mouse, Rat, Human, Marmoset/Rabbit)	1:50	Fluorescence (AlexaFluor 488 Anti-Rabbit)
	FGFR2 (abcam, UK), (Human, Mouse, Rat/Rabbit)	1:500	Fluorescence (AlexaFluor 488 Anti-Rabbit)

Cells were maintained in PBS until were analyzed by Transmitted and Reflected Light Microscope with Apotome 2 (Axio Imager Z1m, Zeiss).

2.3.8.2. Phalloidin Staining

Cytoskeleton actin filaments were stained in hKCs with Phalloidin-Tetramethylrhodamine B isothiocyanate (Phalloidin; Sigma-Aldrich, USA). After fixation, a solution 1:100 of Phalloidin in PBS was incubated for 30 minutes at RT, then the wells were washed and maintained in PBS until were analyzed by Fluorescence Inverted Microscope with Incubation (Axio Observer, Zeiss).

2.3.9. Quantification of Ki67 Positive Cells

In order to quantify the number of positive cells for the proliferation marker, Ki67, ImageJ software was used to analyze 5 different microscopy images for each condition after immunocytochemistry of this

marker (green) and counterstaining with DAPI for the total cell number (blue). Briefly, color images were split in the different channels, and then were adjusted with Threshold or Make binary plug in, to separate the signal from the background and to obtain a more precise area. Then, the area for the green channel was limited with the threshold. Additionally, through the blue channel the number of nuclei was calculated using Analyze Particle plugin, to obtain the total number of cells per image.

The ratio of Ki67 positive cells (Figure 3.7.d and 3.11.d, Chapter 3), was calculated by the following equation:

$$Ki67 \text{ positive cells (\%)} = \frac{\text{Number of Green Nuclei}}{\text{Number of Blue Nuclei}} \times hKCs (\%) \quad (\text{Equation 2.3})$$

2.3.10. Wound Gap Closure *in vitro*

The closure of the wound gap created in the *in vitro* migration assay performed in section 2.2.5. was analyzed by *beWound* software. By drawing lines through the gap in every photo, the area between each side was given. The wound closure area was obtained using the following equation:

$$Wound \text{ Closure (\%)} = \frac{\text{Initial Wound Area} - \text{Actual Wound Area}}{\text{Initial Wound Area}} \times 100 \quad (\text{Equation 2.4})$$

The wound was considered completely closed when the percentage of closure was equal to 100.

2.4. Statistical Analysis

Statistical analysis of data was performed using GraphPad PRISM version 6.0. First, Shapiro-Wilk normality test was used to ascertain the data normality. For the quantitative data of the release for both proteins, showed a normal distribution and were analyzed by two-way ANOVA (several groups), succeeded by Sidak's multiple comparison test. For the data of co-cultures, the normality was rejected and non-parametric Kruskal-Wallis test, followed by Dunn's test for multiple comparisons. The studies using the particles in contact with hKCs, the data passed the normality test and were analyzed by one-way ANOVA with Tukey's post- test and unpaired t-test (one group). The normalization data was analyzed by one-way ANOVA with Tukey's multiple comparison test. The microscope data for Ki67 passed normality and were

analyzed by one-way ANOVA with Tukey's post- test and unpaired t-test (one group). For the migration assay, two-way ANOVA (several groups) was performed, succeeded by Sidak's multiple comparison test. P values lower than 0.05 were considered statistically significant and the results were expressed as median \pm standard deviation.

2.5. References

- [1] P. Matricardi, C. Cencetti, R. Ria, F. Alhaique, T. Coviello, Preparation and Characterization of Novel Gellan Gum Hydrogels Suitable for Modified Drug Release, *Molecules*. 14 (2009) 3376–3391. <https://doi.org/10.3390/molecules14093376>.
- [2] L.P. da Silva, M.T. Cerqueira, R.A. Sousa, R.L. Reis, V.M. Correlo, A.P. Marques, Engineering cell-adhesive gellan gum spongy-like hydrogels for regenerative medicine purposes., *Acta Biomater*. 10 (2014) 4787–4797. <https://doi.org/10.1016/j.actbio.2014.07.009>.
- [3] M.A. O'Neill, R.R. Selvendran, V.J. Morris, Structure of the acidic extracellular gelling polysaccharide produced by *Pseudomonas elodea*, *Carbohydr. Res.* 124 (1983) 123–133. [https://doi.org/10.1016/0008-6215\(83\)88360-8](https://doi.org/10.1016/0008-6215(83)88360-8).
- [4] C.I. (TINCU), A. SAVIN, C. LUNGU, M. POPA, GELLAN. FOOD APPLICATIONS, *Cellul. Chem. Technol.* 50 (2015) 1–13.
- [5] J.D. Oliver, A.A. Rosser, C.M. Fellows, Y. Guillaneuf, J.-L. Clement, M. Gaborieau, P. Castignolles, Understanding and improving direct UV detection of monosaccharides and disaccharides in free solution capillary electrophoresis, *Anal. Chim. Acta.* 809 (2014) 183–193. <https://doi.org/10.1016/j.aca.2013.12.001>.
- [6] V.D. Prajapati, G.K. Jani, B.S. Zala, T.A. Khutliwala, An insight into the emerging exopolysaccharide gellan gum as a novel polymer, *Carbohydr. Polym.* 93 (2013) 670–678. <https://doi.org/10.1016/j.carbpol.2013.01.030>.
- [7] J.T. Oliveira, T.C. Santos, L. Martins, M.A. Silva, A.P. Marques, A.G. Castro, N.M. Neves, R.L. Reis, Performance of new gellan gum hydrogels combined with human articular chondrocytes for cartilage regeneration when subcutaneously implanted in nude mice, *J. Tissue Eng. Regen. Med.* 3 (2009) 493–500. <https://doi.org/10.1002/term.184>.
- [8] J.T. Oliveira, T.C. Santos, L. Martins, R. Picciochi, A.P. Marques, A.G. Castro, N.M. Neves, J.F. Mano, R.L. Reis, Gellan Gum Injectable Hydrogels for Cartilage Tissue Engineering Applications: In Vitro Studies and Preliminary In Vivo Evaluation, *Tissue Eng. Part A.* 16 (2010) 343–353. <https://doi.org/10.1089/ten.tea.2009.0117>.

- [9] C. Wang, Y. Gong, Y. Lin, J. Shen, D.-A. Wang, A novel gellan gel-based microcarrier for anchorage-dependent cell delivery, *Acta Biomater.* 4 (2008) 1226–1234. <https://doi.org/10.1016/j.actbio.2008.03.008>.
- [10] S.J. Chang, Y.-T. Huang, S.-C. Yang, S.-M. Kuo, M.-W. Lee, In vitro properties of gellan gum sponge as the dental filling to maintain alveolar space, *Carbohydr. Polym.* 88 (2012) 684–689. <https://doi.org/10.1016/j.carbpol.2012.01.017>.
- [11] K. Miyamoto, Y. Asakawa, Y. Arai, T. Shimizu, M. Tokita, T. Komai, Preparation of gellan sulfate as an artificial ligand for removal of extra domain A containing fibronectin, *Int. J. Biol. Macromol.* 28 (2001) 381–385. [https://doi.org/10.1016/S0141-8130\(01\)00135-0](https://doi.org/10.1016/S0141-8130(01)00135-0).
- [12] K. Miyamoto, A. Kanemoto, K. Hashimoto, M. Tokita, T. Komai, Immobilized gellan sulfate surface for cell adhesion and multiplication: development of cell-hybrid biomaterials using self-produced fibronectin, *Int. J. Biol. Macromol.* 30 (2002) 75–80. [https://doi.org/10.1016/S0141-8130\(02\)00013-2](https://doi.org/10.1016/S0141-8130(02)00013-2).
- [13] L.P. da Silva, R.P. Pirraco, T.C. Santos, R. Novoa-Carballal, M.T. Cerqueira, R.L. Reis, V.M. Correlo, A.P. Marques, Neovascularization Induced by the Hyaluronic Acid-Based Spongy-Like Hydrogels Degradation Products, *ACS Appl. Mater. Interfaces.* 8 (2016) 33464–33474. <https://doi.org/10.1021/acsami.6b11684>.
- [14] M.T. Cerqueira, L.P. da Silva, T.C. Santos, R.P. Pirraco, V.M. Correlo, A.P. Marques, R.L. Reis, Human Skin Cell Fractions Fail to Self-Organize Within a Gellan Gum/Hyaluronic Acid Matrix but Positively Influence Early Wound Healing, *Tissue Eng. Part A.* 20 (2014) 1369–1378. <https://doi.org/10.1089/ten.tea.2013.0460>.
- [15] M.T. Cerqueira, L.P. da Silva, T.C. Santos, R.P. Pirraco, V.M. Correlo, R.L. Reis, A.P. Marques, Gellan Gum-Hyaluronic Acid Spongy-like Hydrogels and Cells from Adipose Tissue Synergize Promoting Neoskin Vascularization, *ACS Appl. Mater. Interfaces.* 6 (2014) 19668–19679. <https://doi.org/10.1021/am504520j>.
- [16] D.B. Rodrigues, H.R. Moreira, L. Gasperini, M.T. Cerqueira, A.M.P. Marques, R.P. Pirraco, R.L.G. dos Reis, HYDROGEL-LIKE PARTICLES, METHODS AND USES THEREOF, WO/2021/064678, 2021.

- [17] D.K. Chou, R. Krishnamurthy, T.W. Randolph, J.F. Carpenter, M.C. Manning, Effects of Tween 20 and Tween 80 on the Stability of Albutropin During Agitation, *J. Pharm. Sci.* 94 (2005) 1368–1381. <https://doi.org/10.1002/jps.20365>.
- [18] O.A. Douglas-Gallardo, C.G. Gomez, M.A. Macchione, F.P. Cometto, E.A. Coronado, V.A. Macagno, M.A. Pérez, Morphological evolution of noble metal nanoparticles in chloroform: mechanism of switching on/off by protic species, *RSC Adv.* 5 (2015) 100488–100497. <https://doi.org/10.1039/C5RA17529A>.
- [19] A.M. Smith, S. Moxon, G.A. Morris, Biopolymers as wound healing materials, in: *Wound Heal. Biomater.*, Elsevier, 2016: pp. 261–287. <https://doi.org/10.1016/B978-1-78242-456-7.00013-1>.
- [20] J.A. Brydson, Poly(vinyl acetate) and its Derivatives, in: *Plast. Mater.*, Elsevier, 1995: pp. 371–382. <https://doi.org/10.1016/B978-0-7506-1864-9.50020-X>.
- [21] W. Abdelwahed, G. Degobert, S. Stainmesse, H. Fessi, Freeze-drying of nanoparticles: Formulation, process and storage considerations☆, *Adv. Drug Deliv. Rev.* 58 (2006) 1688–1713. <https://doi.org/10.1016/j.addr.2006.09.017>.
- [22] S. Iwaguch, K. Matsumura, Y. Tokuoka, S. Wakui, N. Kawashima, Sterilization system using microwave and UV light, *Colloids Surfaces B Biointerfaces.* 25 (2002) 299–304. [https://doi.org/10.1016/S0927-7765\(01\)00324-1](https://doi.org/10.1016/S0927-7765(01)00324-1).
- [23] E.R. Sanders, Aseptic Laboratory Techniques: Plating Methods, *J. Vis. Exp.* (2012) 1–18. <https://doi.org/10.3791/3064>.
- [24] M.K. Hameed, I.M. Ahmady, H. Alawadhi, B. Workie, E. Sahle-Demessie, C. Han, M.M. Chehimi, A.A. Mohamed, Gold-carbon nanoparticles mediated delivery of BSA: Remarkable robustness and hemocompatibility, *Colloids Surfaces A Physicochem. Eng. Asp.* 558 (2018) 351–358. <https://doi.org/10.1016/j.colsurfa.2018.09.004>.
- [25] M.T. Cerqueira, R.P. Pirraco, T.C. Santos, D.B. Rodrigues, A.M. Frias, A.R. Martins, R.L. Reis, A.P. Marques, Human Adipose Stem Cells Cell Sheet Constructs Impact Epidermal Morphogenesis in Full-Thickness Excisional Wounds, *Biomacromolecules.* 14 (2013) 3997–4008. <https://doi.org/10.1021/bm4011062>.

- [26] Y.C. Lin, T. Grahovac, S.J. Oh, M. Ieraci, J.P. Rubin, K.G. Marra, Evaluation of a multi-layer adipose-derived stem cell sheet in a full-thickness wound healing model, *Acta Biomater.* 9 (2013) 5243–5250. <http://dx.doi.org/10.1016/j.actbio.2012.09.028>.
- [27] M.T. Cerqueira, A.P. Marques, R.L. Reis, Using Stem Cells in Skin Regeneration: Possibilities and Reality, *Stem Cells Dev.* 21 (2012) 1201–1214. <https://doi.org/10.1089/scd.2011.0539>.
- [28] J.G. Rheinwald, H. Green, Serial Cultivation of Strains of Human Epidermal Keratinocytes: the Formation of Keratinizing Colonies from Single Cells, *Cell.* 6 (1975) 331–344. [https://doi.org/10.1016/S0092-8674\(75\)80001-8](https://doi.org/10.1016/S0092-8674(75)80001-8).
- [29] S. Llamas, E. García-Pérez, Á. Meana, F. Larcher, M. del Río, Feeder Layer Cell Actions and Applications, *Tissue Eng. Part B Rev.* 21 (2015) 345–353. <https://doi.org/10.1089/ten.teb.2014.0547>.
- [30] M.T. Cerqueira, A.M. Frias, R.L. Reis, A.P. Marques, Boosting and Rescuing Epidermal Superior Population from Fresh Keratinocyte Cultures, *Stem Cells Dev.* 23 (2014) 34–43. <https://doi.org/10.1089/scd.2013.0038>.
- [31] S. Chapman, X. Liu, C. Meyers, R. Schlegel, A.A. McBride, Human keratinocytes are efficiently immortalized by a Rho kinase inhibitor, *J. Clin. Invest.* 120 (2010) 2619–2626. <https://doi.org/10.1172/JCI42297>.
- [32] M. Yamato, T. Okano, Cell sheet engineering, *Mater. Today.* 7 (2004) 42–47. [https://doi.org/10.1016/S1369-7021\(04\)00234-2](https://doi.org/10.1016/S1369-7021(04)00234-2).
- [33] M. Costa, R.P. Pirraco, M.T. Cerqueira, R.L. Reis, A.P. Marques, Growth Factor-Free Pre-vascularization of Cell Sheets for Tissue Engineering, in: *Methods Mol. Biol.*, 2016: pp. 219–226. https://doi.org/10.1007/7651_2016_362.
- [34] M.J.E. Fischer, *Surface Plasmon Resonance*, Humana Press, Totowa, NJ, 2010. <https://doi.org/10.1007/978-1-60761-670-2>.

- [35] S.A. Burns, R. Hard, W.L. Hicks, F. V Bright, D. Cohan, L. Sigurdson, J.A. Gardella, Determining the protein drug release characteristics and cell adhesion to a PLLA or PLGA biodegradable polymer membrane, *J. Biomed. Mater. Res. Part A.* 94A (2010) 27–37. <https://doi.org/10.1002/jbm.a.32654>.
- [36] J. Stetefeld, S.A. McKenna, T.R. Patel, Dynamic light scattering: a practical guide and applications in biomedical sciences, *Biophys. Rev.* 8 (2016) 409–427. <https://doi.org/10.1007/s12551-016-0218-6>.
- [37] S. Bhattacharjee, DLS and zeta potential – What they are and what they are not?, *J. Control. Release.* 235 (2016) 337–351. <https://doi.org/10.1016/j.jconrel.2016.06.017>.
- [38] M. Kaszuba, J. Corbett, F.M. Watson, A. Jones, High-concentration zeta potential measurements using light-scattering techniques, *Philos. Trans. R. Soc. A Math. Phys. Eng. Sci.* 368 (2010) 4439–4451. <https://doi.org/10.1098/rsta.2010.0175>.
- [39] P.D. Nellist, Scanning Transmission Electron Microscopy, in: *Springer Handbooks Microsc.*, Springer, 2019: pp. 49–99. https://doi.org/10.1007/978-3-030-00069-1_2.
- [40] S.J. Pennycook, A.R. Lupini, M. Varela, A. Borisevich, Y. Peng, M.P. Oxley, K. Van Benthem, M.F. Chisholm, Scanning Transmission Electron Microscopy for Nanostructure Characterization, in: *Scanning Microsc. Nanotechnol.*, Springer New York, New York, NY, 2006: pp. 152–191. https://doi.org/10.1007/978-0-387-39620-0_6.
- [41] L. Graham, J.M. Orenstein, Processing tissue and cells for transmission electron microscopy in diagnostic pathology and research, *Nat. Protoc.* 2 (2007) 2439–2450. <https://doi.org/10.1038/nprot.2007.304>.
- [42] T. Walther, Transmission Electron Microscopy of Nanostructures, in: *Microsc. Methods Nanomater. Charact.*, Elsevier, 2017: pp. 105–134. <https://doi.org/10.1016/B978-0-323-46141-2.00004-3>.
- [43] P.K. Smith, R.I. Krohn, G.T. Hermanson, A.K. Mallia, F.H. Gartner, M.D. Provenzano, E.K. Fujimoto, N.M. Goeke, B.J. Olson, D.C. Klenk, Measurement of protein using bicinchoninic acid, *Anal. Biochem.* 150 (1985) 76–85. [https://doi.org/10.1016/0003-2697\(85\)90442-7](https://doi.org/10.1016/0003-2697(85)90442-7).

- [44] ThermoFisher Scientific, ELISA technical guide and protocols, (n.d.).
- [45] S.J. Ahn, J. Costa, J.R. Emanuel, PicoGreen quantitation of DNA: effective evaluation of samples pre- or post-PCR, *Nucleic Acids Res.* 24 (1996) 2623–2625. <https://doi.org/10.1093/nar/24.13.2623>.
- [46] K.M. McKinnon, Flow Cytometry: An Overview, *Curr. Protoc. Immunol.* 120 (2018) 1–16. <https://doi.org/10.1002/cpim.40>.
- [47] A. Adan, G. Alizada, Y. Kiraz, Y. Baran, A. Nalbant, Flow cytometry: basic principles and applications, *Crit. Rev. Biotechnol.* 37 (2015) 163–176. <https://doi.org/10.3109/07388551.2015.1128876>.
- [48] Z. Pan, Z. Zhou, H. Zhang, H. Zhao, P. Song, D. Wang, J. Yin, W. Zhao, Z. Xie, F. Wang, Y. Li, C. Guo, F. Zhu, L. Zhang, Q. Wang, CD90 serves as differential modulator of subcutaneous and visceral adipose-derived stem cells by regulating AKT activation that influences adipose tissue and metabolic homeostasis, *Stem Cell Res. Ther.* 10 (2019) 355. <https://doi.org/10.1186/s13287-019-1459-7>.
- [49] J. Xiong, D. Menicanin, P.S. Zilm, V. Marino, P.M. Bartold, S. Gronthos, Investigation of the Cell Surface Proteome of Human Periodontal Ligament Stem Cells, *Stem Cells Int.* 2016 (2016) 1–13. <https://doi.org/10.1155/2016/1947157>.
- [50] A.D. Hyatt, T.G. Wise, Immunolabeling, in: *Immunocytochem. Situ Hybrid. Biomed. Sci.*, Birkhäuser Boston, Boston, MA, 2001: pp. 73–107. https://doi.org/10.1007/978-1-4612-0139-7_5.
- [51] A. Nanci, R. Wazen, C. Nishio, S.F. Zalzal, Immunocytochemistry of matrix proteins in calcified tissues: Functional biochemistry on section, *Eur. J. Histochem.* 52 (2008) 201–214. <https://doi.org/10.4081/1218>.
- [52] P.E. Swanson, Foundations of Immunohistochemistry, *Am. J. Clin. Pathol.* 90 (1988) 333–339. <https://doi.org/10.1093/ajcp/90.3.333>.

CHAPTER III.

Results and Discussion

CHAPTER III. Results and Discussion**3.1. Results****3.1.1. Characterization of Gellan Gum Particles**

Each batch of GG particles produced by the technique of double emulsion water-in-oil-in-water was analyzed by DLS, which included size, polydispersity index (PDI) and the ZP of the particles (Table 3.1).

Table 3.1 - Dynamic light scattering parameters: size, polydispersity index and zeta potential.

GG particles	Size (nm) \pm STD	PDI \pm STD	Zeta Potential (mV) \pm STD
Batch 1	206 \pm 49	0.19 \pm 0.02	-43.(2) \pm 8
Batch 2	251 \pm 38	0.11 \pm 0.05	-59.(7) \pm 4
Batch 3	199 \pm 32	0.20 \pm 0.01	-55.(4) \pm 5

For batch 1, the mean particles size was 206 \pm 49 nm, PDI of 0.19 \pm 0.02 and the zeta potential -43.(2) \pm 8 mV. The second batch, the mean particles size was 251 \pm 38 nm, polydispersity index of 0.11 \pm 0.05 and zeta potential -59.(7) \pm 4 mV. The third batch presented a mean size of particles of 199 \pm 32 nm, polydispersity index of 0.20 \pm 0.01 and zeta potential -55.(4) \pm 5 mV. Hence, all the three batches showed similar characteristics after production. Furthermore, the morphology of the particles was analyzed by STEM (Figure 3.1), showing that the particles exhibited a spherical shape with sizes smaller than 100 nm.

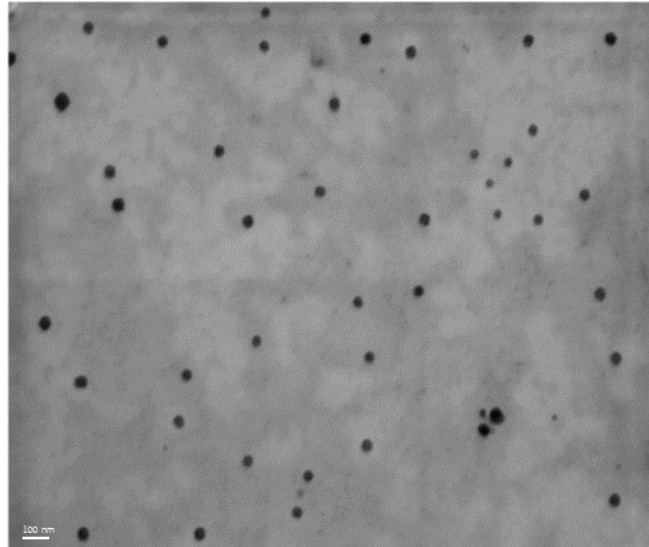


Figure 3.1 - STEM micrograph of gellan gum particles (50 000 x magnification). *Scale bar: 100 nm.*

3.1.2. Protein Loading/Release Strategies

3.1.2.1. Bovine Serum Albumin as a Model Molecule

3.1.2.1.1. Size Effect

Initially, the release assay was performed using polydisperse particles and particles smaller than $1\ \mu\text{m}$ ($< 1\ \mu\text{m}$) (Figure 3.2). Both types of particles were incubated with $10\ \mu\text{g}/\text{mL}$ of BSA.

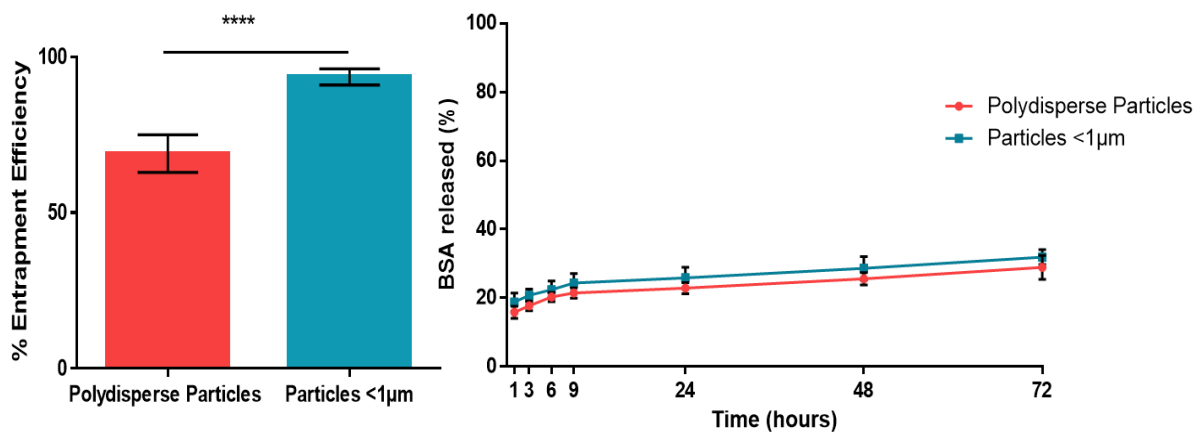


Figure 3.2 - Quantification of **a**) the entrapment efficiency (%) and **b**) BSA released (%) in polydisperse particles (red) and particles $< 1\ \mu\text{m}$ (blue). Statistical differences: **** $p < 0.0001$. The data is expressed as mean \pm standard deviation, $n = 3$.

Regarding the entrapment efficiency (Figure 3.2.a), polydisperse particles were able to entrap around 60% of BSA, whereas particles smaller than 1 μm entrapped almost 90% of BSA. The entrapment percentage of BSA in the polydisperse particles was significantly lower ($p < 0.0001$) when comparing to the smaller ones. The analysis of BSA released (%) over time (Figure 3.2.b) was calculated taking in consideration the entrapment efficiency and showed that both conditions of particles released around 30% of BSA. By comparing both profiles, polydisperse particles released lower percentage of BSA when comparing to the smaller particles.

3.1.2.1.2. Lyophilization Effect

Taking in account the results obtained in section 3.2.1.1.1, particles $< 1 \mu\text{m}$ were then chosen to proceed with the next release studies, as they entrapped and released a higher percentage of BSA. The effect of lyophilization after incubation of BSA was then performed to assess the best condition for the maximum release of this protein (Figure 3.3).

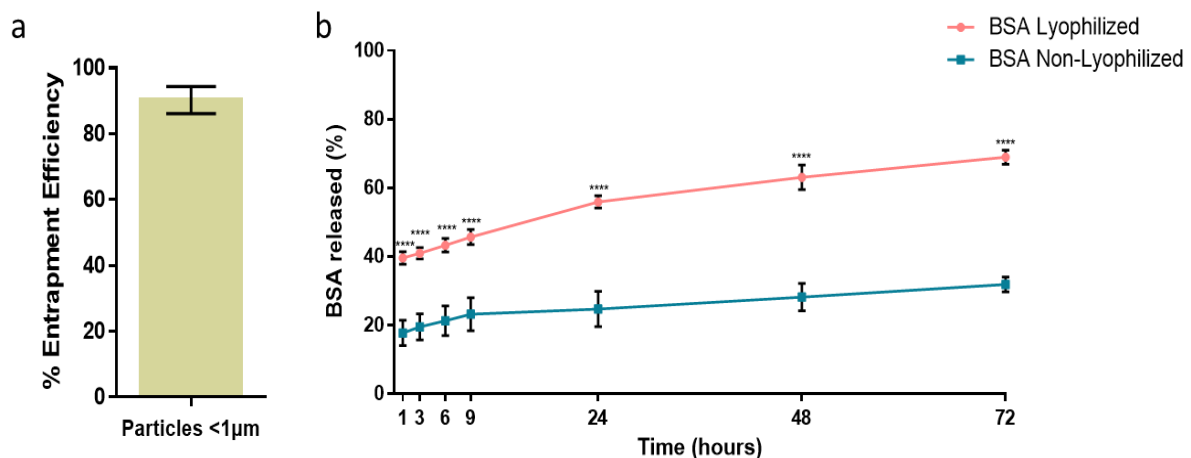


Figure 3.3 - Quantification of **a**) entrapment efficiency (%) and **b**) BSA released (%) in BSA Lyophilized (pink) and BSA Non-Lyophilized (blue) conditions. Statistical differences: **** $p < 0.0001$. The data is expressed as mean \pm standard deviation, $n = 3$.

The entrapment efficiency (Figure 3.3.a) for the chosen particles ($< 1 \mu\text{m}$) was around 90%. The assessment of released BSA (Figure 3.3.b) showed that the condition where BSA was lyophilized released around 30% of BSA at early time points and that after 72 hours, 70% of BSA was released. When BSA

loaded particles were further lyophilized a significantly higher ($p < 0.0001$) percentage of BSA was released, comparing with the non-lyophilized setting.

3.1.2.2. Keratinocyte Growth Factor as Molecule of Interest

3.1.2.2.1. Lyophilization Effect with pH Variation

After optimizing the parameters for the entrapment (particles size), the release of KGF then performed using particles $< 1 \mu\text{m}$. The consequence of a further lyophilization after KGF entrapment and the effect of the release at different pHs were tested (4, 7.4 and 10) with the rationale of recreating the different pHs variations that wounds go through the healing process. The entrapment efficiency and the release profile of KGF are depicted in Figure 3.4.

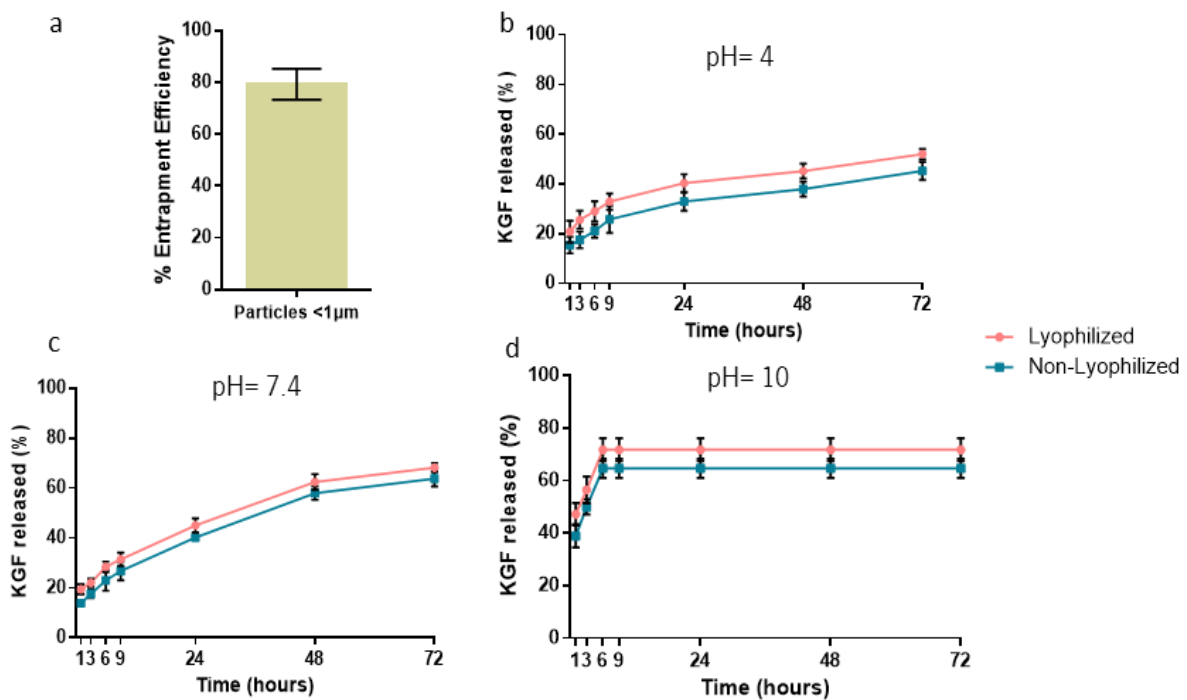


Figure 3.4 - Quantification of **a)** the entrapment efficiency (%) and KGF (%) released at **b)** pH= 4, **c)** pH= 7.4 and **d)** pH= 10. For every pH, both Lyophilized (pink) and Non-Lyophilized (blue) after KGF entrapment were tested. The data is expressed as mean \pm standard deviation, $n= 3$.

The entrapment efficiency (Figure 3.4.a) showed that around 80% of KGF was captured. Regarding the release profile at different pH conditions, a higher amount of KGF was released when

particles were lyophilized after incubation of KGF, although not being significantly different from the non-lyophilized particles. The amount of KGF released at pH= 4 (Figure 3.4.b), was low for both conditions, where lyophilized particles released around 50% of KGF and non-lyophilized particles about 40%. At pH= 7.4 (Figure 3.4.c), both conditions presented gradual release through the 72 hours of study with about 70% of KGF released. On another hand, at pH =10 (Figure 3.4.d), a burst release of 70% of KGF was observed for the lyophilized particles while the non-lyophilized particles released 60% in the first 6 hours of study. From that point on, no further release of KGF was observed, and therefore the cumulative concentration of KGF was the same.

A representation of the concentration of KGF released in all the pH conditions using lyophilized and non-lyophilized particles, was performed to identify the differences between them at 72 hours (Figure 3.5).

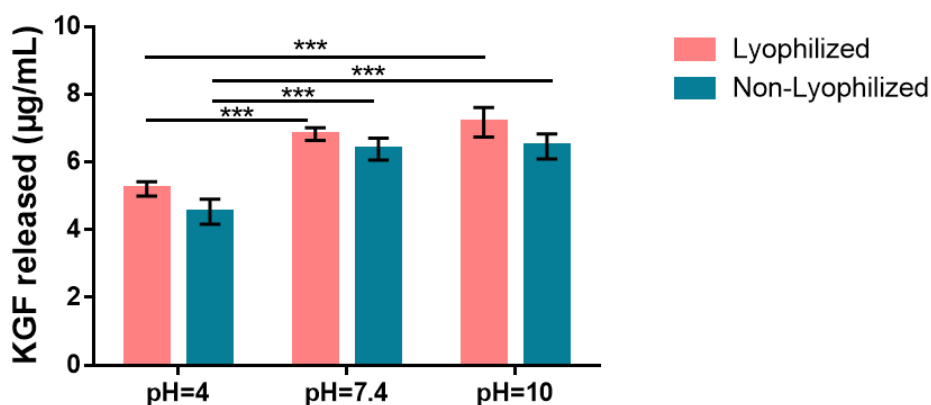


Figure 3.5 - KGF released ($\mu\text{g/mL}$) at pH= 4, pH= 7.4 and pH= 10 using the conditions Lyophilized (red) and Non-Lyophilized (blue) after KGF entrapment at 72 hours. Statistical differences: $***p < 0.001$. The data is expressed as mean \pm standard deviation, $n = 3$.

Within the same pH tested, no significant differences were detected between the 2 conditions. When comparing the condition of lyophilized particles, the release at pH= 4 was significantly lower ($p < 0.001$) than the release at pH= 7.4 and pH= 10. The same tendency was observed for non-lyophilized particles, where the release at pH= 4 was also significantly lower ($p < 0.001$) than the release at pH= 7.4 and pH= 10. However, no statistically relevant differences were detected between release assays performed at pH=7.4 and pH=10.

3.1.3. Biological Assays

3.1.3.1. hKCs and Gellan Gum Particles Direct Contact

3.1.3.1.1. Particles Internalization

In order to study the internalization of GG particles by hKCs, particles were initially functionalized with biotin-FITC (Figure 3.6.a). Then, hKCs were analyzed by flow cytometry to detect any fluorescence signal due to FITC labelled particles (Figure 3.6.b and c).

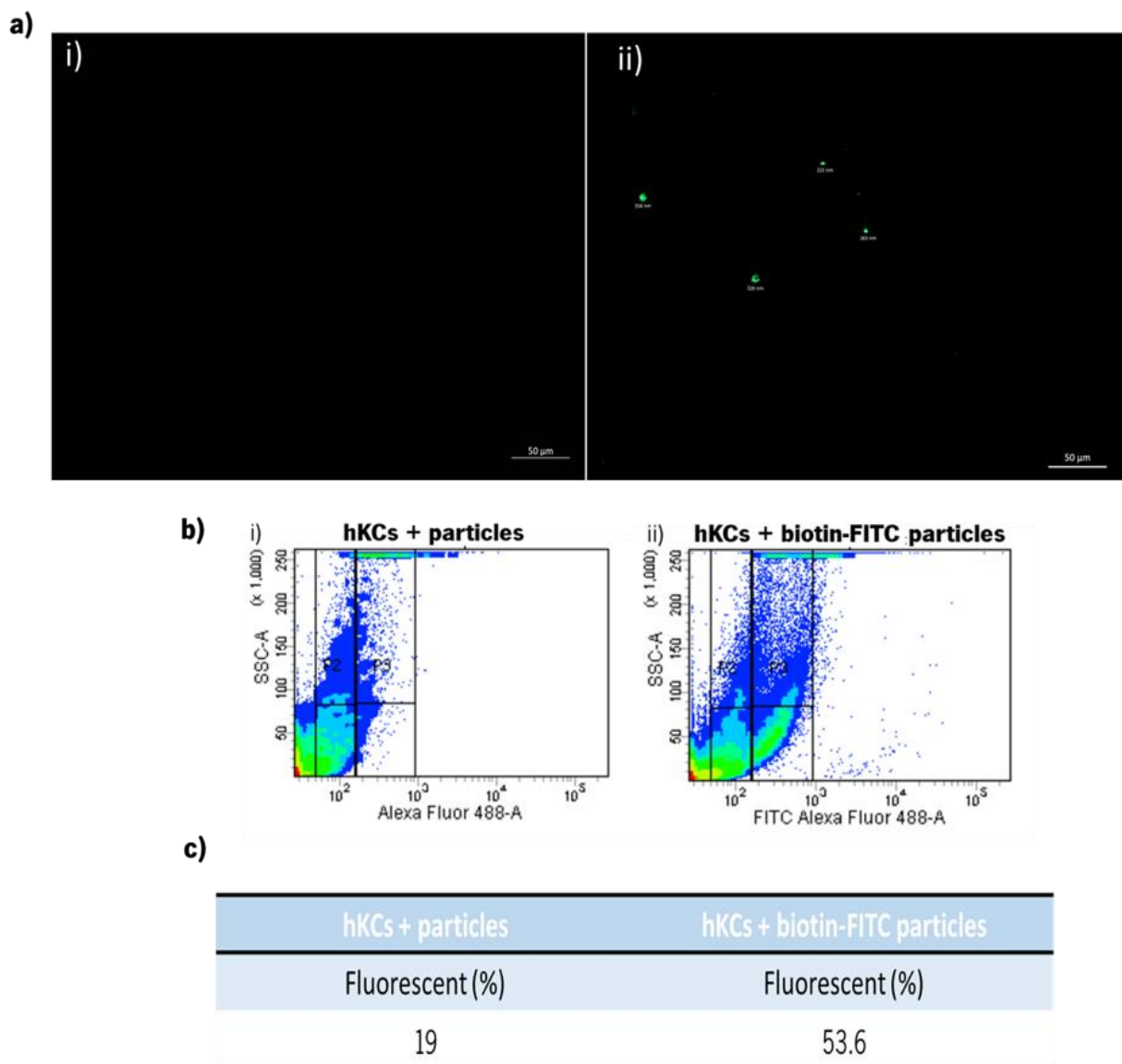


Figure 3.6 - a) Fluorescence microscopy images of GG particles not functionalized with Biotin-FITC (i) and functionalized with Biotin-FITC (ii). **b)** Representative density dot plots of hKCs incubated with non-functionalized particles (i) and functionalized particles (ii). **c)** Percentage of FITC expressing hKCs provided by flow cytometry. *Scale bar: 50 μm.*

As depicted in fluorescence microscopy images (Figure 3.6.a), the functionalization of the particles with biotin-FITC was successfully accomplished. While control particles without any functionalization, no fluorescence signal was detected, particles functionalized with fluorescent molecule FITC displayed green color.

Flow cytometry (Figure 3.6.b) enabled to assess the internalization of FITC-labelled particles by hKCs. A shift in FITC channel was observed with 53.6% of hKCs fluorescent (Figure 3.6.c). hKCs in contact with particles without FITC functionalization were used as control.

Additional internalization studies were performed using transmission electron microscopy (TEM) (Figure 3.7) to support the results obtained by flow cytometry.

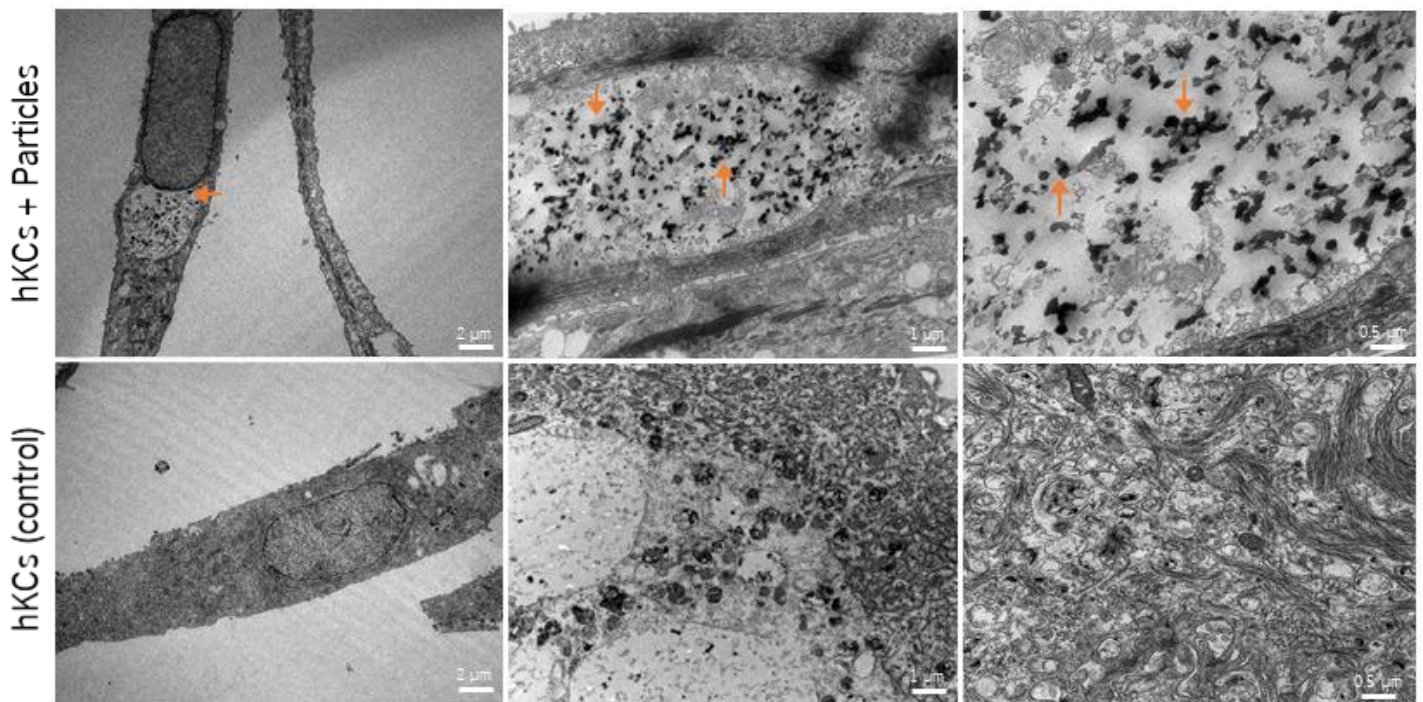


Figure 3.7 - TEM micrographs of hKCs and gellan gum particles (top row) and the control of hKCs (bottom row). The orange arrows indicate GG particles internalized by the cells. *Scale bar: 2 μm ; 1 μm and 0.5 μm .*

In the condition of hKCs with GG particles, small black dots (particles), pointed by the orange arrows, were present in intracellular vesicles. As expected, in the negative control, none of these particles-containing vesicles were observed.

3.1.3.1.2. KGF and dsDNA Quantification

To understand how KGF-loaded particles and GG particles alone influenced hKCs during 72 hours, KGF levels and dsDNA were quantified (Figure 3.8). The concentration of KGF released from the particles was also quantified to know the amount of KGF released from the initially 10 ng KGF-loaded particles. Moreover, the amount of KGF present in the medium after the contact with hKCs was also assessed, in order to understand the quantity of KGF not uptaken by the cells.

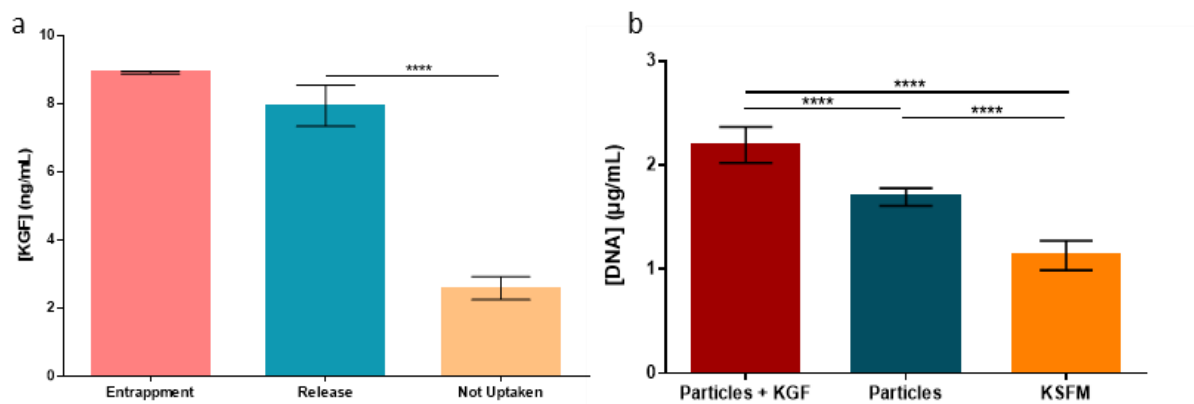


Figure 3.8 - Quantification of **a)** KGF present in the medium (Entrapped and Released by GG particles, and KGF Not Uptaken by the cells) and **b)** dsDNA of hKCs in different conditions (Particles with KGF in contact with hKCs, Particles in contact with hKCs, control of hKCs). Statistical differences: ** $p < 0.01$; *** $p < 0.001$ and **** $p < 0.0001$. The data is expressed as mean \pm standard deviation, $n = 3$.

The amount of KGF entrapped was assessed after 24 hours of incubation in KSFM, prior contact with hKCs, which was around 9 ng out of 10 ng incorporated. From these 9 ng, nearly 8 ng were detected in KSFM after incubating KGF-loaded particles for 72 hours without cells, revealing that this was the amount of KGF being released to hKCs cultured in the same period (Figure 3.8.a). In parallel, KGF content in culture medium after contact of KGF-loaded particles and hKCs (not uptaken by hKCs) turned out to be 3 ng. This means that indirectly, the amount of KGF uptaken by hKCs was statistically significant, as the amount of KGF not uptaken by hKCs was significantly higher ($p < 0.0001$) than quantity of KGF released during the assay.

The results from dsDNA quantification (Figure 3.8.b) showed that the amount of DNA in the condition when hKCs were in contact with the KGF-loaded particles was significantly higher ($p < 0.0001$)

when comparing to the particles alone in contact with hKCs and to the control using KSFM. The condition of the particles alone in contact with hKCs also showed a significantly higher ($p < 0.0001$) amount of DNA when comparing to the control.

3.1.3.1.3. FGFR2 and Ki67 Expression Markers

The expression of FGFR2 and Ki67 markers was confirmed by immunocytochemistry for hKCs when in contact with KGF-loaded particles and hKCs in presence of KSFM (control) (Figure 3.9.a and Figure 3.9.c), as well the negative control (Figure 3.9.b). The ratio of Ki67 positive cells (Figure 3.9.d), was calculated by dividing the number of green nuclei per number of blue nuclei.

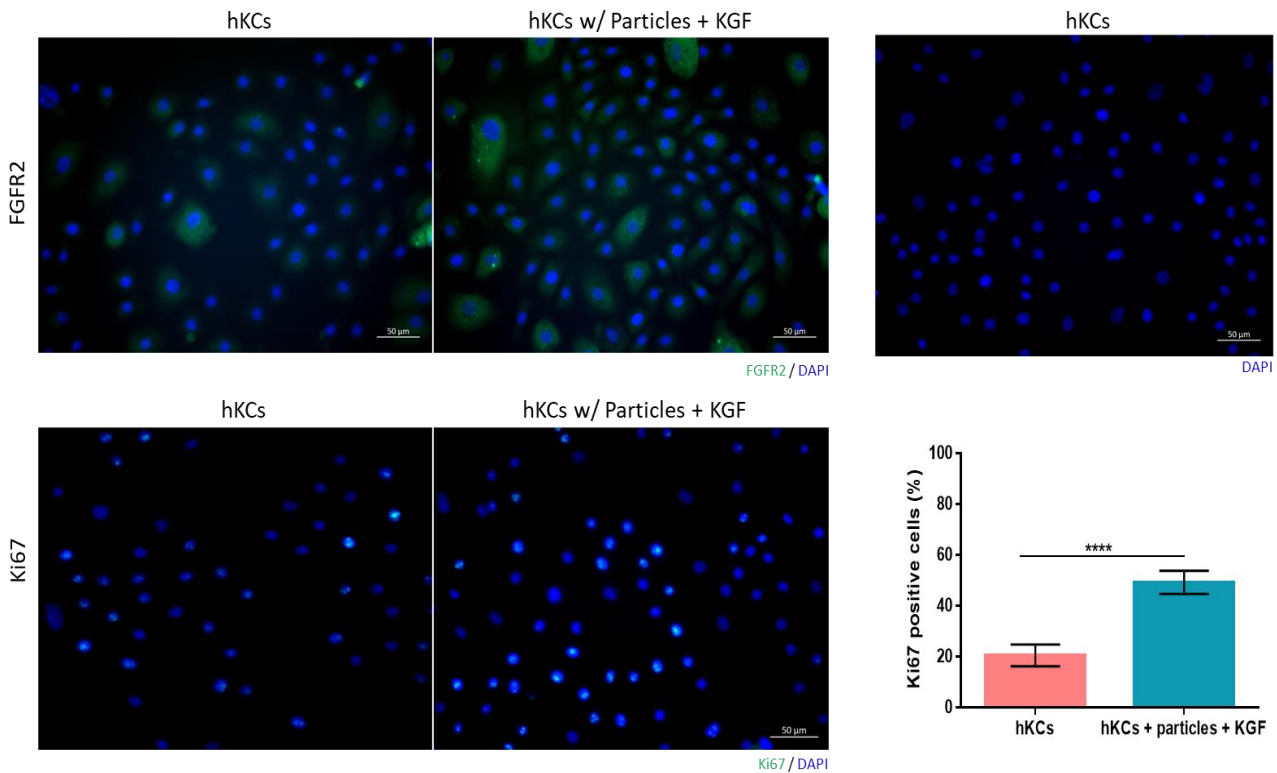


Figure 3.9 - Representative immunocytochemistry images of **a**) the expression of FGFR2 (green), **b**) negative control and **c**) the expression of Ki67 (green), all for the conditions of KGF-loaded particles in contact with hKCs and the control of hKCs at 72 hours. Nuclei were stained with DAPI (blue). **d**) Ratio of Ki67 positive cells (%) of hKCs and hKCs in contact with GG particles incubated with KGF. Statistical differences: **** $p < 0.0001$. The data is expressed as mean \pm standard deviation, $n = 3$. Scale bar: 50 μm .

The expression for the markers FGFR2 and for Ki67 (Figure 3.9.a and c) was present for both conditions. In the negative control (Figure 3.9.b) no unspecific staining from the secondary antibody was detected.

The ratio of Ki67 positive cells (Figure 3.9.d) showed that in hKCs treated with culture medium only 20% of the cells were positive for this marker, in opposition with hKCs treated with the KGF-loaded particles that around 60% of the cells were positive. These results showed that the control of hKCs had a significantly lower ($p < 0.0001$) percentage of Ki67 positive cells when comparing to the condition of hKCs in the presence of the particles and KGF.

3.1.3.1.4. Effect on Migration

The migration assay was performed by culturing hKCs in a wound healing assay setup with KGF-loaded particles, particles alone and KGF. The control condition used was KSFM alongside with KGF antibody to neutralize the action of KGF (Figure 3.10).

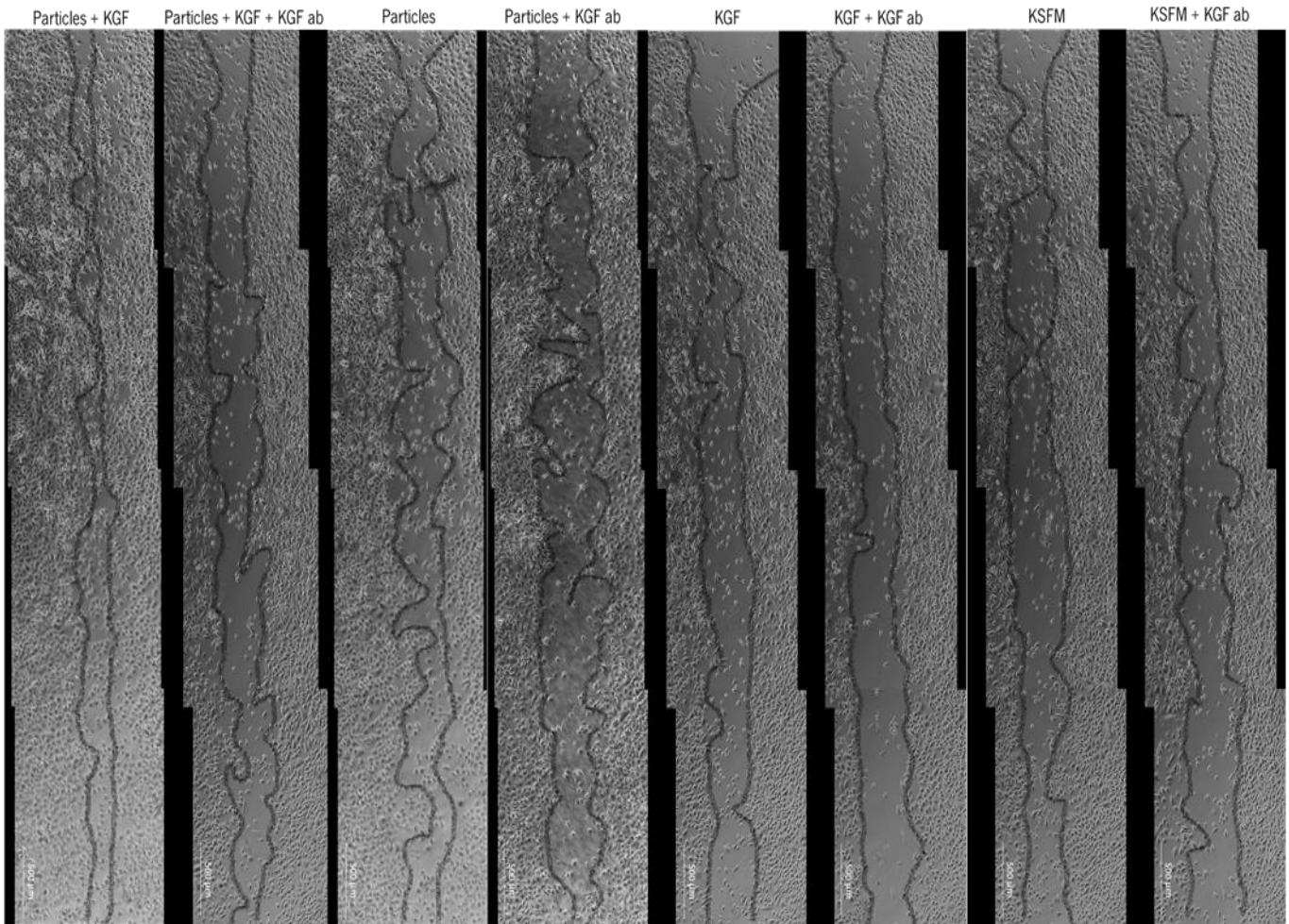


Figure 3.10 - Representative microscopy images showing final gaps of migrating hKCs after 21 hours under different conditions, $n=3$. Scale bar: 500 μm .

In the migration assay (Figure 3.11), after the contact of the particles with hKCs, it was observed that KGF-loaded particles allowed a significantly faster wound gap closure (nearly 100%), when compared to particles ($p<0.0001$), KGF alone ($p<0.01$), KSFM ($p<0.0001$) and KGF particles + KGF antibody ($p<0.0001$) (Figure 3.11). KGF alone promoted a wound gap closure of 70% and significantly higher when comparing to the same condition with KGF antibody ($p<0.01$). In all the conditions that comprised the addition of KGF antibody, the migration was similar to the control condition (KSFM), reaching only 50% of the wound closure.

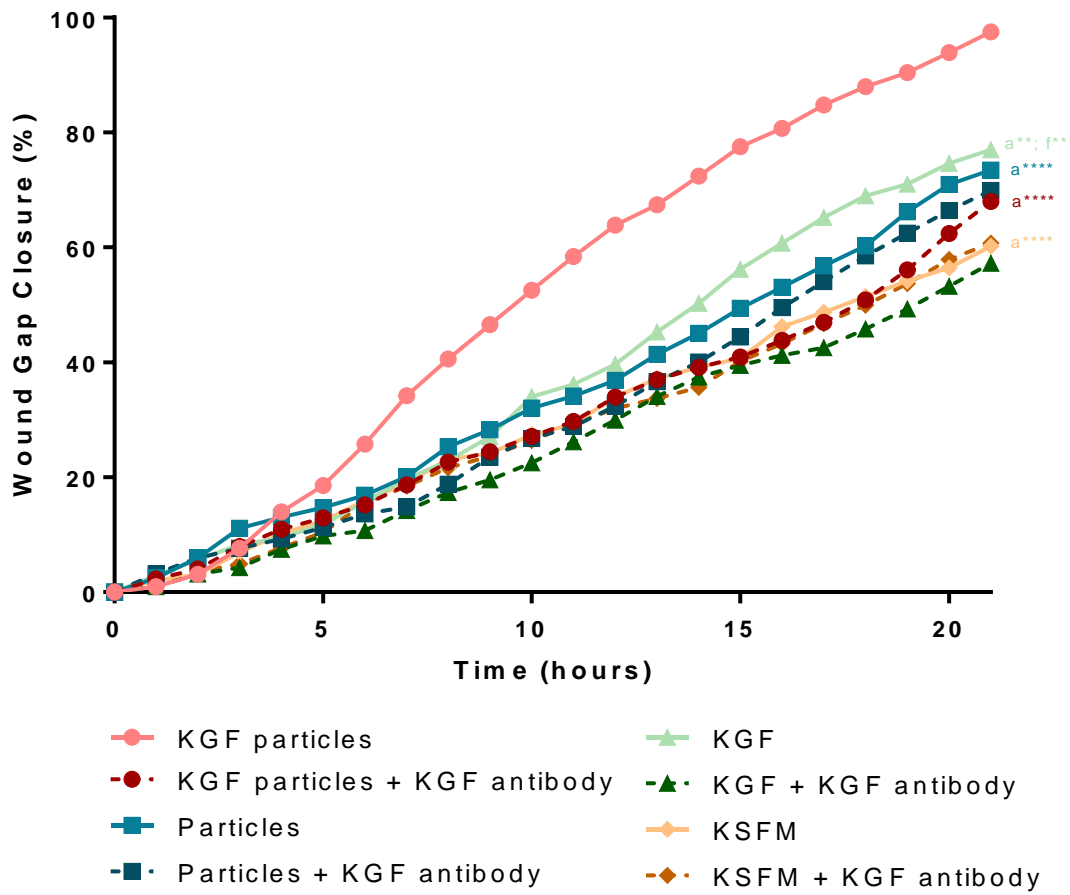


Figure 3.11 - Migration assay conducted using different conditions with hKCs. Data was analyzed by 2way ANOVA, followed by Sidak's multiple comparison test for: *a* denotes significant differences compared to KGF particles, *f* denotes significant differences compared to KGF + KGF antibody. The data is expressed as mean, *n*= 3.

3.1.3.2. hKCs and hASCs Direct Contact

3.1.3.2.1. Effect on Proliferation and KGF Release

In order to study the effect on proliferation of hKCs after contact with hASCs, several assays were performed. The dsDNA was quantified for the different conditions and time points, flow cytometry was used to distinguish the different cell types in co-culture conditions based on phenotypic staining and ultimately the amount of KGF present in the conditioned medium was also quantified. In this sense, by using the percentage of hASCs from each condition, the values of DNA and KGF were normalized in order to understand how the production of KGF was related to the number of hASCs in culture, as hKCs do not produce this factor. The results of all the performed tests are presented in Figure 3.12.

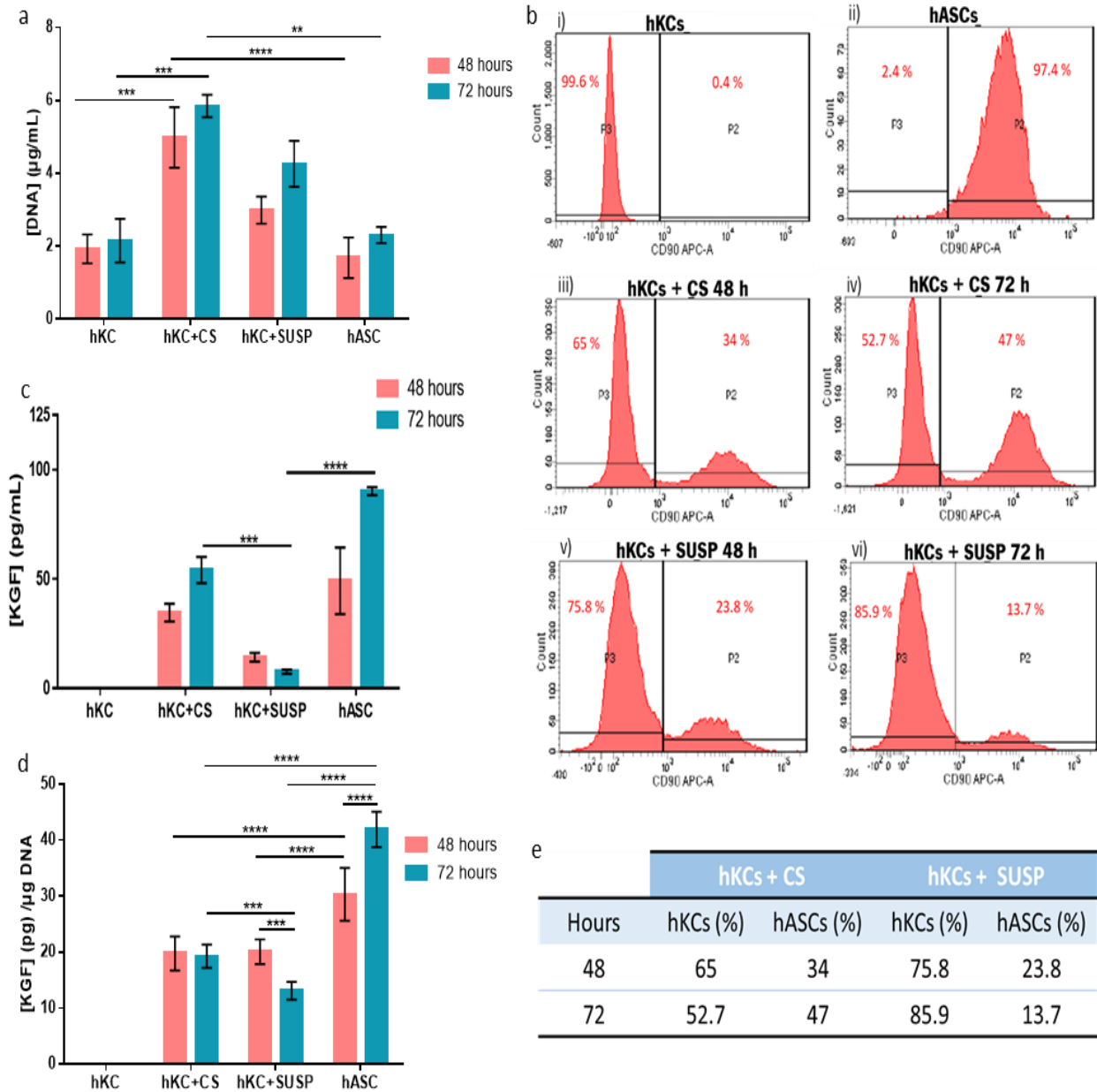


Figure 3.12 - Quantification of **a)** dsDNA; **b)** cellular ratio present in co-culture conditions by flow cytometry: **i)** control of hKCs, **ii)** control of hASCs, hASCs-CS in contact with hKCs **iii)** at 48 hours and **iv)** at 72 hours, hASCs-suspension in contact with hKCs **v)** at 48 hours and **vi)** 72 hours **c)** before and **d)** after normalization taking in account dsDNA and hKCs number present in the different conditions. **e)** Percentage of hKCs and hASCs provided by flow cytometry. Statistical differences: ** $p < 0.01$; *** $p < 0.001$ and **** $p < 0.0001$. The data is expressed as mean \pm standard deviation, $n = 3$.

Experimental results from dsDNA quantification (Figure 3.12.a) showed an increase of DNA amount through time, with no statistical differences within the same condition. These results were used as reference for the normalization of further KGF quantification, in order to have KGF concentration per μg DNA.

Flow cytometry data (Figure 3.12.b) showed an insignificant percentage of hKCs expressing CD90, in opposition of 97% CD90 positive. After 48 hours, in the condition of hASCs-CS in contact with hKCs, 65% of the cells corresponded to hKCs and 34% were hASCs. At 72 hours, the variation of hKCs (52.7%) and hASCs (47%) numbers was observed. When hASCs were in suspension (SUSP) in contact for 48 hours with, 75.8% were hKCs and 23.8% were hASCs. At 72 hours, hKCs increased to 85.9% and hASCs decreased 13.7%. In Figure 3.12.e a table with summarized percentages is displayed.

Regarding the quantification of KGF levels present in the CM (Figure 3.12.c), this factor was not detected in hKCs monocultures in both time points. On the other hand, KGF was found to increase in the conditioned medium collected from either hASCs-CS in contact with hKCs cultures or hASCs monocultures, after 48 hours and 72 hours. While in conditioned medium from hASCs-suspension in contact with hKCs there was a decrease of KGF concentration between the two timepoints. These results were obtained after absolute quantification of KGF present and therefore a further normalization taking in account the cell number (DNA quantification) and type (flow cytometry) was performed.

After normalization of KGF secreted values (Figure 3.12.d), the concentration of KGF through time in hASCs-CS in contact with hKCs was practically the same, in opposition to hASCs-suspension in contact with hKCs that, along time, this amount was significantly lower ($p < 0.001$). Monocultures of hASCs at 72 hours exhibited a significantly increase ($p < 0.0001$) of KGF in the media, compared to 48 hours. In fact, at 48 hours, the control of hASCs, produced a significantly higher ($p < 0.0001$) amount of KGF when comparing to the conditions of hASCs-CS in contact with hKCs and hASCs-suspension in contact with hKCs. At 72 hours, hASCs-CS in contact with hKCs produced significantly higher ($p < 0.001$) amount of KGF by comparison to hASCs-suspension in contact with hKCs. The control of hASCs had a significantly higher ($p < 0.0001$) production when comparing to hASCs-CS in contact with hKCs and hASCs-suspension in contact with hKCs.

3.1.3.2.2. FGFR2 and Ki67 Expression Markers

The expression of specific receptor for KGF and Ki67 proliferation marker was assessed by immunocytochemistry for the conditions above mentioned (Figure 3.13).

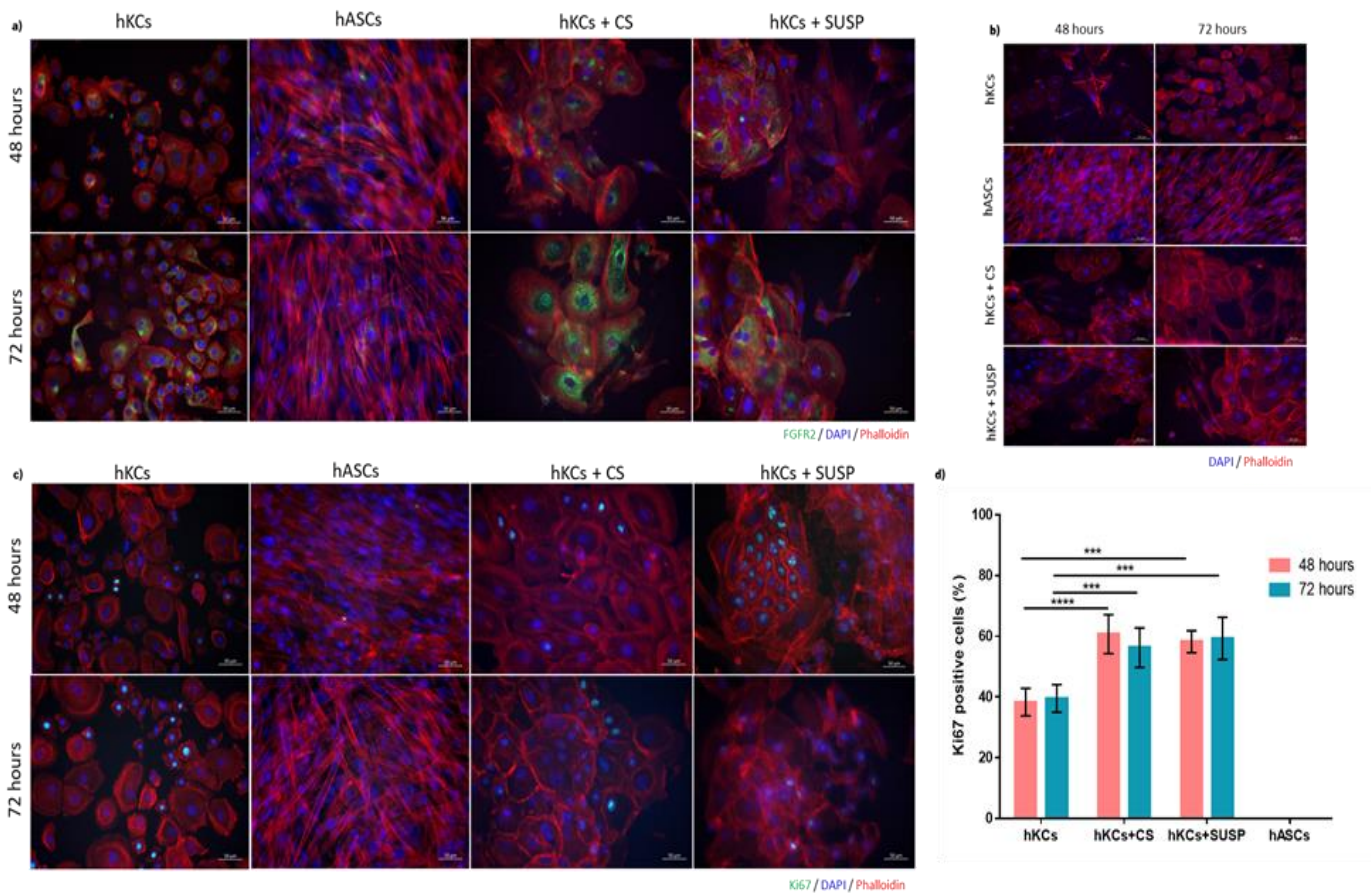


Figure 3.13 - Representative immunocytochemistry images of **a)** the expression of FGFR2 (green), **b)** negative control and **c)** the expression of Ki67 (green), for all the conditions comprising control of hKCs, control of hASCs, hASCs-CS in contact with hKCs and hASCs-suspension in contact with hKCs at 48 hours and 72 hours. Nuclei were stained with DAPI (blue) and cytoplasm with phalloidin-TRITC (red). **d)** Ratio of Ki67 positive cells (%) of hKCs and hASCs as controls, and hASCs-CS in contact with hKCs, hASCs-suspension in contact with hKCs at 48 hours and 72 hours. Statistical differences: ** $p < 0.01$; *** $p < 0.001$ and **** $p < 0.0001$. The data is expressed as mean \pm standard deviation, $n = 3$. Scale bar: 50 μm .

Both markers – Ki67 and FGFR2 - (Figure 3.13.a and c) appear to be present in the conditions of hKCs, hASCs-CS in contact with hKCs and hASCs-suspension in contact with hKCs, at both time points. Regarding the condition of hASCs, the expression for neither of the markers was detected. Negative controls (Figure 3.13.b) did not show any unspecific staining from the secondary antibody. The two cell types showed their typical morphology, while hKCs were rounder and displayed different sizes, hASCs presented a spindle-like shape.

Furthermore, within each condition and between timepoints, no statistical differences were observed for Ki67 positive cells (Figure 3.13.d). When hASCs-CS were in contact with hKCs for 48 hours, around 60% of hKCs were positive for Ki67 and after 72 hours the percentage decreased to 50%, being

non statistically different. hASCs-suspension in contact with hKCs at 48 hours and 72 hours, near 60% of hKCs were positive for Ki67 and the control of hASCs did not present any positive cells for this marker for both time points. Among the different conditions at 48 hours, hKCs in monocultured displayed a significantly lower number of Ki67 cells than when in culture with hASCs-CS ($p < 0.0001$) and hASCs-suspension ($p < 0.001$). The same tendency was observed at 72 hours, where hKCs cultured alone presented again significantly lower ($p < 0.001$) percentage of Ki67 positive cells comparing to when co-cultured with hASCs-CS and hASCs-suspension. Overall, the conditions using hASCs in contact with hKCs presented a higher ratio of Ki67 positive cells than in monoculture.

3.1.3.2.3. Effect on Migration

The migration assay was performed by culturing hKCs in a wound healing assay setup with different CM recovered after 72 hours (hKCs + CS; hKCs + SUSP; hASCs). The control condition used was KSFM, alongside with KGF antibody to neutralize the action of KGF (Figure 3.14).

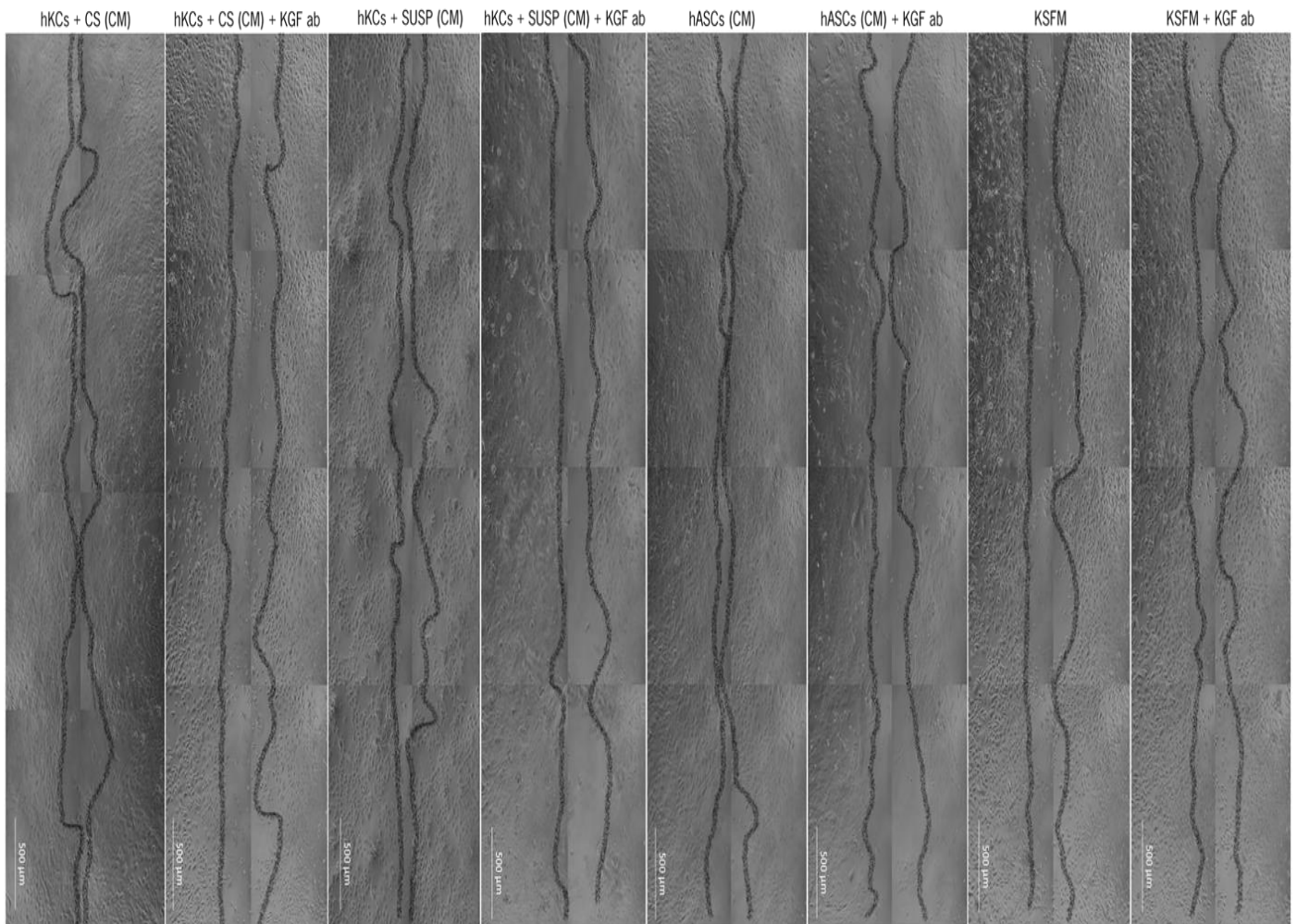


Figure 3.14 - Representative microscopy images showing final gaps of migrating hKCs after 21 hours under different conditions, $n=3$. Scale bar: 500 μm .

After the contact of the different CM with hKCs up to 21 hours (Figure 3.15) it was observed that hASCs (CM) allowed a significantly faster wound gap closure ($p < 0.0001$), (nearly 100%), when compared to hKCs + CS (CM), hKCs + SUSP (CM), hASCs (CM) + KGF antibody and KFSM (Figure 3.15). The conditions comprising hKCs + CS (CM) and hKCs + SUSP (CM) were the second and third condition, respectively to promote faster wound gap closure. These conditions were significantly different between them and between their condition with KGF antibody ($p < 0.0001$), both conditions were also significantly higher comparing to KFSM ($p < 0.0001$). In all the conditions where KGF antibody was added, the migration was similar to the control condition (KFSM) (around 50% of wound gap closure).

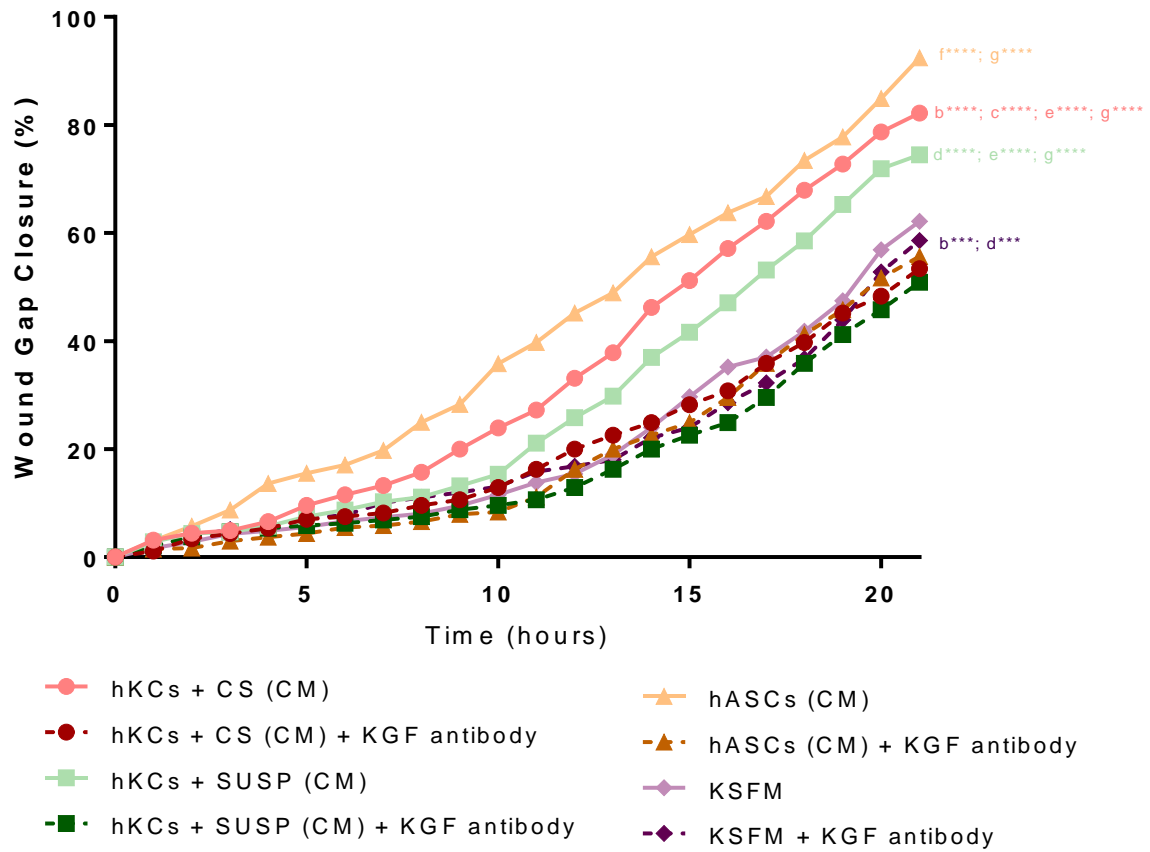


Figure 3.15 - Migration assay conducted using different conditions with hKCs. Data was analyzed by 2way ANOVA, followed by Sidak's multiple comparison test for: *b* denotes significant differences compared to hKCs + CS + KGF antibody, *c* denotes significant differences compared to hKCs + SUSP, *d* denotes significant differences compared to hKCs + SUSP + KGF antibody, *e* denotes significant differences compared to hASCs, *f* denotes significant differences compared to hASCs + KGF antibody, *g* denotes significant differences compared to KSFM. The data is expressed as mean percentages, n= 3.

3.2. Discussion

Impaired production of GFs in wounds can lead to malfunction of different cells that are crucial during re-epithelialization, namely KCs. Keratinocyte growth factor is a key player on promoting migration and proliferation of these cells and a wide range of strategies aiming to improve its therapeutic efficacy have been described [1–27]. In this work in particular, GG particles and hASCs were explored for KGF delivery systems.

The GG particles herein produced displayed a polydispersity index smaller than 0.2, being in the range of the values found for a solution of particles to be homogeneous and an indication of a narrow range of size distribution according to published guidelines [28]. The associated changes in values (from -59.70 mV to -43.20 mV), indicated that the formulation was stable according to the standards of literature [29]. The negative values observed could be related to the contribution of glucuronic acid, a weak acid present in the GG structure [30]. When comparing the sizes obtained by DLS and STEM, the sizes of the particles in DLS were larger. The difference in sizes could be explained due to the requirement of vacuum in STEM technique, because without it, the electrons aiming at the sample would be deflected, and for that, the liquid present in the sample evaporated [31]. The evaporation of the liquid led for the particles to be dried, and therefore smaller when compared to the particles in solution measured by DLS. This was in accordance to the literature, where DLS results typically showed larger sizes than the ones found with microscopy techniques [32]. In this way, the sizes using both techniques could not be compared, and STEM was used to confirm the spherical shape of GG particles.

Bovine Serum Albumin is known to be a standard protein (66 kDa) used in several experiments, due to its similar properties, molecular weight and amino acid sequence to human serum albumin [33]. Release assays using BSA demonstrated that polydisperse GG particles, less protein was entrapped than the condition where particles are filtered ensuring a size smaller than 1 μm . This was possibly related with the presence of aggregates in the non-filtered condition as in this one, the surface area was smaller and that, according to the literature, particles comprising lower surface area have naturally lower reactive surface sites for BSA to bind to GG particles [34]. Particles with subsequent lyophilization, BSA release was significantly higher, since this freeze-drying technique is known to allow the creation of new porous that can directly enhance the release process [35]. The pH is highly dependent on physiologic state of the skin. In normal skin the pH varies between 4 and 6, while in healing and non-healing wounds the pH is normally between 7.15 and 8.9 [36,37]. Release assays using KGF in different pHs, demonstrated that depending on the pH, the amount of KGF as well as the associated release profile varied, which can be

justified by the charges inherent to GG and to KGF. Gellan gum pKa is 3.5 and this value is essential for understanding chemical reactions, revealing the protonation state of the molecule in a particular solvent in a certain pH, meaning that all pHs above the value of pKa GG is deprotonated due to the dissociation of the carboxylate residues and the surface negatively-charged, pHs below GG is protonated and consequently the surface is positively-charged [38–40]. On the other hand, KGF (18.9 kDa) presents an isoelectric point (pI)=9.29, which is the pH of the solution where the net charge of KGF becomes zero [41–43]. For pH=4 and pH=7.4, the KGF in solution has predominantly positively-charged surface, since it is below the pI, demonstrating attractive interactions to negatively-charged surfaces of GG [42]. At pH=10, most of KGF surface is negatively-charged, exhibiting repulsive interactions to GG particles [42], therefore not presenting a sustained release, but instead a fast burst release in the first 6 hours was observed [44]. Particle-based systems have been used for consecutive and long-term administration of drugs/growth factors suitable for treatment of wounds [45,46]. The delivery of KGF by GG particles led to higher proliferation of hKCs also confirmed by the higher percentage of hKCs expressing Ki67 proliferation marker, which meets similar administered systems of particles produced with other materials [25,27]. The migration of hKCs when using KGF-loaded particles was significantly enhanced to a greater degree than KGF alone. This could be attributed not only to a protection of KGF degradation by the encapsulation process in the GG particles, but also by a cumulative effect of the internalized particles *per se*, as in this condition alone hKCs also migrate faster. These observations go in line with data from another study, where fibrin nanoparticles with entrapped KGF, lead to a stabilization of KGF and an enhancement of hKCs migration *in vitro* [20]. Additionally, the reduced stimulatory activity of KGF in keratinocyte migration in the presence of neutralizing antibody against KGF, supports the hypothesis that KGF released by the particles was exhibiting a mitogenic and mitogenic effect in hKCs, as observed in the literature [1]. Furthermore, the enhanced impact on migration and proliferation of KCs by GG particles alone, could be related with the effect somehow promoted by the process of cellular internalization of the particles. Different mechanisms have been described and recently reviewed [47], nonetheless no specific studies on this topic were herein conducted.

Mesenchymal stem cells are known to promote tissue regeneration and to release GFs [48,49]. Adipose-derived stem cells have been one of the most promising stem cells population known to be capable of secreting numerous GFs and cytokines, including KGF, that are critical for wound healing [50,51]. Using two different methodologies to promote proliferation and migration of hKCs, hASCs were used in co-culture with hKCs, as cell sheets and cell suspension. Through time, hKCs were not able to produce any KGF since, as has been described, it is solely produced by various types of stromal cells but

not by epithelial cells [52]. Through time, hASCs-CS did not present differences of KGF secreted values, in contrary to hASCs-SUSP, which showed to decrease. This could be related to the fact that the percentage of hASCs in CS form was practically the same as the one for hKCs after 72 hours, in contrary to the hASCs in suspension form that decreased while KCs increased, suggesting that more cells were consuming KGF comparing to the ones producing this GF. The specific receptor for KGF showed to be expressed on hKCs and not on hASCs, because despite being low expressed on mesenchymal cells, it is not located on hASCs, but is highly expressed on epithelial cells, namely on hKCs [53]. The mitogenic effect of KGF on hKCs was detected on the conditions in contact with hASCs, where hKCs showed to be highly proliferative [54]. The migratory stimuli by the CM of hASCs, CS and SUSP have shown to be in accordance to the expression of KGF present in the media, where through a paracrine release of KGF supported the migration of hKCs, not needing cell-to-cell contact [16]. The neutralization of KGF partially inhibited the inductive effect of migration, being similar to the migration found in the control. These results could be a suggestion of the implication of additional growth factors such EGF (known to induce KC migration and present as a supplement in the medium in control conditions), together with the fact that small concentrations of EGF are normally produced by hASCs [55–57].

Overall, these studies using either KGF-loaded particles or hASCs potentiated the migration and mitogenic activity of hKCs *in vitro*, being possibly a therapeutic strategy for wounds with impaired re-epithelialization.

3.3. References

- [1] R. Tsuboi, C. Sato, Y. Kurita, D. Ron, J.S. Rubin, H. Ogawa, Keratinocyte Growth Factor (FGF-7) Stimulates Migration and Plasminogen Activator Activity of Normal Human Keratinocytes, *J. Invest. Dermatol.* 101 (1993) 49–53. <https://doi.org/10.1111/1523-1747.ep12358892>.
- [2] S. Karvinen, S. Pasonen-Seppänen, J.M.T. Hyttinen, J.-P. Pienimäki, K. Törrönen, T.A. Jokela, M.I. Tammi, R. Tammi, Keratinocyte Growth Factor Stimulates Migration and Hyaluronan Synthesis in the Epidermis by Activation of Keratinocyte Hyaluronan Synthases 2 and 3, *J. Biol. Chem.* 278 (2003) 49495–49504. <https://doi.org/10.1074/jbc.M310445200>.
- [3] Y. Qu, C. Cao, Q. Wu, A. Huang, Y. Song, H. Li, Y. Zuo, C. Chu, J. Li, Y. Man, The dual delivery of KGF and bFGF by collagen membrane to promote skin wound healing., *J. Tissue Eng. Regen. Med.* 12 (2018) 1508–1518. <https://doi.org/10.1002/term.2691>.
- [4] S.A. Burns, R. Hard, W.L. Hicks, F. V Bright, D. Cohan, L. Sigurdson, J.A. Gardella, Determining the protein drug release characteristics and cell adhesion to a PLLA or PLGA biodegradable polymer membrane, *J. Biomed. Mater. Res. Part A.* 94A (2010) 27–37. <https://doi.org/10.1002/jbm.a.32654>.
- [5] J. Oh, E. Lee, Engineered dressing of hybrid chitosan-silica for effective delivery of keratin growth factor and acceleration of wound healing, *Mater. Sci. Eng. C.* 103 (2019) 109815. <https://doi.org/10.1016/j.msec.2019.109815>.
- [6] M. Bienert, M. Hoss, M. Bartneck, S. Weinandy, M. Böbel, S. Jockenhövel, R. Knüchel, K. Pottbacker, M. Wöltje, W. Jahnen-Dechent, S. Neuss, Growth factor-functionalized silk membranes support wound healing in vitro, *Biomed. Mater.* 12 (2017) 045023. <https://doi.org/10.1088/1748-605X/aa7695>.
- [7] M.G. Jeschke, G. Richter, F. Höfstädter, D.N. Herndon, J.-R. Perez-Polo, K.-W. Jauch, Non-viral liposomal keratinocyte growth factor (KGF) cDNA gene transfer improves dermal and epidermal regeneration through stimulation of epithelial and mesenchymal factors., *Gene Ther.* 9 (2002) 1065–74. <https://doi.org/10.1038/sj.gt.3301732>.

- [8] C.T. Pereira, D.N. Herndon, R. Rocker, M.G. Jeschke, Liposomal Gene Transfer of Keratinocyte Growth Factor Improves Wound Healing by Altering Growth Factor and Collagen Expression, *J. Surg. Res.* 139 (2007) 222–228. <https://doi.org/10.1016/j.jss.2006.09.005>.
- [9] G. Marti, M. Ferguson, J. Wang, C. Byrnes, R. Dieb, R. Qaiser, P. Bonde, M. Duncan, J. Harmon, Electroporative transfection with KGF-1 DNA improves wound healing in a diabetic mouse model, *Gene Ther.* 11 (2004) 1780–1785. <https://doi.org/10.1038/sj.gt.3302383>.
- [10] C. Dou, F. Lay, A.M. Ansari, D.J. Rees, A.K. Ahmed, O. Kovbasnjuk, A.E. Matsangos, J. Du, S.M. Hosseini, C. Steenbergen, K. Fox-Talbot, A.T. Tabor, J.A. Williams, L. Liu, G.P. Marti, J.W. Harmon, Strengthening the Skin with Topical Delivery of Keratinocyte Growth Factor-1 Using a Novel DNA Plasmid, *Mol. Ther.* 22 (2014) 752–761. <https://doi.org/10.1038/mt.2014.2>.
- [11] M.J. Escámez, M. Carretero, M. García, L. Martínez-Santamaría, I. Mirones, B. Duarte, A. Holguín, E. García, V. García, A. Meana, J.L. Jorcano, F. Larcher, M. Del Río, Assessment of Optimal Virus-Mediated Growth Factor Gene Delivery for Human Cutaneous Wound Healing Enhancement, *J. Invest. Dermatol.* 128 (2008) 1565–1575. <https://doi.org/10.1038/sj.jid.5701217>.
- [12] G. Erdag, D.A. Medalie, H. Rakhorst, G.G. Krueger, J.R. Morgan, FGF-7 Expression Enhances the Performance of Bioengineered Skin, *Mol. Ther.* 10 (2004) 76–85. <https://doi.org/10.1016/j.ymthe.2004.04.013>.
- [13] L. Staiano-Coico, J.G. Krueger, J.S. Rubin, S. D'limi, V.P. Vallat, L. Valentino, T. Fahey, A. Hawes, G. Kingston, M.R. Madden, Human keratinocyte growth factor effects in a porcine model of epidermal wound healing., *J. Exp. Med.* 178 (1993) 865–878. <https://doi.org/10.1084/jem.178.3.865>.
- [14] J. Kopp, G.Y. Wang, P. Kulmburg, S. Schultze-Mosgau, J.N. Huan, K. Ying, H. Seyhan, M.D. Jeschke, U. Kneser, A.D. Bach, S.D. Ge, S. Dooley, R.E. Horch, Accelerated Wound Healing by In vivo Application of Keratinocytes Overexpressing KGF, *Mol. Ther.* 10 (2004) 86–96. <https://doi.org/10.1016/j.ymthe.2004.04.016>.

- [15] M. Denzinger, A. Link, J. Kurz, S. Krauss, R. Thoma, C. Schlensak, H.P. Wendel, S. Krajewski, Keratinocyte Growth Factor Modified Messenger RNA Accelerating Cell Proliferation and Migration of Keratinocytes, *Nucleic Acid Ther.* 28 (2018) 335–347. <https://doi.org/10.1089/nat.2018.0737>.
- [16] V.-I. Alexaki, D. Simantiraki, M. Panayiotopoulou, O. Rasouli, M. Venihaki, O. Castana, D. Alexakis, M. Kampa, E.N. Stathopoulos, E. Castanas, Adipose Tissue-Derived Mesenchymal Cells Support Skin Reepithelialization through Secretion of KGF-1 and PDGF-BB: Comparison with Dermal Fibroblasts, *Cell Transplant.* 21 (2012) 2441–2454. <https://doi.org/10.3727/096368912X637064>.
- [17] B.-R. Zhou, Y. Xu, S.-L. Guo, Y. Xu, Y. Wang, F. Zhu, F. Permatasari, D. Wu, Z.-Q. Yin, D. Luo, The Effect of Conditioned Media of Adipose-Derived Stem Cells on Wound Healing after Ablative Fractional Carbon Dioxide Laser Resurfacing, *Biomed Res. Int.* 2013 (2013) 1–9. <https://doi.org/10.1155/2013/519126>.
- [18] M.T. Cerqueira, R.P. Pirraco, T.C. Santos, D.B. Rodrigues, A.M. Frias, A.R. Martins, R.L. Reis, A.P. Marques, Human Adipose Stem Cells Cell Sheet Constructs Impact Epidermal Morphogenesis in Full-Thickness Excisional Wounds, *Biomacromolecules.* 14 (2013) 3997–4008. <https://doi.org/10.1021/bm4011062>.
- [19] M. Hamada, T. Iwata, Y. Kato, K. Washio, S. Morikawa, H. Sakurai, M. Yamato, T. Okano, Y. Uchigata, Xenogeneic transplantation of human adipose-derived stem cell sheets accelerate angiogenesis and the healing of skin wounds in a Zucker Diabetic Fatty rat model of obese diabetes, *Regen. Ther.* 6 (2017) 65–73. <https://doi.org/10.1016/j.reth.2017.02.002>.
- [20] S. Li, Q. Tang, H. Xu, Q. Huang, Z. Wen, Y. Liu, C. Peng, Improved stability of KGF by conjugation with gold nanoparticles for diabetic wound therapy, *Nanomedicine.* 14 (2019) 2909–2923. <https://doi.org/10.2217/nnm-2018-0487>.
- [21] Y. Ni, D. Turner, K. Yates, I. Tizard, Stabilization of Growth Factors Relevant to Wound Healing by a Plant Cell Wall Biomaterial, *Planta Med.* 73 (2007) 1260–1266. <https://doi.org/10.1055/s-2007-990225>.

- [22] H. Waldeck, A.S. Chung, W.J. Kao, Interpenetrating polymer networks containing gelatin modified with PEGylated RGD and soluble KGF: Synthesis, characterization, and application in vivo critical dermal wound, *J. Biomed. Mater. Res. Part A.* 82A (2007) 861–871. <https://doi.org/10.1002/jbm.a.31054>.
- [23] D.J. Geer, D.D. Swartz, S.T. Andreadis, Biomimetic Delivery of Keratinocyte Growth Factor upon Cellular Demand for Accelerated Wound Healing in Vitro and in Vivo, *Am. J. Pathol.* 167 (2005) 1575–1586. [https://doi.org/10.1016/S0002-9440\(10\)61242-4](https://doi.org/10.1016/S0002-9440(10)61242-4).
- [24] S. Sen-Britain, W.L. Hicks, R. Hard, J.A. Gardella, Differential orientation and conformation of surface-bound keratinocyte growth factor on (hydroxyethyl)methacrylate, (hydroxyethyl)methacrylate/methyl methacrylate, and (hydroxyethyl)methacrylate/methacrylic acid hydrogel copolymers, *Biointerphases.* 13 (2018) 06E406. <https://doi.org/10.1116/1.5051655>.
- [25] A. Pan, M. Zhong, H. Wu, Y. Peng, H. Xia, Q. Tang, Q. Huang, L. Wei, L. Xiao, C. Peng, Topical Application of Keratinocyte Growth Factor Conjugated Gold Nanoparticles Accelerate Wound Healing., *Nanomedicine.* 14 (2018) 1619–1628. <https://doi.org/10.1016/j.nano.2018.04.007>.
- [26] I. Muhamed, E.P. Sproul, F.S. Ligler, A.C. Brown, Fibrin Nanoparticles Coupled with Keratinocyte Growth Factor Enhance the Dermal Wound-Healing Rate., *ACS Appl. Mater. Interfaces.* 11 (2019) 3771–3780. <https://doi.org/10.1021/acsami.8b21056>.
- [27] P. Koria, H. Yagi, Y. Kitagawa, Z. Megeed, Y. Nahmias, R. Sheridan, M.L. Yarmush, Self-assembling elastin-like peptides growth factor chimeric nanoparticles for the treatment of chronic wounds., *Proc. Natl. Acad. Sci. U. S. A.* 108 (2011) 1034–9. <https://doi.org/10.1073/pnas.1009881108>.
- [28] N. Salim, M. Basri, M.B. Rahman, H. Basri, Modification of palm kernel oil esters nanoemulsions with hydrocolloid gum for enhanced topical delivery of ibuprofen, *Int. J. Nanomedicine.* 7 (2012) 4739–4747. <https://doi.org/10.2147/IJN.S34700>.
- [29] S. Jayaprakash, S. A, J. S, Optimization of Process Variables for the Preparation of Gellan Gum-Raloxifene Nanoparticles Using Statistical Design, *Am. J. Pharm. Heal. Res.* 2 (2014) 34–49.

- [30] R. Mao, J. Tang, B.G. Swanson, Gelling Temperatures of Gellan Solutions as Affected by Citrate Buffers, *J. Food Sci.* 64 (1999) 648–652. <https://doi.org/10.1111/j.1365-2621.1999.tb15103.x>.
- [31] P.D. Nellist, Scanning Transmission Electron Microscopy, in: *Springer Handbooks Microsc.*, Springer, 2019: pp. 49–99. https://doi.org/10.1007/978-3-030-00069-1_2.
- [32] P. Eaton, P. Quaresma, C. Soares, C. Neves, M.P. de Almeida, E. Pereira, P. West, A direct comparison of experimental methods to measure dimensions of synthetic nanoparticles, *Ultramicroscopy*. 182 (2017) 179–190. <https://doi.org/10.1016/j.ultramic.2017.07.001>.
- [33] M.K. Hameed, I.M. Ahmady, H. Alawadhi, B. Workie, E. Sahle-Demessie, C. Han, M.M. Chehimi, A.A. Mohamed, Gold-carbon nanoparticles mediated delivery of BSA: Remarkable robustness and hemocompatibility, *Colloids Surfaces A Physicochem. Eng. Asp.* 558 (2018) 351–358. <https://doi.org/10.1016/j.colsurfa.2018.09.004>.
- [34] A.B. Asha, R. Narain, Nanomaterials properties, in: *Polym. Sci. Nanotechnol.*, Elsevier, 2020: pp. 343–359. <https://doi.org/10.1016/B978-0-12-816806-6.00015-7>.
- [35] T. Garg, O. Singh, S. Arora, R.S.R. Murthy, Scaffold: A Novel Carrier for Cell and Drug Delivery, *Crit. Rev. Ther. Drug Carr. Syst.* 29 (2012) 1–63. <https://doi.org/10.1615/CritRevTherDrugCarrierSyst.v29.i1.10>.
- [36] L.A. Schneider, A. Korber, S. Grabbe, J. Dissemond, Influence of pH on wound-healing: a new perspective for wound-therapy?, *Arch. Dermatol. Res.* 298 (2007) 413–420. <https://doi.org/10.1007/s00403-006-0713-x>.
- [37] G. Gethin, The significance of surface pH in chronic wounds, *Wounds*. 3 (2007) 52–56.
- [38] K.S. Alongi, G.C. Shields, Theoretical Calculations of Acid Dissociation Constants: A Review Article, in: *Annu. Rep. Comput. Chem.*, Elsevier BV, 2010: pp. 113–138. [https://doi.org/10.1016/S1574-1400\(10\)06008-1](https://doi.org/10.1016/S1574-1400(10)06008-1).
- [39] S. de Jong, F. van de Velde, Charge density of polysaccharide controls microstructure and large deformation properties of mixed gels, *Food Hydrocoll.* 21 (2007) 1172–1187. <https://doi.org/10.1016/j.foodhyd.2006.09.004>.

- [40] C.J. Ferris, L.R. Stevens, K.J. Gilmore, E. Mume, I. Greguric, D.M. Kirchmajer, G.G. Wallace, M. in het Panhuis, Peptide modification of purified gellan gum, *J. Mater. Chem. B.* 3 (2015) 1106–1115. <https://doi.org/10.1039/C4TB01727G>.
- [41] FGF7 (human), (n.d.). <https://www.phosphosite.org/proteinAction?id=24297&showAllSites=true>.
- [42] P. Novák, V. Havlíček, Protein Extraction and Precipitation, in: *Proteomic Profiling Anal. Chem.*, Elsevier, 2016: pp. 51–62. <https://doi.org/10.1016/B978-0-444-63688-1.00004-5>.
- [43] Animal-Free Recombinant Human KGF (FGF-7), (n.d.). <https://www.peprotech.com/en/recombinant-human-kgf#productreviews>.
- [44] C. Andrade, Sustained-Release, Extended-Release, and Other Time-Release Formulations in Neuropsychiatry, *J. Clin. Psychiatry.* 76 (2015) e995–e999. <https://doi.org/10.4088/JCP.15f10219>.
- [45] W. ABDELWAHED, G. DEGOBERT, S. STAINMESSE, H. FESSI, Freeze-drying of nanoparticles: Formulation, process and storage considerations☆, *Adv. Drug Deliv. Rev.* 58 (2006) 1688–1713. <https://doi.org/10.1016/j.addr.2006.09.017>.
- [46] F. Oyarzun-Ampuero, A. Vidal, M. Concha, J. Morales, S. Orellana, I. Moreno-Villoslada, Nanoparticles for the Treatment of Wounds, *Curr. Pharm. Des.* 21 (2015) 4329–4341. <https://doi.org/10.2174/1381612821666150901104601>.
- [47] N.D. Donahue, H. Acar, S. Wilhelm, Concepts of nanoparticle cellular uptake, intracellular trafficking, and kinetics in nanomedicine, *Adv. Drug Deliv. Rev.* 143 (2019) 68–96. <https://doi.org/10.1016/j.addr.2019.04.008>.
- [48] M.T. Cerqueira, R.P. Pirraco, A.P. Marques, Stem Cells in Skin Wound Healing: Are We There Yet?, *Adv. Wound Care.* 5 (2016) 164–175. <https://doi.org/10.1089/wound.2014.0607>.
- [49] B. Dash, Z. Xu, L. Lin, A. Koo, S. Ndon, F. Berthiaume, A. Dardik, H. Hsia, Stem Cells and Engineered Scaffolds for Regenerative Wound Healing, *Bioengineering.* 5 (2018) 23. <https://doi.org/10.3390/bioengineering5010023>.

- [50] Y.-C. Lin, T. Grahovac, S.J. Oh, M. Ieraci, J.P. Rubin, K.G. Marra, Evaluation of a multi-layer adipose-derived stem cell sheet in a full-thickness wound healing model, *Acta Biomater.* 9 (2013) 5243–5250. <https://doi.org/10.1016/j.actbio.2012.09.028>.
- [51] M.T. Cerqueira, A.P. Marques, R.L. Reis, Using Stem Cells in Skin Regeneration: Possibilities and Reality, *Stem Cells Dev.* 21 (2012) 1201–1214. <https://doi.org/10.1089/scd.2011.0539>.
- [52] H.-D. Beer, M.G. Gassmann, B. Munz, H. Steiling, F. Engelhardt, K. Bleuel, S. Werner, Expression and Function of Keratinocyte Growth Factor and Activin in Skin Morphogenesis and Cutaneous Wound Repair, *J. Investig. Dermatology Symp. Proc.* 5 (2000) 34–39. <https://doi.org/10.1046/j.1087-0024.2000.00009.x>.
- [53] Cell type atlas - FGFR2 - The Human Protein Atlas, (n.d.). <https://www.proteinatlas.org/ENSG00000066468-FGFR2/celltype>.
- [54] J. Rubin, Keratinocyte growth factor, *Cell Biol. Int.* 19 (1995) 399–412. <https://doi.org/10.1006/cbir.1995.1085>.
- [55] M.A. Seeger, A.S. Paller, The Roles of Growth Factors in Keratinocyte Migration, *Adv. Wound Care.* 4 (2015) 213–224. <https://doi.org/10.1089/wound.2014.0540>.
- [56] Keratinocyte SFM (1X), (n.d.). <https://www.thermofisher.com/order/catalog/product/17005042#/17005042>.
- [57] R. Noverina, W. Widowati, W. Ayuningtyas, D. Kurniawan, E. Afifah, D.R. Laksmiawati, R. Rinendyaputri, R. Rilianawati, A. Faried, I. Bachtiar, F.F. Wirakusumah, Growth factors profile in conditioned medium human adipose tissue-derived mesenchymal stem cells (CM-hATMSCs), *Clin. Nutr. Exp.* 24 (2019) 34–44. <https://doi.org/10.1016/j.yclnex.2019.01.002>.

CHAPTER IV.

General Conclusions
and Future Work

CHAPTER IV. General Conclusions and Future Work

Upon skin injury, wound re-epithelialization is one of the major milestones of the healing process. This is especially difficult to achieve on hard-to-heal wounds that are often open for long periods, as the dysregulation of the growth factors involved in this response contributes for an impaired proliferation and migration of KCs. KGF plays a central role in this problematic, as it is a potent factor that in the normal healing scenario promotes direct proliferation and migration of epidermal cells, consequently impacting re-epithelialization.

In this thesis, GG particles were developed to enable a controlled and sustained release of KGF using different pHs, aiming to induce wound regeneration. During healing cascade, wounds pass through different states that have different associated pH variations. Therefore, by adapting these release profiles for specific pHs, a better healing could be targeted. The proliferation and migration of hKCs was increased in the conditions treated with KGF-loaded particles, as well as with particles alone, possibly due to the associated internalization of GG particles by hKCs, when compared to control conditions. Overall, these results suggested that the developed delivery system is likely to be more effective than the administration of KGF in free form, as a small dose released in a controlled manner showed to be efficient under this context. As an alternative approach, previous works have shown the involvement of hASCs in the re-epithelialization through KGF effect. By either using hASCs in cell sheet and suspension forms, hASCs showed to be natural producers of KGF, inducing an improvement of proliferation and migration of co-cultured KCs. Both strategies, either using KGF delivery from a natural source or via the KGF-loaded particles, promoted *in vitro* proliferation and migration of hKCs, necessary for wound re-epithelialization.

The use of GG particles encapsulated with KGF may help solve one of the major shortcomings of drug delivery, namely the growth factor stability, sustained release and prolonged activity of KGF. While hASCs-based strategies can be explored taking advantage of their KGF production capacity, as well as other important features for wound healing. The study of the internalization process of GG particles deserves attention in order to unravel the contribution to hKCs motogenic activity. Alongside, the use of human skin *ex vivo* models or excisional wounds in rodents *in vivo* models would allow the validation of the produced KGF-loaded particles and hASCs-CS over the re-epithelialization process. Moreover, the incorporation of additional factors relevant for the cutaneous healing process opens the possibility of a multi-factor sophisticated system to target the different phases more efficiently, going beyond the proposed target of re-epithelialization.